Università degli Studi di Palermo

AREA RICERCA E TRASFERIMENTO TECNOLOGICO
SETTORE DOTTORATI E CONTRATTI PER LA RICERCA
U. O. DOTTORATI DI RICERCA

Corso di Dottorato in Biomedicina, Neuroscienze e Diagnostica Avanzata

Dipartimento di Biomedicina, Neuroscienze e Diagnostica Avanzata

Settore Scientifico Disciplinare MED/12A

Frequency and clinical correlates of brain gadolinium deposition in patients with Multiple Sclerosis

IL DOTTORE
Dott. Salvatore Iacono

IL COORDINATORE
Prof. Fabio Bucchieri

IL TUTOR
Prof. Filippo Brighina

CICLO XXXVIII
ANNO CONSEGUIMENTO TITOLO 2025

TABLE OF CONTENTS

ABSTRACT

Multiple sclerosis (MS) is a chronic neuroinflammatory disease of the central nervous system (CNS) representing a common cause of neurological disability in your people. While the relapsing-remitting phenotype is the most frequent form at disease onset, many patients experience an unrelenting disability progression over time.

To date, many disease modifying treatments (DMTs) are available to counteract disease activity even if the finding of an effective drug on progressive MS forms is still an unmet need. Several studies showed that the early initiation of high effective DMT is the best treatment strategy of MS. Whilst the achievement of the highest anti-inflammatory effect is the mainstream of neurologists and researchers, it is worth noting that greater is the efficacy of that DMT and greater is the risk of causing related adverse events. For this reason, many DMTs require focused and rigorous surveillance.

Natalizumab (NTZ) is a high effective DMTs for the treatment of MS. Since 2006, when it has been commercialized, it changed the natural history of MS becoming one of the most prescribed DMT worldwide. NTZ inhibits the extravasation of peripheral lymphocytes into CNS limiting the intrathecal inflammation. If this mechanism of action lead to the reduction of MS activity, on the other hand, it exposes patients to higher risk of opportunistic CNS infections, especially progressive multifocal leukoencephalopathy (PML) caused by the intrathecal reactivation of John Cunningham virus (JCV).

The brain MRI monitoring strategy in patients with MS is vastly different worldwide ranging from one MRI scans every 6 months to one year. It is worth noting that the MRI monitoring strategy gains even more relevance in patients under treatment with NTZ to detect the early appearance of PML pathological changes. In this case, the monitoring range is highly variable across different MS clinics depending mainly by serum JCV status and treatment duration. Of note, before the recommendations of the 2021 MAGNIMS consensus, the administration of gadolinium was routinely employed in patients with MS.

The aim of this study is to explore the effect of recurrent gadolinium exposition in patients with MS treated with NTZ who routinely underwent brain MRI scan for the PML-risk surveillance purpose

1. MULTIPLE SCLEROSIS

Multiple Sclerosis (MS) is a chronic, inflammatory, autoimmune disease of the central nervous system (CNS) characterized by the immune-mediated aggression to oligodendrocytes leading to myelin loss and axonal damage. The incidence of MS is increasing worldwide representing one of the major causes of non-traumatic disability in younger people. The first description of MS was given by the French neurologist J.M. Charcot who termed the disease "sclerosis in plaques" due to the peculiar dissemination of oval lesion in brain and spinal cord white matter. To date, it is known that these lesions are sites of elevated inflammatory activity damaging both myelin and gray matter. Several factors have been studied as contributors of MS pathogenesis, (e.g., smoking, vitamin D deficiency, Epstein-Barr Virus (EBV) infection), but its etiology remains unknown. Despite MS has been recognized as a T-cell-mediated disease, the effectiveness of new anti-CD20 drugs in reducing disease activity has cast doubt on the original pathogenetic hypothesis. In 85% of cases, the clinical presentation is the relapsing-remitting MS (RRMS), while in the remaining cases, the phenotype is a progressive form from the onset, known as primary progressive MS (PPMS). However, after 15-20 years from onset, nearly 80% of patients with RRMS undergo secondary progression (SPMS) characterized by an inexorable disability progression over time.

1.1. Epidemiology

Approximately 2.8 million people worldwide are affected by MS, and 1.2 millions of whom are in Europe. The global MS prevalence ranges from 1 every 3.000 people up to 1 in every 300 people in countries with the highest prevalence. It affects mainly women (female to male ratio=3:1) and has the highest incidence between 20 and 50 years of age (1). It has been tradionally thought that prevalence and incidence of MS were higher in temperate zones far from equator such as New Zeeland, United States and Northen Europe while they were lower in tropical and subtropical regions leading to a South to North prevalence gradient. This peculiar distribution suggests that the etiopathogenesis of MS depends from a complex interaction between genetic, environmental and socioeconomic factors (2). However, in the last decades the incidence of MS has been increasing worldwide with the loss of the typical geographical gradient. This discrepancy between the previous and current data may be related to the erroneous interpretation to the latitudinal gradient in Europe which was based mainly on prevalence studies (3). It is worth noting that the MS incidence peak is around 35 years while the prevalence peak is around 50 years thus the crude prevalence and incidence rates could therefore depend on the age distribution in the MS patient population. The age-standardization with reference to a standard global population could be the leading factor of the loss of the latitudinal incidence gradient (4). For instance, the incidence and prevalence of MS have been increasing in Italy in a not

dependent manner from latitude; Italy is a higher-risk region for MS and this may be explained by environmental factors in addition to the genetic background (5). To date, the global incidence of MS is 5.2/100.000 people per year, while the prevalence is 112/100.000 people per year (6). The heat map of the MS prevalence is depicted in Figure 1.

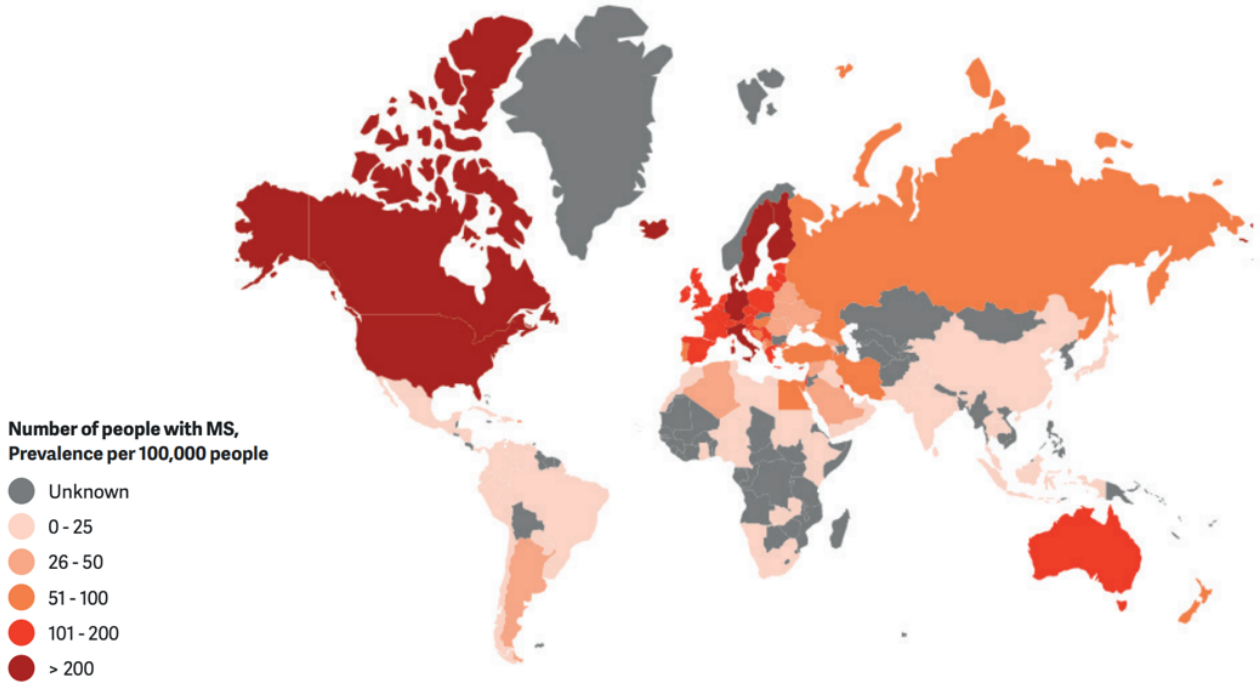

Figure 1 Heat map showing the prevalence of MS worldwide. Warmer colors indicate high-prevalence region. Data from the 2020 Atlas of MS, Third Edition, Multiple Sclerosis International Federation, MSIF.

Moreover, the number of patients with the MS onset before 18 (pediatric MS) and above 50 years (late onset MS) is increasing to date. While pediatric MS has an estimated prevalence of 3.1 every 100.000 people, late onset MS account for 5% of all MS cases (1). Interestingly, late onset MS is characterized by attenuated female to male ratio and higher frequency of progressive course from its onset (7).

1.2. Etiology

The etiology of MS is still unknown probably resulting from the complex interplay between genetic, environmental and socioeconomic factors. Among factors traditionally associated to higher risk of MS there are Epstein Barr Virus (EBV) infection, positive familiar history, smoking obesity and lower exposition to UV rays.

- *UVB rays and Vitamin D:* several epidemiological studies highlighted the role of UVB rays and Vitamin D in MS etiopathogenesis since sixties. The lower exposure to UVB rays lead to hypovitaminosis D which is a common finding in patients with MS. The association between vitamin D and MS is not established and is only putative since vitamin D has an important role in the regulation of T CD4 lymphocytes and in the myelinization processes.

- *Genetic background:* although there are no causative genes, one every 8 MS patients have a positive familiar history and the concordance between identical twins is around 30% (8,9). One-hundred genes have been studies as predisposing factors for MS pathogenesis. Accordingly, genes codifying for the major histocompatibility complex II (MHC II) including the allele HLA-DRB1*1501 of DR2 gene and DQB1*0602, DRB5*0101 and DQA1*0102 are the main genetic predisposing factors in Caucasians. Of interest, the risk of developing MS is 3 and 6-fold higher in the case of heterozygous and homozygous genotype for the haplotype HLA-DRB1*1501, respectively (10). More recently, by using genome wide association studies (GWAS) at least 150 polymorphisms of genes codifying for interleukins and other inflammation molecules (CD58, IL2RA, IL7R, CD6, TNFR1, BAFF, CYP2R1 e AHI-1) were found to increase the risk of MS by 10-20% (11–16).

- *Smoking:* It increases the risk of MS by approximately 50% and may explain up to 40% of the increase in MS incidence in women since the use of smoked tobacco increased disproportionately in women after the Second World War, in parallel with the increase of MS incidence (17). Particularly, the risk of MS is enhanced by smoked tobacco rather than chewed tobacco suggesting a potential role of post-translational modifications induced by smoking in the lungs. Smoking has also a negative impact on the course of the disease, risk of relapses, response to drugs, mental state and quality of life.

- *Obesity*: GWAS studies have shown that genetic predisposition to a high BMI is strongly associated with the risk of MS. In particular, each one-point increase of BMI standard deviation appears to confer a 41% increase in MS risk. The mechanisms by which obesity may contribute to the increased risk of MS are unknown. Several mechanisms have been proposed, including the induction of a pro-inflammatory stat typical of obesity and increased leptin production and reduced adiponectin with consequent reduction of regulatory T lymphocytes (Tregs) (18).

- *Epstein-Barr Virus infection (EBV):* The role of EBV infection in the pathogenesis of MS has attacked interest since many years. EBV persists in a latent form in B lymphocytes throughout the life of the host altering the dynamics of the immune response. Furthermore, some studies have found the EBV genome in demyelinating lesions in subjects with MS (19). However, given that EBV infection is ubiquitous (95% of the population), causality studies have been largely hindered. Recently, a study conducted on 10,000 American soldiers, in which the incidence of MS in EBV-negative and -positive patients was compared over a 20-year period, concluded that EBV-infected subjects have a risk of developing MS greater than 32 times higher than uninfected subjects or subjects infected with other viruses such as, for example, cytomegalovirus. Furthermore, seroconversion after EBV infection has been associated with increased serum neurofilaments in a pre-clinical phase of MS, concluding that EBV infection is the main cause of MS (20). On the other hand, considering that all MS patients are EBV positive but not all EBV-infected patients develop MS, in this scenario EBV infection appears as a necessary but not sufficient factor for the development of the disease.

- *Diet habits and microbiota:* recently, the microbiota has attracted the interest of many researchers as contributor of MS pathogenesis. Accordingly, it would seem to be involved in the regulation of the host immune system in response to external factors and this imbalance could be the trigger of damage to the blood-brain barrier (BBB) with subsequent pro-inflammatory shift within the CNS. In particular, dysbiosis supported by unhealthy dietary habits (e.g. diet rich in saturated fats, poor vitamin D intake, etc.) would lead to the increase of gut Firmicutes and Bacterioides with consequent reduction in the production of anti-inflammatory metabolites such as propionate and butyrate and subsequent reduction of Treg lymphocytes, increase of Th17, over expression of genes involved in antigen presentation to B and T lymphocytes and activation of the complement and coagulation cascades with increased intestinal permeabilization and systemic inflammation that could contribute to the pathogenesis of MS (21).

The etiology of MS seems to be multifactorial involving genetic (e.g., HLA genes), individual (e.g., smoking, obesity) and environmental (e.g., infections) factors.

1.3. Neuropathogenesis

MS is an autoimmune disease characterized by the lymphocyte-mediated destruction of oligodendrocytes. Historically, it has been defined as an organ-specific, T-lymphocyte-mediated autoimmune disease, although the effectiveness of anti-CD20 drugs in modifying its course has strongly modified this concept (22). The first photogenetic model was the "*immunoallergic theory*" which was based on that observed in mice model of experimental autoimmune encephalomyelitis (EAE). Of note, EAE is induced by the inoculation in mice of myelin-targeted T lymphocyte. Recent studies showed that the unbalance between T lymphocyte subsets is a feature of the MS pathogenesis. Specifically, is has been observed the increase of T helper (Th)-1 and Th17 lymphocytes producing interleukin (IL)-1, interferon γ (IFN- γ) and IL-17 and IL-22, respectively, with proinflammatory effects and BBB permeabilization. This may allow to the entering of cytotoxic T lymphocytes (T CD8+) into CNS causing direct myelin damage. However, resident microglia and astrocytes seem to have a role in the maintaining as well as compartmentalization of the intrathecal inflammation (23). In the following section the role of lymphocytes and microglia has been briefly reviewed.

- *T CD4+lymphocytes:* Th1 lymphocytes produce IFN-γ, a pro-inflammatory cytokine which is able to exacerbate inflammation in experimental model of MS. The target cell of Th1 lymphocytes is microglial cells. They produce pro-inflammatory cytokines such as IL-1 and IFN-γ that promote the activation of microglial cells towards a pro-inflammatory and neurotoxic phenotype called M1-like. Moreover, Th 17 lymphocytes producing IL-17A may promote the disruption of BBB allowing the penetration of autoreactive Th1 and TCD8 into CNS. In addition, the IL-17A receptors is located also on the surface of astrocytes, and this is the reason why pro-inflammatory Th17 cells may also promote astrogliosis and astrocyte degeneration (24).

- *T regulatory lymphocytes (Treg):* they suppress the inflammatory response by producing anti-inflammatory cytokines such as IL-10 and IL-4. Although the role of Treg in the pathogenesis of MS is not completely understood, a dysregulation of these cells, in terms of reduction and/or impaired functioning, has been proposed as further pathogenetic pitfall of MS (25).

- *T CD8+ lymphocytes:* These cells have been found in greater quantities than TCD4 lymphocytes, in both gray and white matter lesions, and they lead to neurotoxicity through the production of granzyme, perforin as well as apoptosis by the interaction between FAS and

FAS-L. They also produce proinflammatory cytokines such as IL-17 and chemotactic factors (e.g., IL-16) for TCD4 allowing the self-sustaining of inflammation (25).

- *B cells:* the neurotoxic action of B lymphocytes is multifaceted. While they can differentiate into plasma cells producing antibodies directed against CNS structures, they also function as antigen-presenting cells to T lymphocytes, activating them and reiterating inflammatory processes. Furthermore, they are capable of generating ectopic meningeal foci, or secondary lymphoid follicles, responsible for maintaining a pro-inflammatory environment within the CNS. Therefore, they not only actively participate to the initial remitting-relapsing phase but their role may be prominent for disease progression (26).

- *Innate immunity:* Among these, mast cells, involved in the permeabilization of the BBB, peripheral macrophages, neutrophils and resident microglia have been implicated in MS pathogenesis (25).

The trafficking of autoreactive lymphocytes from peripheral circulation into CNS has a key role in MS pathogenesis. Accordingly, it has been hypothesized that production of autoreactive T cells in response to unknown antigens or allergens with their subsequent CNS infiltration was the starting point of demyelination. Resident microglia, in turn, shift towards a pro-inflammatory phenotype amplifying the inflammatory processes into CNS (27). However, the pathogenetic model is more complex and is not fully understood. Whilst the lymphocytes infiltration into CNS in a waves fashion from peripheral circulation is underlying the demyelinating attack (MS relapse), the compartmentalization of the inflammation is a key feature of MS progression. From a clinical perspective, the recurrence of inflammatory waves into CNS is underlying the relapsing-remitting RRMS while the compartimentalized inflammation is underlying the SPMS. Accordingly, neuropathological studies showed that active demyelinating lesions in RRMS are enriched by T CD8+ lymphocytes and, in part, by B lymphocytes and plasma cells with prominent demyelination and relative sparing of axons. On the contrary, the progressive phase is characterized by chronic lesions with an inactive core and a microglia and macrophages rich border (28,29). In this case, the number of B cells and plasma cells as well as the axonal loss are higher compared to the relapsing phases. These neuropathological changes are in parallel with the transition from RRMS to progressive MS. Based on these premises, several types of lesions were identified in CNS of patients with MS according the disease phase (30).

- *Active lesions:* characterized by a central core enriched by pro-inflammatory cells including Th1, Th17, B cells, macrophages and activated microglia.

- *Chronic active lesions (CALs):* characterized by an inactive core containing astrocytes and a microglia and macrophages rich border. Two types of CALs have been identified, the paramagnetic rim lesions (PRLs) and slowly expanding lesion (SELs). Whilst the former has an iron-rich border, the latter expand over time. However, both kind of CALs have been associated with faster disease progression (31).

- *Inactive lesions:* have a well-defined border, hypocellular both in the core and border, typical of late MS phases. They are characterized by complete loss of myelin with denuded and atrophic axons, accompanied by reactive astrogliosis. Occasionally, remyelination processes can be observed.

- *Shadow plaque:* they appear after 4-8 weeks from a demyelinating event representing the epiphenomenon of the remyelination process. The remyelination is promoted by protective microglia (M2-like). These cells are able to phagocytose myelin debris as well as to produce neurotrophic factors (32). The remyelination processes are more efficient in subcortical area rather than periventricular and in lesions proximal to neuronal soma (32). It is worth noting that remyelination decreases with increasing resulting more efficient before 55 years of age and within ten years from MS onset (32).

- *Gray matter lesions:* they exhibit a lower degree of inflammation, edema, microglial activation, and macrophage recruitment compared to white matter. Depending their localization, they can be classified into four types: 1) cortico-subcortical junction; 2)intracortical and perivenous; 3) subpial layers of the cortex; 4) involving the entire cortical ribbon.

The neurological impairment is not fully explained by demyelination alone but it appears also related to secondary axonal damage (33). As introduced before, the progressive infiltration of CNS by peripheral lymphocytes alongside with the pro-inflammatory switch of resident microglia lead to compartimentalized inflammation. Specifically, TCD8+ lymphocytes, plasma cells and B cells promote a chronic pro-inflammatory environment at perivascular or meningeal level affecting also the pro-inflammatory response of microglia and astrocytes (34–36). Interestingly, the TCD8+

memory cells undergo repeated activation by target antigen promoting the perpetuation of the inflammation (37). However, the mechanisms underlying the compartmentalization are not understood. According to the surface-in model, it has been proposed pro-inflammatory cytokines (IFNγ, TNFα, LTα e IL-6) contained in cerebrospinal fluid cause meningeal inflammation and cortical damage with the formation of subpial cortical lesion with a decreasing gradient of neuronal damage from ependyma to deep gray matter (34,38–40). Therefore, at this level TCD8+ cells may be constantly activated by EBV-positive B cells (38,41). However, B cells not only may act as antigen presenting cells but they may also produce neurotoxin such as LTα and other with subsequent neuronal damage (42,43). The interplay between meningeal inflammasome and resident microglia would underlie to compartmentalization of the inflammation and chronic CNS damage. Finally, several mechanisms of neurodegeneration have been proposed: 1)mitochondrial damage with impaired axonal transport; 2) neurons apoptosis due to oxidative stress; 3) Wallerian axonal degeneration due to myelin loss; 4) glutamate toxicity; 5) neurotoxic action of complement (34,36,44). Thus, the coexistence of different type of lesions (e.g, active, chronic active, inactive, etc) and in different area of CNS in the same patient and the different lesional pattern between patients are the basis of intra and interindividual variability of MS neuropathology.

1.4. *Clinical features*

The clinical features of MS are heterogeneous and they depend mainly by the localization of CNS damage resulting in a highly interindividual variation. The typical presentation of MS is the attack or relapse characterized by the acute or subacute onset of focal or multifocal neurological symptoms lasting 24h at least not associated with fever or infections followed by partial or total recovery (45). The first demyelinating attack is known as clinically isolated syndrome (CIS). It is worth noting that the entity of recovery decreases over time leading to disability accrual. It is worth noting many CNS lesions are clinically silent due to the involvement of non-eloquent CNS areas and it has been estimated that around ten asymptomatic lesions may be found for each relapse. The most common presenting symptoms are limb paresthesia (43%), optic neuritis (25%), brainstem or cerebellar symptoms (20%), pyramidal tract signs (15%), Lhermitte signs (2%) and sphincters disturbances (1%). However, in 14% of cases the MS onset is multifocal. Rarely, it is possible to find a full compatible magnetic resonance imaging (MRI) finding without clinical symptoms namely radiologically isolated syndrome (RIS). For the first time, four phenotypes of MS were identified by US MS Society in 1996 including RRMS, SPMS, PPMS and progressive-relapsing MS (PRMS). These phenotypes were substantially revised in 2014 with the introduction of CIS and the suppressing

of the PRMS phenotype since it was enclosed within the definition of PPMS (46). At the same time, the progressive forms of MS were divided into active and not active ones (Figure 2).

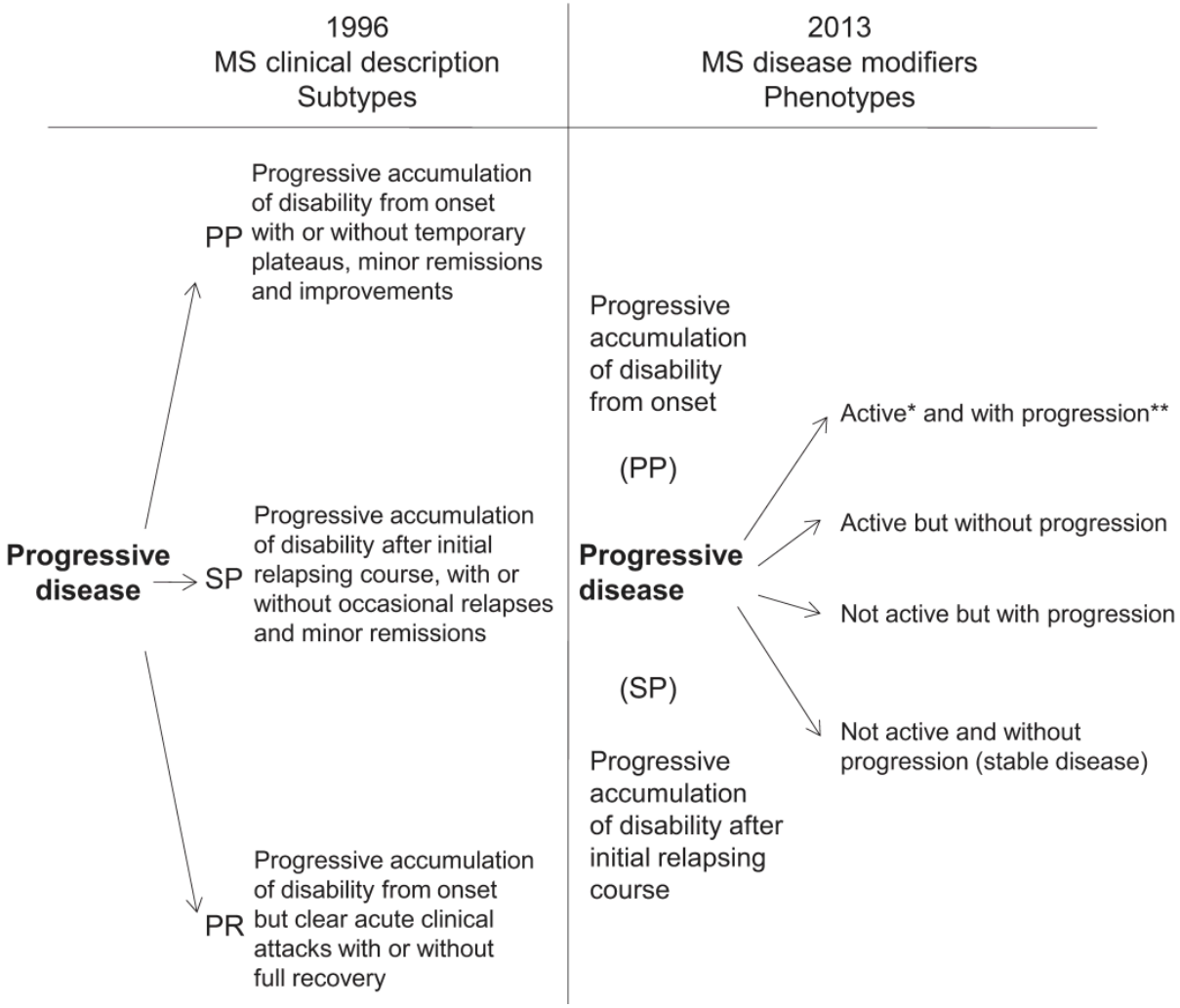

Figure 2 Clinical phenothype of Multiple Sclerosis according to the 2013 revision. Adapted from "Defining the clinical course of Multiple Sclerosis: the 2013 revision", Lublin F et al, 2014.

- *Clinically isolated syndrome (CIS):* this is the first neurological attack highly suggestive of MS. It is characterized by the acute or subacute onset of focal or multifocal neurological symptoms. A high number of T2 brain lesion and the presence of oligoclonal band in CAS are factors that enhance the risk of conversion to MS (47).

- *Relapsing-remitting MS (RRMS):* RRMS is the clinical course in about 85% of patients and it is characterized by the alternance of relapsing and remitting phases (Figure 3). Approximately the 80% of relapses full recovery although this percentage falls over time. It has been estimated that the mean frequency of relapses was 1.5 per year. It is worth noting that a relapse is an unpredictable event with random frequency (47).

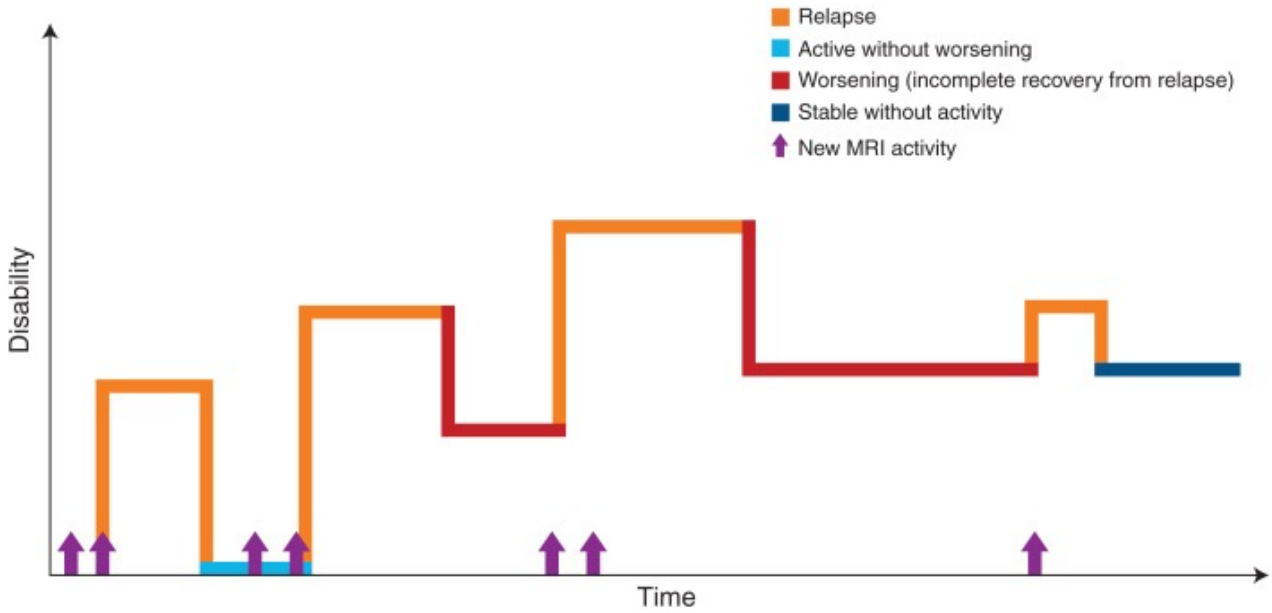

Figure 3 Clinical course of the relapsing-remitting Multiple Sclerosis over time. Adapted from "Clinical Course of Multiple Sclerosis", Klineova S, Lublin F, 2018.

- *Secondary progressive MS (SPMS):* this phase is characterized by the unrelenting and inexorable disability progression over time (Figure 4). It has been estimated that about 50% of MS patients evolve into SPMS after 10-15 years from disease onset. Among others, late onset MS, male sex, higher disability at baseline, higher number of relapses and early involvement of spinal cord are negative prognostic factors that enhance the risk of SPMS conversion (48). Recently, it has been proposed that MS patients acquire disability over time through the accumulation of neurological sequela from relapses (relapse-associated worsening, RAW) or progression independent of relapsing activity (PIRA) (49). However, the two processes are not mutually exclusive and they are both present since the early phases of MS contributing to disease progression and disability accrual over time.

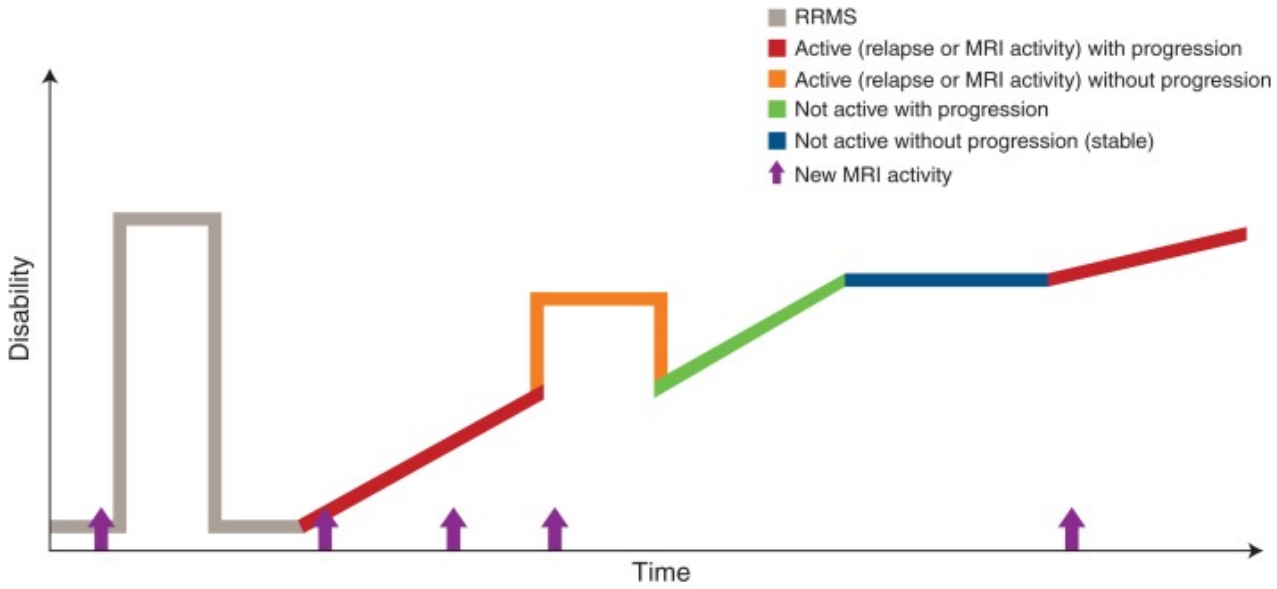

Figure 4 Clinical course of the secondary progressive Multiple Sclerosis over time. Adapted from "Clinical Course of Multiple Sclerosis", Klineova S, Lublin F, 2018.

- *Primary progressive MS (PPMS):* it is characterized by abrupt and unrelenting progression since the MS onset, with or without relapses (Figure 5). Fortunately, it is more rare accounting for about the 5-15% of MS phenotype (50). Although PPMS and SPMS are similar, patients with SMSP usually have a higher number of T2 brain lesion while those with PPMS have a higher frequency of new Gd enhancing lesions (48).

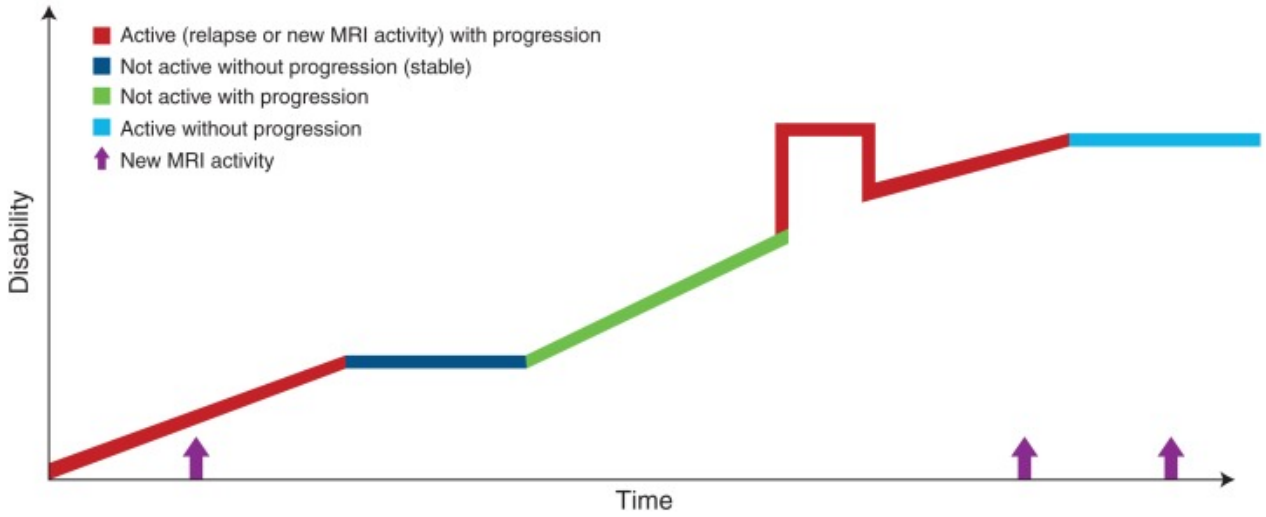

Figure 5 Clinical course of the primary progressive Multiple Sclerosis over time. Adapted from "Clinical Course of Multiple Sclerosis", Klineova S, Lublin F, 2018.

From the pathogenetic perspective, MS could be considered a neurodegenerative disease with a spectrum of clinical manifestation ranging from a prodromic phase to PPMS, RRMS and SPMS depending on the grade and type of CNS involvement (Figure 6) (36).

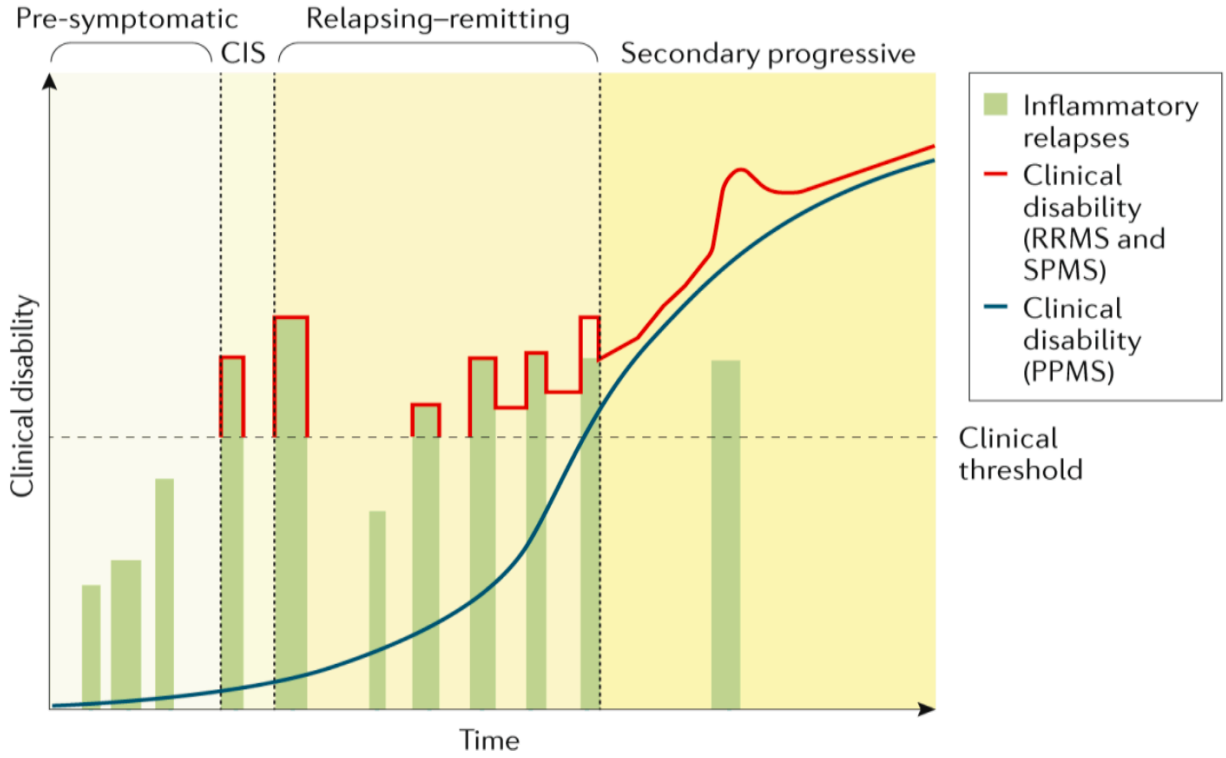

Figure 6 Clinical course of Multiple sclerosis over time. Adapted from Filippi et al. 2018, Nat Rev Dis Primer 2018.

1.5. *Diagnostic criteria*

The diagnosis of MS was classically based on clinical criteria by the demonstration of its core features which are the dissemination on time (DIT) and space (DIS). In the pre-MRI era, the diagnostic criteria required the demonstration of DIT and DIS by the recurrence of clinical relapses indicating the involvement of multiple CNS sites over time (51). Twenty years later, the relevance of oligoclonal band (OCB) was suggested by Poser (52). The development of MRI has given a major contribution in the diagnosis of MS since it allowed a faster recognition of DIT and DIS before the occurrence of new clinical relapses. The role of MRI in the diagnosis of MS by demonstrating DIT and DIT was highlighted since the 2001 McDonald criteria which have been updated over time until the latest version in 2017 (53). According to 2017 McDonald criteria, DIS is demonstrated by the presence of one lesion in T2-weighted imaging (T2-WI) at least in two of typical CNS areas including periventricular, iuxtacortical, infratentorial and spinal cord; DIT is demonstrated by the finding of new T2-WI lesion or the presence of T1 Gd-enhancing lesion or the contemporary presence of both

T2-WI and T1 Gd-enhancing lesion or the presence of oligoclonal band in CSF (53). A brief summary of the 2017 McDonald criteria for the diagnosis of RRMS and PPMS is reported in Table 1.

Table 1 The 2017 McDonald criteria for the diagnosis of RRMS and PPMS

RRMS			
No. attacks	**No. sites**	**Additional data**	**Diagnostics**
≥2	≥2	None	
≥2	1	DIS	One lesion in two typical CNS site on MRI New relapse involving different CNS site
≥1	≥2	DIT	New T2 lesion or T1 Gd enhancing lesion New relapse Presence of OCB in CSF
≥1	1	DIT + DIS	One lesion in two typical CNS site on MRI New T2 lesion or T1 Gd enhancing lesion Presence of OCB in CSF New relapse involving different CNS site
PPMS			
Disability progression within one year from onset regardless relapse activity retrospectively or prospectively assessed plus two out of the additional features.			One lesion in two typical brain sites on MRI Two or more spinal cord lesions on MRI Presence of OCB in CSF

RRMS, relapsing-remitting multiple sclerosis; DIS, dissemination in space; DIT, dissemination in time; CNS, central nervous system; MRI, magnetic resonance imaging; OCB, oligoclonal bands; CSF, cerebrospinal fluid; PPMS, primary progressive multiple sclerosis.

The 2017 McDonald criteria have a sensitivity about 85% although with lower specificity (60%) thus the rate of misdiagnosis is relevant whether they are employed without a strong clinical suspicion (54). The fulfilling of 2017 McDonald criteria doesn't mean that the diagnosis of MS is correct before the exclusion other mimicking disease according the principle of the "no better explanation". On the other hand, the availability of even more accurate MRI machines alongside the formulation of even more sensitive diagnostic criteria allowed the reduction of diagnostic delay over time as well as the level of disability at diagnosis (55).

1.6. Evaluation and prognosis

Patients with MS usually undergo longitudinal assessments of disability through the calculation of the Expanded Disability Status Scale (EDSS), published in 1983 by Kurtzke (56). To date the EDSS is the most common measure of neurological impairment due to MS worldwide and is employed to estimate disability progression in clinical practice as well as in clinical trial. The EDSS is a composite score based on clinical examination of eight functional system score (FSS): visual, pyramidal, brainstem, cerebellar, sensory, bowel and bladder, mental and ambulation. Depending the neurological examination, each FSS may be scored from 0 to 5 resulting than in the final EDSS which is not however the simple sum of each FSS grade. The EDSS ranges from 0 (all FSS equal to 0) to 10 (death due to MS) and provides several intermediate steps indicating an increasing level of disability as shown in Figure 7.

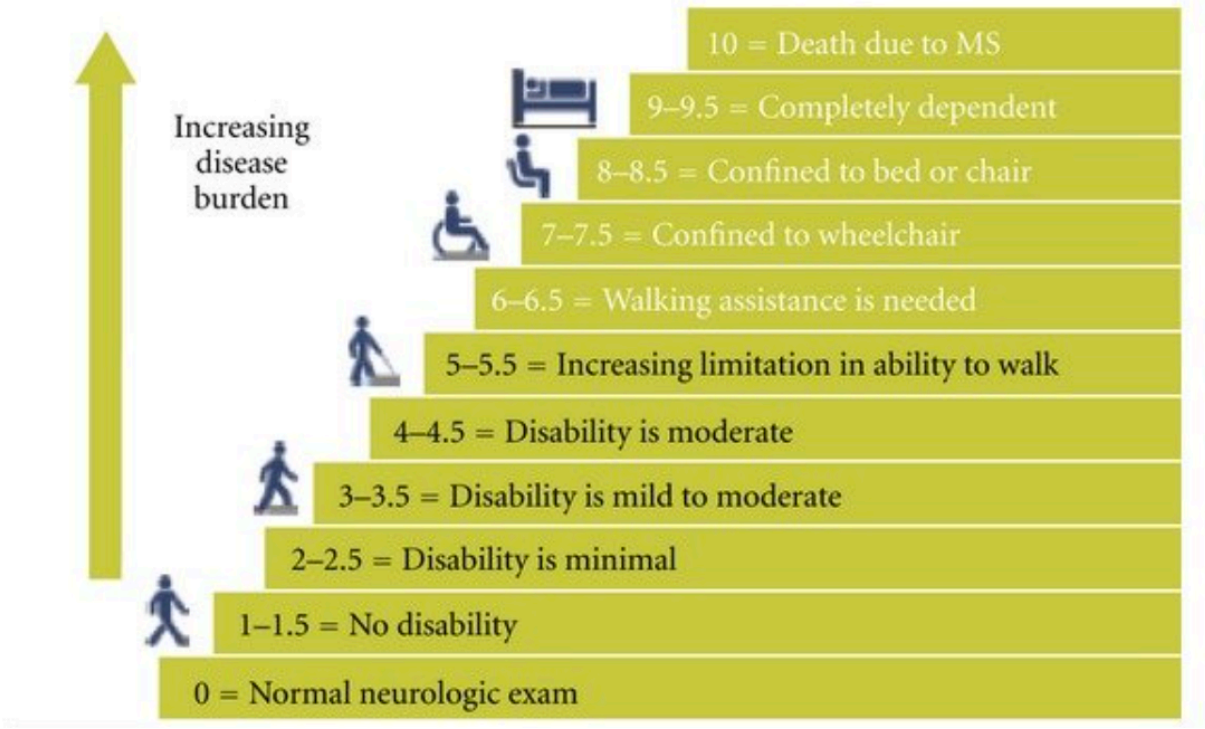

Figure 7 Schematic representation of the main step of Expanded Disability Status Scale. Adapted from "Theranostic Implications of Nanotechnology in Multiple Sclerosis: A Future Perspective".

The limitations of EDSS are the interoperator variability, a limited sensitivity for cognitive impairment and its heavy weighting on walking ability. Several clinical factors may affect negatively MS prognosis including male sex, late onset MS, progressive course from onset, early spinal cord and/or brainstem involvement, poor recovery from relapses and chronic comorbidities (57,58). More recently, some MRI findings such as brain or spinal cord atrophy, higher number of black hole and presence of CALs have been associated with a worse prognosis (59)

2. THERAPIES

The development of a curative treatment of MS has been hindered by the lack of defined etiology and an uncertain pathogenesis. To date, the goals of therapies are to achieve a full recovery from a relapse, to prevent the occurrence of new relapses as well as to slow disease progression and disability accrual. In this perspective, disease modifying treatments (DMTs) including immunosuppressant and immunomodulant drugs are able to modify MS course reducing the occurrence of new CNS lesions, relapses and disability accrual (60). On the other hand, corticosteroids are commonly employed to counteract the acute phase of a relapse favouring a good and prompt recovery.

2.1. *Therapy of the acute attack*

The prompt infusion of intravenous methylprednisolone is the gold standard therapy for the treatment of MS attack. Corticosteroids reduce the entity of clinical attack by exerting a powerful anti-inflammatory effect and recovering of BBB permeability. The standard of care is the administration of intravenous methylprednisolone at the dose of 1000mg daily for 5 days with or without tapering (61,62). Therapeutical plasma exchange or immunoglobulin should be taken into account in the cases of steroid-refractory or highly severe attacks (23,63).

2.2. *Disease modifying treatments*

To date several DMTs have been approved for the treatment of MS and they are divided into first- and second-line therapies according their efficacy. Several drug agencies including Italian one recommends the use of DMTs in an escalating strategy, thus employing the second line after the failure of the first line therapies (64). However, it is well known that the early intervention with high-efficacy DMTs (HE-DMTs) may represent the best window of opportunity to delay irreversible central nervous system damage and MS-related disability progression (65). Considering the neuropathological changes over time in patients with MS (e.g., compartimentalized inflammation), it is not surprising that the early intervention with HE-DMTs is more convenient than the use of first line immunosuppressants. It is worth noting that the frequency of adverse events related to immunosuppression (e.g., infections) increase with the increase of DMT power making the patient's safety another relevant aspect of the MS treatment algorithm. In the next section a brief overview of available first- and second-line therapies is provided.

- *Interferon-beta (IFN-β1a):* it was the first specific DMT approved for the treatment of MS in 1993 by Food and Drug Administration (FDA) followed by IFN-β-1b and peghilated IFN-β-1a. The interferon compounds have been employed for decades in the treatment of MS despite

their mechanism of action is almost not understood. Despite they did not change significantly the natural history of MS, some patients showed a good response to interferons namely good responder probably due to genetic background (66,67).

- *Glatiramer acetate:* it is a peptide mix mimicking the myelin composition. It is mechanism of action is to act as false target for autoreactive cells favouring the lymphocytes shifting toward Th2 phenotype. Although it reduces the relapse rate, it has a modest impact on MS course (60).

- *Dimethyl-fumarate:* the precise mechanism of action of DMF is unknown although it is able to activate the erythroid-derived nuclear factor 2 (Nrf2) which, in turn, suppresses the activation of transcriptional factor Nf-kB exerting anti-inflammatory and neuroprotective effect. Body flushing, nausea, diarrhea and abdominal pain are common side effects while rare cases of progressive multifocal leukoencephalopathy have been reported (60).

- *Teriflunomide:* it acts as reversible inhibitor of dihydroorotate dehydrogenase, reducing the pyrimidine synthesis and the proliferation of T and B cells as consequence. Thus, teriflunomide is an immunosuppressant. Commonly reported side effects include increases of liver enzymes, hypertension, cough, dyspnea and leukopenia. It is worth noting that is a teratogenic drug (60).

- *Natalizumab (NTZ):* is a humanized monoclonal antibody targeting the α4β1 integrin expressed on the surface of lymphocytes inhibiting their infiltration into CNS. NTZ was the first monoclonal antibody for the treatment of MS and it changed the natural history of the disease by dramatically reducing the relapsing rate, the increasing of brain lesion as well as the disease progression (68). However, the treatment with NTZ is associated to higher risk of PML due to its immunosuppressive effect on CNS. The risk factors of PML as well as the MRI monitoring strategies are explored in the next section.

- *Sphingosine 1-phosphate receptors modulators (S1PRm):* the mechanism of action of S1PRm is through binding S1PR subtype 1 on lymphocytes resulting in an internalization of lymphocyte into lymph nodes. The reduction of circulating lymphocytes presumably limits the inflammatory cell migration into CNS (69). Four S1PRm have been approved for MS including Fingolimod, Siponimod, Ozanimod and Ponesimod. Fingolimod was the first oral

HE-DMT and compared to placebo it reduced the relapse rate up to 55-60% (70). Of note, Fingolimod is the only DMT approved for the treatment of pediatric MS in Italy (71). Siponimod is the only DMT together with Ocrelizumab which has been approved for the treatment of patients with active SPMS since it reduced the disability progression in these patients (60,72). Ozanimod share the same receptor selectivity with Siponimod although it has been approved for the treatment of RRMS and Chron disease being a good choice in the case of that comorbidity. The last approved S1PRm is Ponesimod which acts exclusively on S1PR limiting thus the side effects of other S1PRm, especially cardiovascular ones (73). However, S1PRm share the same side effects including moderate to severe leukopenia, atrioventricular conduction block and infection (e.g., Varicella Zoster Virus).

- *Ocrelizumab:* is a humanized anti-CD20 mAb administered every six months via intravenous route. It targets mature B cells exerting mainly an antibody-dependent cellular toxicity. Ocrelizumab strongly reduces the number of relapses, the accumulation of new CNS lesion as well as disease progression. To date, is the only drug approved for the treatment of active PPMS and SPMS (60).

- *Ofatumumab:* is a fully human anti-CD20 monoclonal antibodies administered once per month via subcutaneous route. It mechanism of action is quite different compared to ocrelizumab since it binds two different epitopes of CD20 killing the B cell via both complement activation and antibody-dependent cellular cytotoxicity. It is a highly effective DMT with a favorable safety profile (74).

Despite several DMTs are available and recent evidence are supporting the early use of HE-DMTs, many drug agencies recommend the use of an escalation therapeutical strategy. However, the first goal of neurologists is to prevent the disability accrual since the first phases of the MS maintaining a good safety profile at the same time. A possible solution to overlook these issues is to custom the treatment according to individual features of the patient (Figure 8) (60)

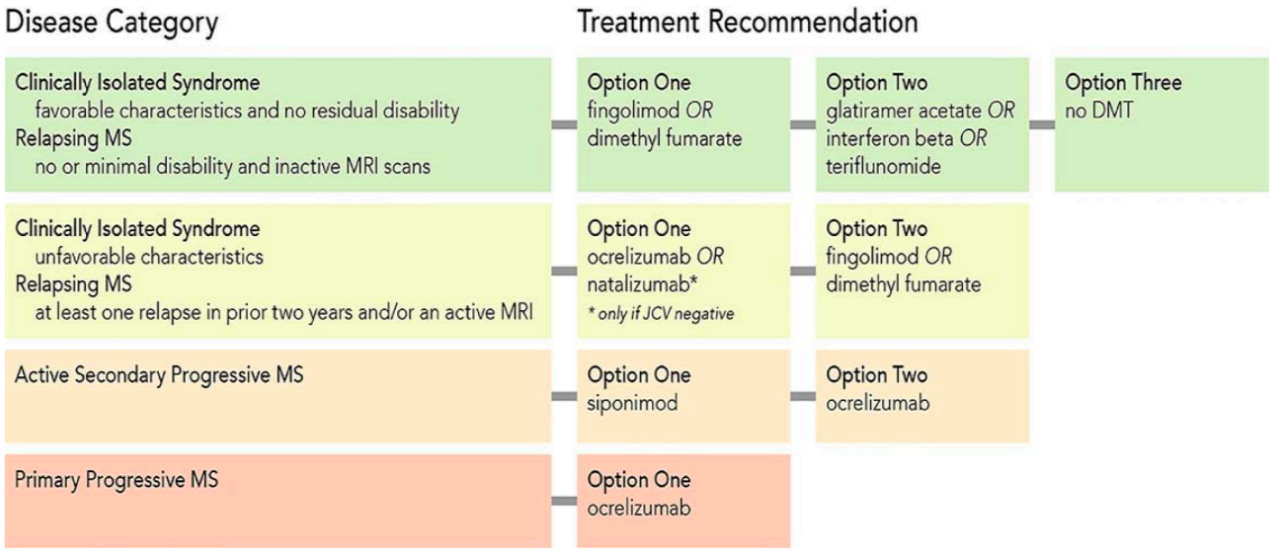

Figure 8 Recommendations for the use of disease modifying treatment according to MS clinical. Adapted from Hauser et al 2020.

2.3. *Symptomatic treatment*

Patients with MS usually experience annoying symptoms which are not under control of DMTs such as subtle cognitive changes, urinary disturbances, pain, fatigue, and spasticity. These symptoms significantly affect the activity of daily of living of pwMS reducing their quality of life. Of note, spasticity is one of the most common disabling symptoms in MS patients (40-84%) affecting mobility and ambulation (75). A lot of symptomatic drugs are employed to counteract these symptoms such as anticholinergic drugs, anticonvulsant against neuropathic pain (e.g., gabapentin, pregabalin) and antispastic drugs such as baclofen (45)

3. MAGNETIC RESONANCE IMAGING IN MULTIPLE SCLEROSIS

3.1. *Role of MRI in multiple sclerosis*

The evidence supporting the use of brain MRI for MS diagnosis originates from the first application of MRI in patients with MS by Young et al. in 1981 (76). Interestingly, they found that MRI detected a higher number of MS plaques compared to computed tomography (76). Since its introduction, the clinical applications of MRI have increased over time alongside the advancement of technology and the development of MS-specific sequences. MRI has become the most important tool for the diagnosis and monitoring of MS. Interestingly, the role of brain and spinal MRI in the diagnosis of MS has been officially recognized with the introduction of 2001 McDonald criteria as they provided the use of MRI for the detection of DIS and DIT (77). It has been established the type of mandatory MRI sequences for MS diagnosis are the T2-weighted, fluid attenuated inversion recovery (FLAIR), non-enhanced T1-weighted imaging (T1-WI) and T1-WI with gadolinium-based contrast agents (GBCAs) administration at the magnetic field of 1.5T. The use of MRI has gained further relevance with the introduction of 2017 McDonald criteria (53). Moreover, the central vein sign (CVS) has been proposed as novel MRI biomarker to improve sensitivity and specificity of MRI in distinguishing MS from other mimics (78). Even if the CVS has not been included in latest MS diagnostic criteria, its evaluation through dedicated sequences (e.g., gradient echo) is recommended (79,80). Nevertheless, the utility of MRI stems from its sensitivity to longitudinal changes including those in overt lesions and, with advanced MRI techniques, in normal-appearing brain tissue. Conventional MRI techniques, including lesion detection and measurement of atrophy from T1- or T2-weighted images, have been the mainstay for monitoring disease activity in clinical trials, in which the use of gadolinium with T1-weighted images adds additional sensitivity and specificity for areas of acute inflammation (81). Other relevant application of MRI could be the detection of CALs. It has been shown that the number and the type of CALs is a negative prognostic factor making their longitudinal characterization relevant for the estimation of MS prognosis. However, this requires significant efforts from radiologists as well as the use of specific sequencies such as the susceptibility weighted imaging (82). It is worth noting that powerful magnets (e.g., 3T and 7T) and advanced sequences have higher costs and usually their use is limited to University Hospitals. To standardize the use of MRI in MS, in 2021 the Magnetic Resonance Imaging in Multiple Sclerosis (MAGNIMS) and the Consortium of Multiple Sclerosis Centers (CMSC) published the recommendations on the use of MRI in patients with MS (83). These include he use at diagnostic purpose as well as monitoring treatment effectiveness and drug safety (83). Despite the recommendation of MAGNIMS, the use of MRI is still heterogeneous across different MS clinics especially in particularly conditions which are poor defined by guidelines.

3.2. *The risk of PML*

The increasing number of DMTs approved for the treatment of MS has led to the need of standardized MRI-monitoring strategy to assess the treatment effectiveness (84). Whilst the achievement of the highest anti-inflammatory effect is the mainstay of MS treatment, on the other hand, the use of DMTs with higher impact on immune system raised several safety concerns. Accordingly, the spectrum of DMT-related adverse events is wide ranging from vascular diseases, CNS tumor and opportunistic infection (85,86). Of note, PML is a well-known, rare, adverse event of the treatment with NTZ despite its occurrence has been reported also during the treatment with other DMTs such as Fingolimod, Dimethyl-fumarate and Alemtuzumab (87–89). PML is a rare infection of the CNS caused by the John Cunningham Virus (JCV) which may have fatal consequences or neurological sequala in 20 % and 40%, respectively, of those affected (90). The risk of PML during NTZ treatment has been largely investigated in the last years. This PML-risk is higher in the case of positive JCV serum status, duration of NTZ treatment >24 months and prior use of immunosuppressive therapies (90). The classical MRI finding of PML are the presence of multifocal demyelinating lesions of the deep white matter that may mimic the occurrence of new MS lesions. In early stages, around the 48% of PML lesions originate in the frontal lobe and in most cases are unilobar with a progressive enlarging over time (91). PML lesions shows high signal intensity in diffusion-weighted imaging (DWI) with a not corresponded low signal in apparent coefficient diffusion (ADC) imaging suggesting that these lesions are resulting from intracellular oedema. Contrast-enhancement can be observed in 30%−40% of the patients in the early natalizumab-associated PML stages suggesting inflammatory PML characteristics (91). Within and near to the main PML lesion, small T2-lesions with a microcystic appearance may be observed with a star-like distribution pattern described as “milky way” appearance (92). Usually, lesion expands over time, often becoming confluent, with the involvement of corpus callosum, cortico-spinal tract and superior longitudinal fasciculus and posterior fossa. This massive irreversible demyelination which is promoted by the infection of oligodendrocytes and astrocytes lead to neurodegeneration with fatal outcome within weeks or months (92). Several strategies have been investigated to counteract the risk of PML. Firstly, patients with positive JCV serum antibody after two years of NTZ undergo to extended interval dosing (EID), thus receiving NTZ every 6 instead 4 weeks with a reduction of PML risk but with unchanged efficacy (93). Secondly, an intensive MRI-monitoring protocol is suggested in pwMS at higher risk of PML consisting to perform a brain MRI scan every 3-4 months with the aim to reveal PML as early as possible in order to achieve a better outcome (94) (95). However, the 2021 MAGMIMS guidelines, stated that the administration of GBCAs should be only provided in the case of PML suspicion as well as to monitor PML lesions over time.

3.3. Gadolinium-based contrast agents

GBCAs were introduced in 1988 to enhance the parenchymal MRI contrast to improve the detection and characterization of CNS lesions. It has been estimated that 750 million doses have been administrated up to 2023 and around 40% of these have used in neuroradiology (96). GBCAs contain the trivalent Gd ion (Gd^{3+}), a strong ferromagnet metal belonging to lanthanides, which shortens the T1 and T2 relaxation time increasing the signal intensity of T1-WI. It is worth noting that the unchelated Gd^{3+} ions are highly toxic due to its capacity to bind calcium ions interfering with the calcium-mediated biological processes (96). Thus, Gd^{3+} is enclosed within an organic ligand in GBCA preventing its free releasing in human tissues. GBCAs may be distinguished in ionic and non-ionic as well as in linear and macrocyclic ones according their chemical structure. While linear GBCAs are characterized by flexible and open-chain ligands surrounding the Gd^{3+} ion, macrocyclic GBCAs provides a more rigid and encapsulation of Gd^{3+} iones (97). From this perspective, linear GBCAs are less stable and are more prone to release Gd^{3+} ions subsequently (98). On the other hand, GBCAs may be classified as ionic (i.e, electrically charged and interact with other opposite-charged ions) and non-ionic (i.e., electrically neutral). However, this ionic property would not seem to affect the GBCAs stability. Conversely, two chemical parameters may affect GBCAs stability: 1) thermodynamic stability, which is influenced by tissues pH; 2) kinetic inertness indicating how fast the GBCAs disaggregates. Thus, the dissociation of Gd^{3+} from GBCAs depends on chemical and physical properties of the chelating agents as well as by tissue chemical characteristics. In this perspective, macrocyclic GBCAs agent with a more solid structure and higher kinetic inertness may have higher stability in vivo compared to other ones (99). In Europe, several GBCAs both macrocyclic (Gadobutrol, Gadoterate, Gadoteridol) and linear (Gadodiamide, Gadopentetate, Gadobenate, Gadoxetate) have been commercialized as shown in Table 2. Despite the different concentration of Gd^{3+} in various GBCAs (Table 2), the amount of pure Gd^{3+} administered per each MRI scan is the same for each GBCA (0.1 mmol/kg) and it depends on the patient's weight.

Table 2. List of linear and macrocyclic GBCAs, their concentration in commercial formulation and their indicated dosage for central nervous system investigation

Linear GBCA	Gd (mmol/ml)	Gd mg/ml	Dose ml/kg
Gadodiamide (Omniscan®)	0.5	78.6	0.2
Gadopentetate (Magnevist®)	0.5	78.6	0.2
Gadobenate (Multihance®)	0.5	78.6	0.2
Gadoxetate (Primovist®)	0.25	39.4	0.4

Macrocyclic GBCA			
Gadobutrol (Gadovist®)	1.0	157,2	0.1
Gadoterate (Dotarem®, Dotagraf®, Claricyclic®)	0.5	78.6	0.2
Gadoteridol (ProHance®)	0.5	78.6	0.2

Gd, gadolinium; GBCAs, gadolinium-based contrast agents.

3.4. Gadolinium clearance and retention

The first evidence of GBCAs toxicity was provided in 2006 by the report of Marckmann et al. that described the nephrogenic systemic fibrosis (NSF) as consequence of GBCAs administration in patients with severe renal impairment (100). GBCAs were designed for rapid renal excretion even if their in-vivo behavior depends on chelating agent stability and tissues biological properties. GBCAs have a wide distribution to extracellular volume and their elimination is mainly renal. Both linear and macrocyclic GBCAs have a half elimination life lesser than 2h and the 95% of the GBCA is completely cleared by the kidney after 12h. However, a small amount of Gd^{3+} may have a deeper distribution with a long-lasting residual excretion which is faster for macrocyclic compared to linear GBCAs (101). This difference in long-lasting excretion is correlated to higher chemical stability and lower rate of transmetallation of macrocyclic GBCAs. Accordingly, it has been shown that the tissue releasing of Gd^{3+} is higher for linear GBCAs (20%) compared to macrocyclic ones (0.1%) (98). Recently, Gd^{3+} ions from both linear and macrocyclic GBCAs were found into three different forms in rats including intact chelate, free Gd^{3+} and aggregate to macromolecules (102). Thus, it is clear that the process of Gd^{3+} deposition in human tissues is multifaceted and may include several mechanisms: 1) transmetallation; 2) acidic dissociation in lysosomes; 3) in-vivo generation of Gd-containing nanoparticles. Through a chemical reaction known as transmetallation, the Gd^{3+} ions may be exchanged with other metal ions (e.g., Zn^{2+}, Cu^{2+}, Fe^{3+}, Ca^{2+}) with the subsequent release of free and toxic Gd^{3+} (103). It is worth noting that stable GBCAs may not cross the BBB and they reach the CSF though the choroid plexus and the brain tissue via the glymphatic system alongside perineural sheaths and perivascular spaces (104). It has been hypothesized that transmetallation between Gd^{3+} and other metals such as Zn^{2+}, Cu^{2+} and Fe^{3+} take place in the extravascular space. Thus, the glymphatic system may have a central role in the Gd clearance since may serve as pathway for its deposition (105,106). Several factors may affect transmetallation such as chemical stability, exposure duration, concentration of competing metals and chemical properties of the tissues. Based on the premises, it is not surprising that transmetallation is increased for linear GBCAs (e.g., less stable) or in patients with impaired renal function (e.g., prolonged exposition) or in metal-enriched tissues (107,108). Interestingly, the accumulation of Gd^{3+} in dentati nuclei (DN) and globi pallidi (GP) might

further be explained by the increased metal content in these areas, facilitating transmetallation. The acidic dissociation is another mechanism which may explain the Gd deposition in specific cellular compartments such as lysosomes. Since the chemical stability of GBCAs decrease with decreasing pH of tissue, linear GBCAs with lower kinetic inertness may be more prone to acidic-driven dissociation compared to macrocyclic ones (109). It is worth noting that precipitated Gd^{3+} does not cause T1-shortening at brain MRI thus other mechanisms of its deposition should be taken into account. Accordingly, some authors suggested the generation of insoluble Gd-containing nanoparticles which may occur for both linear and macrocyclic GBCAs (110). Recently, Henderson et al. showed that both linear and macrocyclic GBCAs can dechelate and precipitate as gadolinium oxalate in an acidic environment; this was confirmed also for macrocyclic GBCAs especially in the presence of proteins and acid tissue pH (111). It is worth noting that other endogenous anions such as phosphate and citrate may promote Gd^{3+} precipitation. This mechanism offers a plausible explanation of Gd^{3+} deposition beyond just transmetallation suggesting that also macrocyclic GBCAs may dechelate in specific conditions. Regardless the mechanism through Gd^{3+} accumulates into human tissues, it may activate several downstream pathogenetic pathways. Firstly, free Gd^{3+} may interfere the calcium-dependent biological process (e.g., ion channels, cascade signalling, etc) directly disrupting several cellular functions (103,112). Secondly, the deposition of Gd may activate a local pro-inflammatory response promoting tissue fibrosis. Thirdly, Gd deposits may enhance oxidative stress with mitochondrial dysfunction and apoptosis. Finally, Gd-containing nanoparticles may exert a distinct toxicity effect by interacting with cells membrane or act as reservoir for gradual Gd release (97).The proposed mechanism of tissue Gd deposition are summarized in Figure 9.

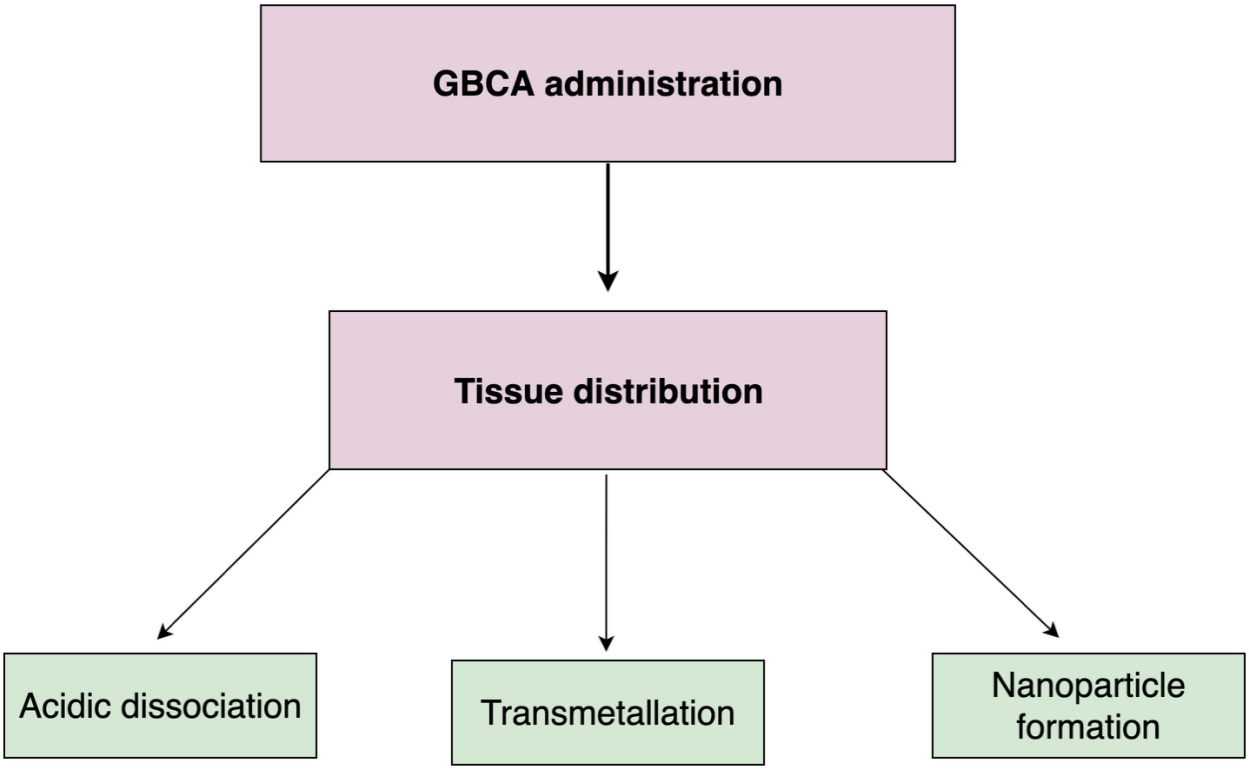

Figure 9 Mechanisms of gadolinium deposition in human tissues. GBCA, gadolinium-based contrast agents. Created with GitMind.

3.5. Brain gadolinium deposition

The first study reporting the association between neuroradiological abnormal findings and the exposition to GBCAs has been published in 2014. Kanda et al. reported a linear, positive, correlation between the T1-WI signal intensity of GP and DN with the number of GBCAs administrated in 19 patients regardless the renal function (113). The cohort of Kanda et al. did not include pwMS. Interestingly, six years before the study of Kanda et al., some authors found that the 19.3% of a cohort of 119 pwMS had hyperintensity of DN on unenhanced T1-WI (114). However, authors interpreted those radiological findings as epiphenomenon of MS progression since they were associated with progressive course, higher EDSS and higher brain atrophy (114). At the end of 2014, a positive association was demonstrated between the increase of T1-WI signal intensity of DN and the number of administrated doses of gadodiamide in pwMS even if the clinical consequences were not investigated (115). Since the first reports, a lot of animal and retrospective human studies have investigated the effect of GBCAs exposition in brain tissue. Interestingly, the use of linear GBCAs has been associated to Gd deposition in rat and dog brains in a dose-dependent manner regardless the presence of renal dysfunction, especially in DN and GP (116–120). In addition, Gd deposits were found in pulvinar, pons, frontal lobe cortex and white matter, cerebellum and pituitary gland (116,121,122). Notably, Gd deposition reached higher concentration in active inflamed area of mouse

brain (123). Whilst brain deposits of Gd and macromolecules have been found for linear GBCAs, only traces of intact chelated have been found for macrocyclic ones with complete wash-out over time suggesting that more stable Gd compounds (macrocyclic GBCAs) are completely cleared rather than linear GBCA (124,125). Most of the published studies were focused on signal intensity changes in the DN providing the evidence that 1)linear GBCAs are correlated with a T1-WI signal intensity increase of DN; 2) non-ionic linear GBCA (i.e., gadodiamide) causes a stronger T1-WI signal intensity increase than ionic linear GBCAs (i.e., gadopentetate and gadobenate); 3) macrocyclic GBCAs are less or not associated with T1-WI signal intensity increase of DN and GP compared to linear GBCAs. However, the reason why Gd accumulates in specific brain regions such as GP and DN is intriguing. This may depend from the structural anatomy of these structures in terms of vascularization and/or by the presence of an environment rich in metal ions making these structures prone to transmetallation and dechelation. In rat brain three chemical form of Gd were found including intact GBCA, insoluble Gd salt and Gd bound to endogenous macromolecules (126). Whilst intact GBCA was found for both linear and macrocyclic GBCAs, the remaining compounds were found only after the administration of linear GBCAs. More specifically, complexes of Gd^{3+} with ferritin and other endogenous molecules as well as in the form of amorphous structures and insoluble salt with calcium and phosphate were found in rats after the exposure to gadobenate and gadodiamide (127,128). Given that precipitated Gd^{3+} is not responsible for any change in MRI signal, it is plausible that Gd bound to macromolecules is responsible for the signal increase in T1-WI (129). Accordingly, in the majority of studies, macrocyclic GBCAs did not lead to visible signal change on T1-WI indicating that linear GBCAs promote the formation of tissue deposits by the precipitation of Gd and endogenous molecules which are responsible detectable hyperintensity in T1-WI (96). Regardless the mechanism of deposition, it has been well documented that the Gd brain deposition was more common following the administration of linear GBCAs rather than macrocyclic ones in animal models. Neverthless, the findings concerning macrocyclic GBCAs are limited compared linear ones and often conflicting. A brief overview of the published studies exploring the association between GBCAs administration and Gd brain deposition in animal models is reported in Table 3.

Table 3. Animal studies exploring the Gd deposition in brain tissue

Linear GBCA		**Reference**
Gadodiamide	Hyperintensity in DN and GP on T1-WI	(130–137)
	Gd found as intact chelate, soluble and insoluble forms	(129)
	25-40% washout of brain within 12 months	(125,138)

	Higher T1-WI changes in DN than macrocyclic GBCA	(139)
	No increase in Gd levels after radiotherapy	(140)
	Persistent hyperintensity in DN and GP after 12 months	(125,138)
	No ultrastructural or metabolic changes	(130,132,133,141)
Gadopentetate	Normal T1-WI signal intensity of DN and GP	(135)
	Increase of T1-WI signal intensity of DN and GP	(134,137)
	10-40% washout of brain within 12 months	(142)
	No increase in Gd brain levels after radiotherapy	(140)
	Increased Gd levels after brain inflammation	(143)
	Gd found as intact chelate, soluble and insoluble forms	(129)
Gadobenate	Gd found as intact chelate, soluble and insoluble forms	(129)
	Higher T1-WI changes in DN than macrocyclic GBCA	(139)
	Hyperintensity in DN and GP on T1-WI	(119,120,139,144)
	Increased Gd levels after abdominal sepsis	(136)
Gadoxetate	Normal T1-WI signal intensity of DN and GP	(145)
Macrocyclic GBCA		
Gadobutrol	Normal T1-WI finding of DN and GP in adult and children	(135,146)
	More than 85% washout of brain within 12 months	(142)
	No detectable Gd levels in brain	(144)
	Gd only found as intact chelate	(129)
	Higher Gd brain level compared to Gadoteridol	(147–149)
Gadoterate	Gd only found as intact chelate	(134,135,150,151)
	More than 85% washout of brain within 12 months	(142)
	No detectable Gd levels in brain	(144)
	Higher Gd level in brain compared to Gadoteridol	(147–149)
	Normal T1-WI signal intensity of DN and GP	(129)
Gadoteridol	Gd only found as intact chelate	(128)
	Minimum T1-WI signal intensity changes of DN	(139)
	No detectable Gd levels in brain	(144)
	More than 65% washout of brain within 12 months	(142)
	Lower Gd level in brain compared to other macrocyclic	(147–149)

GBCAs, gadolinium-based contrast agents; Gd, gadolinium; DN, dentati nuclei; GP, globi pallidi; WI, weighted imaging.

All the information concerning the association between GBCAs administration and brain deposition in humans come from indirect finding from observational and retrospective studies. In Table 4 are listed the current evidence of the association between GBCAs and brain Gd deposition in humans.

Table 4 Human studies exploring the Gd deposition in brain tissue

Linear GBCA		**References**
Gadodiamide	T1-WI hyperintensity of DN and GP	(113,152–154)
	T1-WI hyperintensity of anterior pituitary gland	(155,156)
	Normal T1-WI signal intensity of DN after radiotherapy	(157)
	Increased T1WI signal intensity thalamus, DN, GP, RN, SN, CP	(158)
Gadopentetate	Hyperintensity in DN and GP on T1-WI in adult and children	(146,159–162)
	Hyperintensity in DN in patients with MS	(163)
	Increase T1-WI signal intensity of thalamus, SN, RN, CP, DN, GP	(158)
	Increase T1-WI signal intensity in whole GM, thalamus, DN, GP	(164)
Gadobenate	T1-WI hyperintensity of DN and GP	(159,162,165)
	Increase T1-WI signal intensity of thalamus, SN, RN, CP, DN, GP	(158)
	Increase T1-WI signal intensity of DN and GP in children after radiochemotherapy	(166)
Gadoxetate	Signal increase in DN but not in GP on T1-WI	(167)
Macrocyclic GBCA		
Gadobutrol	Normal T1-WI signal intensity of DN in MS patient after 22 MRI	(168)
	Normal T1-WI signal intensity of DN in pwMS	(163)
	Normal T1-WI signal intensity of DN and GP in pwMS and tumors	(162)
	Increase T1-WI signal intensity of DN and GP in pwMS	(169,170)
	Normal R1 relaxometry finding of DN	(168,171)
	Increase brain Gd accumulation following radiotherapy	(172)
	Increased magnetic susceptibility in GP and DN evaluated by QSM	(173,174)
Gadoterate	Normal T1-WI signal intensity of DN and GP in pwMS and tumor	(162)
	Increase T1-WI signal intensity in DN and GP in pwMS	(170)
Gadoteridol	No evidence of Gd retention in women undergoing breast MRI	(175)

GBCAs, gadolinium-based contrast agents; Gd, gadolinium; DN, dentati nuclei; GP, globi pallidi; SN, substantia nigra; RN, red nucleus; CP, cerebellar peduncle; WI, weighted imaging; MRI, magnetic resonance imaging; pwMS, patients with MS. QSM, quantitative susceptibility mapping

As reported in Table 4, the toxic properties of linear GBCAs have been well documented while the finding about macrocyclic GBCAs are conflicting. However, Gadobutrol showed a stronger association with T1-WI signal changes compared to other macrocyclic GBCAs but this has never been confirmed to date.

4. MATERIALS AND METHODS

4.1. Objective

To explore the frequency of brain Gd deposition and its neurological clinical correlates in a cohort of pwMS treated with Natalizumab who underwent a long-term MRI monitoring follow-up for PML-risk surveillance. The primary analysis aims to explore frequency and localization of brain Gd deposits in a cohort of pwMS as well as the critical thresholds of Gd enhanced-MRI number and cumulative Gd dose associated with the presence of Gd deposition in DN and GP. The secondary analyses aim to explore: 1)whether the presence of brain Gd deposition is associated with parkinsonism evaluated by the Unified Parkinson's Disease Rating Scale part III (UPDRS-III); 2) whether presence of brain Gd deposition is associated with changes in the symbol digit modalities test (SDMT); 3) association between cumulative Gd dose and renal function.

4.2. Study design and participants

This is a cross-sectional and retrospective study including patients attending to the MS clinic of the Hospital Fondazione Istituto G. Giglio, Cefalù, Palermo, Italy. The study inclusion criteria were to have: 1) a diagnosis of MS; 2) a history ≥ 1 year of NTZ treatment 3) an MRI follow-up history in Cefalù Hospital. Patients with lacking data or/and those who received less than 12 NTZ infusions or/and those who were lost to follow-up or/and who did not perform MRI at the Cefalù Hospital were excluded.

4.3. MRI data acquisition

All patients underwent the standard MRI acquisition protocol for MS that included T1-WI, T2-WI, T2-FLAIR, DWI, ADC and GBCA-enhanced T1-WI. All MR examinations were performed on a Philips Achieva 1.5-T system (Philips Medical Systems, Best, The Netherlands) and on a General Electric (GE) Signa 1.5-T scanner (Milwaukee, WI). A 16-channel SENSE neurovascular coil was used as receiver coil. Imaging sequences included: T2 sequence in axial and sagittal plane, T1 sequence in axial plane with and without intravenous GBCAs injection, axial Diffusion-Weighted Imaging (DWI) with a b-value of at 1000 s/mm^2, 3D Fluid-Attenuated Inversion Recovery (FLAIR) with fat saturation (Fat Sat) (1mm, gap of 0, isotropic voxel), acquisition in the sagittal plane, 3D gadolinium-enhanced T1-weighted spin echo (SE) with fat saturation (1mm, gap of 0, isotropic voxel) acquisition in the sagittal plane. All enhanced-MRI were performed by the administration of the standard dose of 0.1 mmol/kg of Gd (15.72mg/kg), regardless the type of GBCAs. The scheduled frequency of monitoring MRI ranged between 3 and 6 months according to JCV serum status and the

duration of NTZ treatment. All the MRI scans were performed at Fondazione Istituto G. Giglio, Cefalù, and they were archived into the electronic system (Olomedia, Healthcare solution, Palermo, Italy) of Radiology and Neurology departments.

4.4. MRI data analysis

Enhanced and non-enhanced T1-WI of brain MRI scans for each MS patient included in this study have been reviewed. The MRI imaging reviewing procedure was carried out by the same operator (S.I) between June 2024 and December 2024 by using the PC Desktop HP 24-cr0076nl with a 24-inchs Full HD monitor and the integrated graphic equipment UHDIntel®. The presence of brain Gd deposits was defined by the presence of eye-visible hyperintensity of GP and/or DN in non-enhanced T1-WI sequences. If a patient did not have an eye-visible T1-WI hyperintensity of DN or GP on the last available brain MRI scan, he or she was classified as not having brain Gd deposition. For each study participants, all MRI scans were reviewed retrospectively until the finding or not the T1-WI hyperintensity of DN or GP. The revision of brain MRI ended as the first finding of T1-WI hyperintensity. All the MRI scans of pwMS in charge in MS outpatient service are stored in digital archives of Fondazione Istituto G. Giglio, Cefalù, and their visualization is available in a dedicate software (OloHealth, Olomedia Healthcare Software, Palermo).

4.5. Data collection

Demographic and clinical data of study participants were prospectively collected during each visit in the MS outpatient service and stored in the local database. The following information were collected: sex, weight, date of birth, date of MS onset, date of MS diagnosis, type of MS course, DMTs history, NTZ infusion history, JCV serum status at the start and the end of NTZ. Disability of MS patients was evaluated through the EDSS (176). The first EDSS at diagnosis was the baseline disability level whilst the EDSS at the day of follow-up was the latest disability level. By reviewing the MRI history, for each patient the following variables were calculated: 1) total number of MRI with GBCAs administration; 2) number of MRI with GBCAs during the treatment with NTZ; 3) number of MRI with GBCAs before or after NTZ treatment.

4.6. Exposition to gadolinium

The exposition to Gd was defined as having undergone at least one MRI scan with GBCAs administration. By accounting for patient's weight and the standard Gd dose of 15.72 mg/kg, the administered Gd dose per each MRI scan was calculated (mgGd/MRI). By multiplying the total Gd dose administered per each MRI scan for the total number of MRI with GBCAs administration and

then dividing for the patient's weight, the cumulative Gd dose received lifetime by each participant has been calculated (mgGd/kg). For the analyses purpose, the cumulative Gd dose was divided into four quartiles.

4.7. UPDRS collection

The UPDRS-III is the third part of the UPDRS employed in clinical practice to assess the motor signs of Parkinson disease (177). Due to its comprensive evalutation of basal ganglia and other extrapiramydal pathways functioning, UPDRS-III was used to assess whether or not Gd-deposits in DN and GP had a clinical impact in study participants. The performance of participants in each motor UPDRS task was scored according to guidelines (177). UPDRS was consecutively administered during the scheduled follow-up visit in study participants with an EDSS lower than 7 and in those with active follow-up. Patients with an EDSS equal or higher than 7, those who were lost to follow-up as well as those who was tested one year after the last MRI scan were excluded from the UPRDS analysis.

4.8. SDMT collection

The SDMT has been largely used as tool for the assessment of cognitive processing speed in pwMS (178). As a part of neurological examination, MS patients underwent oral version of SDMT each year. Specifically, the patient is presented with a page headed by a key that pairs the number 1-9 to corresponding symbols. After completing 10 items for demo, patients are asked to link orally each digit with symbol as fast they can in a time of 90 seconds (179,180). The total score is the number of correct associations between symbol and digit within 90 seconds; it ranges from 0 to 110 with a normative cut-off data for Italian subjects of 34.2 (180). For the analyses purpose, only patients with one available SDMT within one year from the last MRI scan were included in the SDMT analysis.

4.9. Renal function

Serum creatinine was routinely collected at each patients visit. For the analysis purpose, the last value of creatinine (mg/mL) was used to compute the glomerular filtrate rate (GFR as ml/min/1.73m^2) by using the 2021 Chronic Kidney Disease Epidemiology Collaboration equation. The renal function was classified as G1, normal (GFR $\geq$ 90 ml/min); G2, mildly decreased (GFR 60-89 ml/min); G3, moderate to severe decreased (GFR 44-59 ml/min); G4 severe decrease (GFR 15-29 ml/min); G5, kidney failure (GFR <15 ml/min) according literature (181).

4.10. Statistical analyses

Shapiro-Wilk's test was employed to check normality of continuous variables. Continuous variables were reports as median and interquartile range while categorical data were reported as number and relative percentage. Quantitative variables between groups were compared by using Mann and Whitney or Kruskal Wallis tests, as appropriate. Chi-square and Fisher exact tests were employed for the comparison of proportion and trend. The number of MRI per year of follow-up was calculated by carrying out the binomial negative regression with the total number of MRI as response variable and the natural logarithm of the follow-up time as offset variable. To estimate the grade of association between the quartiles of cumulative Gd doses and the presence of brain Gd deposits a multivariate logistic regression model were employed. The association was expressed as odds ratio (OR) with its 95% confidence intervals (CI). To recognize the critical treshold of MRI number and *cumulative Gd dose mg/kg* associated with brain Gd deposits, the receiver operating characteristic (ROC) curves with the calculation of the area under the curve (AUC) were built. The recognition of the best predicting thresholds with sensitivity, specificity and negative predictive value (NPV) were estimated by using the Youden Index (YI) as its higher values indicated the best cut off. Multivariable linear regression models were employed to estimate the association between linear variables. The level of the statistical significance has been set at $p < 0.05$. All the analyses were performed by using SPSS (2019. IBM SPSS Statistics per MacOS, Versione 26.0. Armonk, NY: IBM Corp).

5. RESULTS

Out of n=271 pwMS treated with NTZ, a total of n=205 were included in this study for the primary analysis according to study inclusion criteria (Figure 10).

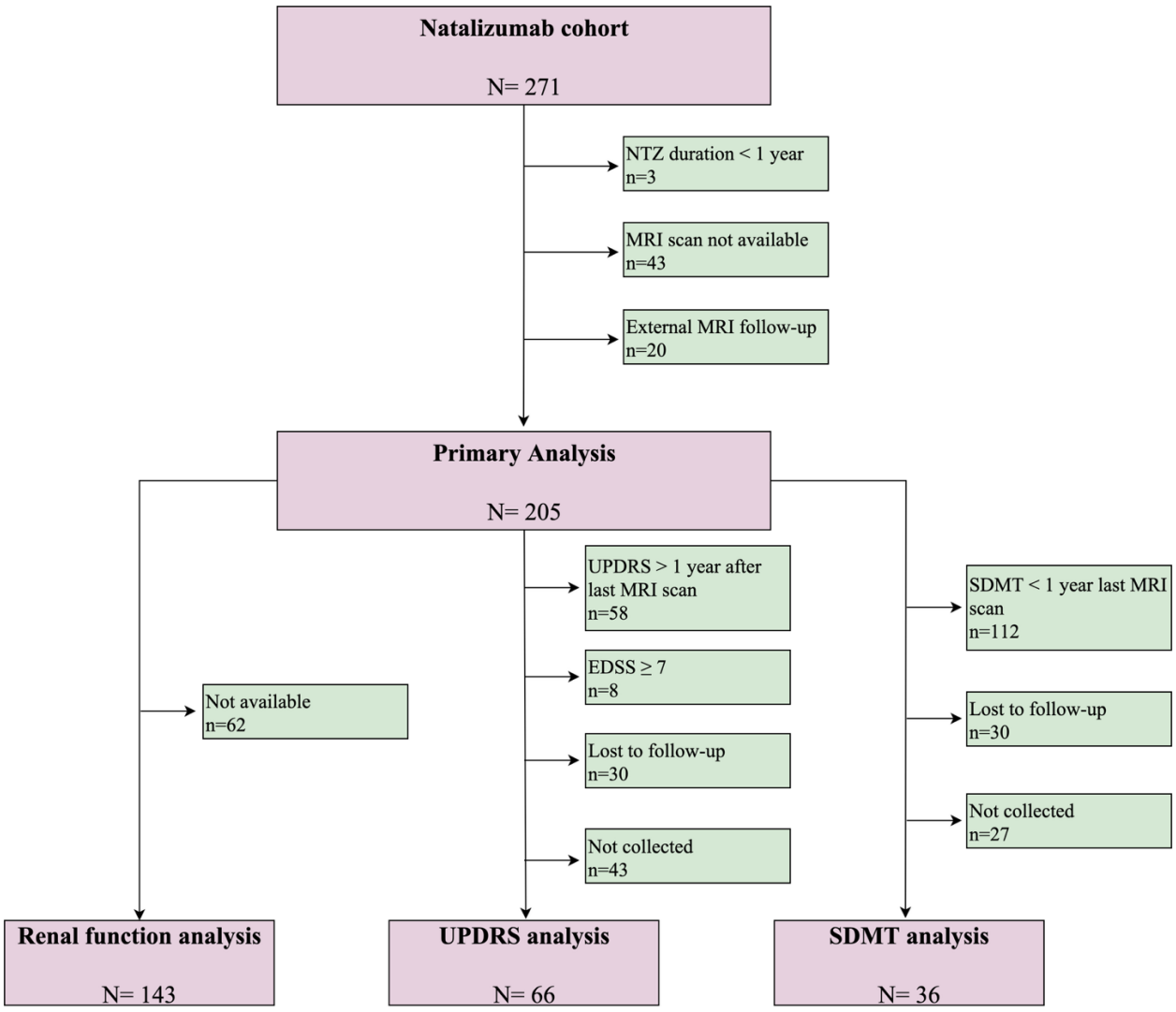

Figure 10. Flow-chart showing inclusion and exclusion procedures. MS, multiple sclerosis; NTZ, natalizumab; MRI, magnetic resonance imaging; EDSS, expanded disability status scale; CKD-EPI, Chronic Kidney Disease Epidemiology Collaboration; UPDRS, Unified Parkinson's Disease Rating Scale.

The secondary analyses that aimed to explore the effect of prolonged Gd exposure to renal function, extrapyramidal system and cognitive function were carried out by including n=143, n=66 and n=36 subjects, respectively (Figure 10).

5.1 Demographic and clinical features

Most of the participants were female (70.2%) and were RRMS (70.2%) at the follow-up date. The median age at study follow-up was 42.2 years (35.7-49) with a median follow-up time of 13.3 years (9.7-17.6); the median EDSS at last visit was 2 (1-4). Among participants, n=133 (64.9%) tested positive for serum JCV while even higher proportion of them received NTZ in EID (n=185, 90.2%) and underwent 3-months MRI-monitoring protocol (n=148, 72.2%). The complete demographic and clinical features of study participants are reported in Table 5.

Table 5 Demographic and clinical features of study cohort

Demographic features	
Female, n (%)	146 (70.2)
Age at follow-up, median (IQR)	42 (37-49)
Weight, kg, median (IQR)	65 (60-70)
Clinical features	
RRMS, n (%)	146 (70.2)
Follow-up duration, y, median (IQR)	15 (11-20)
Baseline EDSS, median (IQR)	1.5 (1-2)
EDSS at follow-up, median (IQR)	2.0 (1-4)
Natalizumab treatment	
JCV positive at baseline, n (%)	113 (55.1)
JCV positive at follow-up, n (%)	133 (64.9)
Ongoing, n (%)	183 (89.3)
Extended interval dosing, n (%)	185 (90.2)
Treatment duration, y, median (IQR)	7.3 (4-11)
MRI monitoring	
Every 3 months, n (%)	148 (72.2)
Every 6 months, n (%)	59 (28.4)
Number of total Gd-enhanced MRI, median (IQR)	31 (20-38)
Exposition to Gd	
Dose of Gd, mg/MRI, median (IQR)	1022 (943-1179)
Cumulative Gd dose, mg/lifetime, median (IQR)	30182 (19820-42130)
Cumulative Gd dose, mg/kg, median (IQR)	487.3 (309-597)

IQR, interquartile range; RRMS, relapsing-remitting multiple sclerosis; y, years; EDSS, Expanded Disability Status Scale; JCV, John Cunningham Virus; MRI, magnetic resonance imaging; Gd, gadolinium.

Participants underwent a median of 31 (20-38) GBCA-enhanced MRI scans with a rate of 2.2 (2-2.5) MRI scans per patient per year of follow-up. Overall, participants were exposed to a median Gd dose of 1022 mg/MRI resulting in median cumulative Gd dose of 30182 mg or 487.3 mgGd/kg. Patients underwent a higher number of enhanced-MRI scan per year of follow-up during the treatment with NTZ (2.77 [95% IC: 2.4-3.2]) rather than the NTZ-free period (1.60 [95% IC: 1.4-1.9]), p<0.0001 (Figure 11).

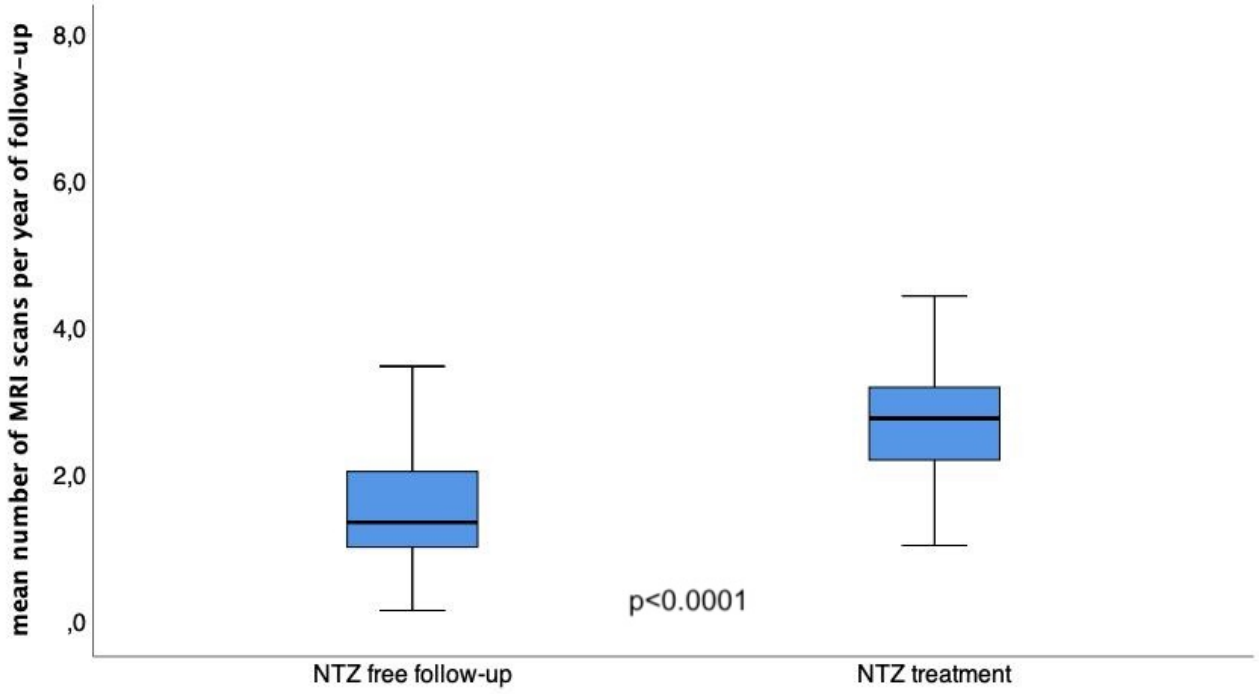

Figure 11 Box-plot showing the difference of the number of MRI scans during the treatment with NTZ and during the NTZ free follow-up time

JCV positive patients underwent higher number of MRI scans (34 [IQR: 24-41] vs (21 [IQR: 16-32]) and were exposed to a higher cumulative Gd dose (535 mg/kg [IQR 393-635] vs 338 mg/kg [244-508]) as depicted in Figure 12.

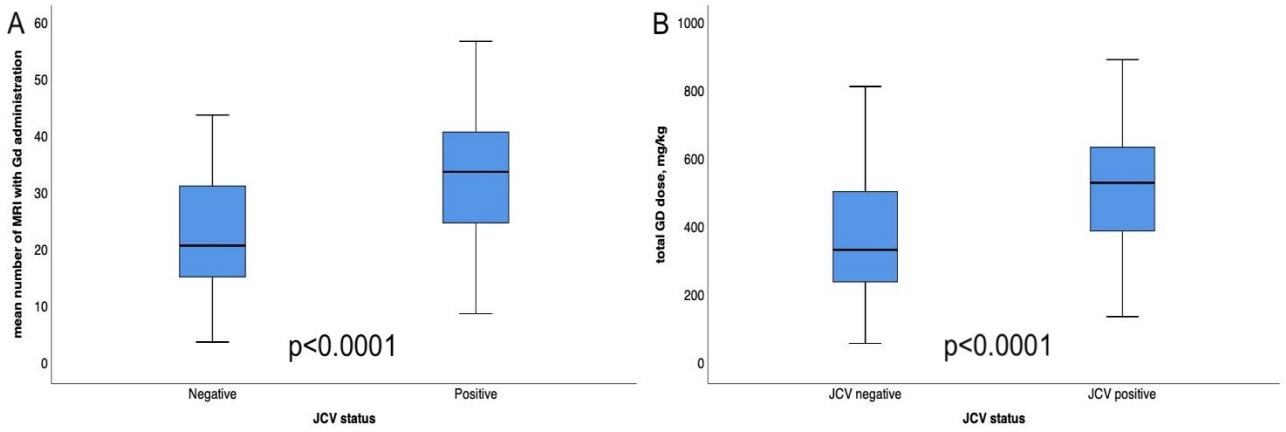

Figure 12 Box-plot showing the difference of the number of MRI scans (A) and total GD dose (B) in patients with and without positive JCV serum status.

5.2 Frequency and type of brain gadolinium deposits

Out of 205 participants, n=33 (16.1%) showed the presence of T1-WI hyperintensity of GP and DN (Figure 13A). Most of them had an involvement of both (n=18, 54.5%) while n=13 (39.4%) and n=2 (6.1%) had the isolated involvement of GP and DN, respectively (Figure 13B).

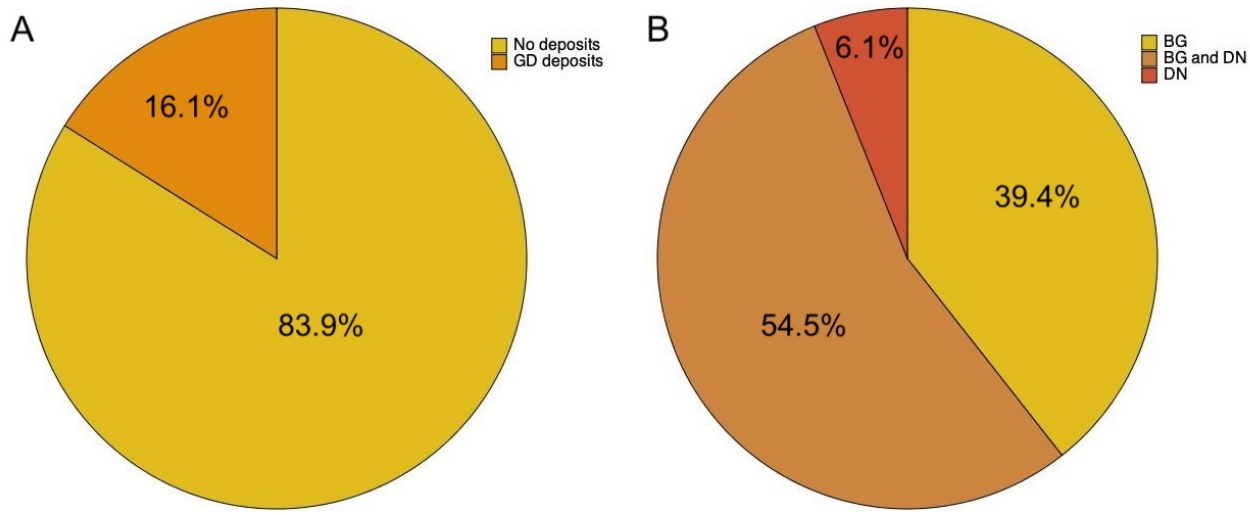

Figure 13 Frequency of T1-WI hyperintensity in study participants (A) and their relative frequency according to anatomical localization (B). Gd, gadolinium; BG, basal ganglia; DN, dentati nuclei.

Patients with DN and GP T1-WI hyperintensity had a longer follow-up time compared to those without it (13 years [10-17] vs 19 years [15-22]) and they underwent a higher number of MRI scans lifetime ($p<0.0001$) as well as during the treatment with NTZ ($p<0.0001$). They had higher age ($p<0.0001$) and were exposed to higher cumulative Gd dose ($p<0.0001$). Finally, a higher proportion of patients with SPMS was found in those with brain T1-WI hyperintensity ($p=0.038$). However, sex, EDSS, proportions of JCV positive patients and GFR did not differ between groups (all $p>0.05$). The complete comparison between patient with and without brain T1-WI hyperintensity are reported in Table 6.

Table 6 Comparison of demographic and clinical features in study participants with and without DN and GP T1-WI hyperintensity

	T1-WI normal N=172	**T1-WI Hyp N=33**	***p***
Men, n (%)	49 (28.5)	13 (39.4)	0.21
SPMS, n (%)	47 (27.3)	15 (45.5)	0.038
Age at MS onset, y, median (IQR)	25 (21-32)	25 (25-34)	0.88
Age at follow-up, y, median (IQR)	42 (36-48)	46 (40-61)	0.004

Follow-up duration, y, median (IQR)	13 (10-17)	19 (15-22)	<0.0001
EDSS, median (IQR)	2 (1-4)	2.5 (1-5.5)	0.24
Weight, kg, median (IQR)	65 (58-72)	69 (60-80)	0.29
NTZ duration y, median (IQR)	7 (4-11)	12 (9-15)	<0.0001
NTZ free-time y, median (IQR)	5 (3-8)	7 (4-9)	0.15
Extended interval dosing, n (%)	172 (88.4)	33 (100)	0.049
JCV serum status, n (%)	107 (62.2)	26 (78.8)	0.068
No. total Gd-enhanced MRI, median (IQR)	27 (20-36)	41 (34-48)	<0.0001
Cumulative Gd dose, mg/kg, median (IQR)	425 (314-568)	634 (539-754)	<0.0001

WI, weighted imaging; Hyp, hyperintensity; Gd, gadolinium; MS, multiple sclerosis; IQR, interquartile range; EDSS, Expanded Disability Status Scale; NTZ, natalizumab; JCV, John Cunningham Virus; MRI, magnetic resonance imaging; CKD-EPI, chronic kidney disease epidemiologic collaboration.

To explore the association between the cumulative Gd dose received by participants, a multivariate logistic regression analysis was carried out. Particularly, the exposition to increasing cumulative Gd dose, was associated with the increasing odd of having DP and GP T1-WI hyperintensity (Q3 vs Q1-2: aOR=7.01 [95%CI: 1.79-27.37]; Q4 3vs Q1-Q2: aOR=16.2 [95%CI: 4.3-61.9]) as shown in Model 1 (Table 7)

Table 7 Multivariate logistic regression analysis exploring the association between the quartiles of the cumulative Gd dose and the odds to have GP and DN T1-WI hyperintensity

Model 1	**B**	**SE**	**Wald**	**aOR**	**95% CIs**		**p**
					Lower	Upper	
Men (Women ref)	0.40	0.44	0.83	1.49	0.63	3.53	0.36
Age	0.03	0.02	2.08	1.03	0. 98	1.07	0.15
Gd dose mg/kg			16.85				
Q3 vs Q1-Q2	1.95	0.70	7.85	7.01	1.79	27.4	0.005
Q4 vs Q1-Q2	2.79	0.68	16.61	16.2	4.3	61.9	<0.0001

SE, standard error; aOR; adjusted odd ratios; CIs, confidence intervals; Gd, gadolinium; Q, quartile.

At the same time, a positive association emerged between higher BMI and the finding of T1-WI hyperintensity of GP and DN although this was not statistically significant as shown in Model 2 (Table 8).

Table 8 Multivariate logistic regression analysis exploring the association between BMI and the odds to find GP and DN hyperintensity adjusted by age and sex and Gd dose.

Model 2*	B	SE	Wald	aOR	95% CIs		p
					Lower	Upper	
Men (Women ref)	0.49	0.88	0.003	1.05	0.19	5.9	0.96
Age	1.27	0.85	2.21	3.54	0.67	18.8	0.14
Gd dose, quartiles	1.07	0.50	4.52	2.91	1.09	7.8	0.033
BMI							
Overweight vs Normal	0.49	0.99	0.24	1.63	0.23	11.5	0.62
Obese vs Normal	1.30	1.01	1.65	3.66	0.51	25.6	0.20

SE, standard error; aOR; adjusted odd ratios; CIs, confidence intervals; Gd, gadolinium; BMI, body mass index. *This analysis was conducted including 51 subjects from the study participants for whom BMI was collected.

The ROC analysis revealed an AUC of 0.82 (95% CI: 0.76-0.88) for the recognition of T1-WI hyperintensity of GP and DN by evaluating the number of total Gd-enhanced MRI performed by participants (Figure 14).

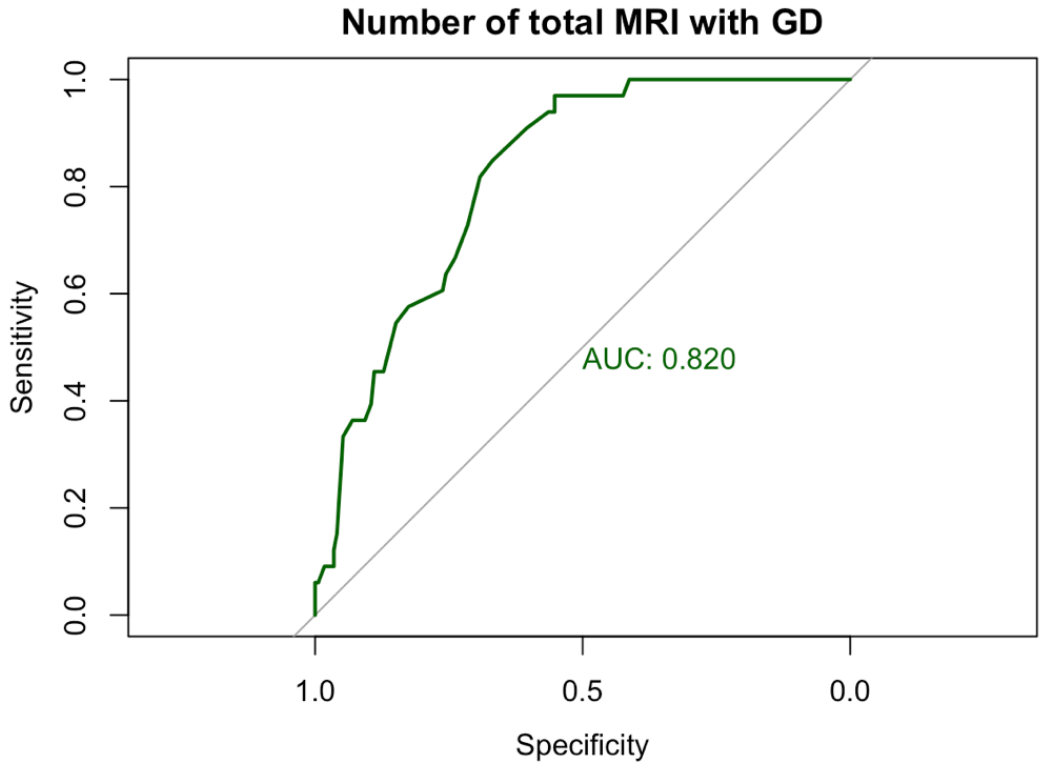

Figure 14 ROC curve showing the accuracy of total number of Gd-enhanced MRI for the recognition of brain T1-WI hyperintensity. Specificity is on the x axis and sensitivity on y axis. AUC, area under the curve.

A threshold of 29 GBCAs-enhanced MRI had a sensitivity of 97% and a specificity of 55.2% with a NPV of 99% (YI=0.522) for the recognition of brain T1-WI hyperintensity (Table 9).

Table 9 Cut-off values of total number of GBCAs-enhanced MRI and their sensitivity, specificity, positive and negative predictive values and Youden Index for the recognition of brain T1-WI hyperintensity.

Cut-off	Sensitivity	Specificity	PPV	NPV	YI
10	100	6.4	17.0	100	0.064
11	100	7.6	17.2	100	0.075
12	100	8.1	17.3	100	0.081
13	100	11.0	17.7	100	0.110
14	100	15.1	18.4	100	0.151
15	100	16.3	18.6	100	0.163
16	100	17.4	18.9	100	0.174
17	100	20.9	19.5	100	0.209
18	100	22.1	19.8	100	0.220
19	100	26.2	20.6	100	0.261
20	100	29.7	21.4	100	0.297
21	100	32.0	22.0	100	0.312
22	100	35.5	22.9	100	0.355
23	100	37.8	23.6	100	0.378
24	100	41.3	24.6	100	0.413
25	97.0	42.4	24.4	98.6	0.394
26	97.0	46.5	25.8	98.8	0.434
27	97.0	48.8	26.7	98.8	0.458
28	97.0	52.9	28.3	98.9	0.498
29	97.0	55.2	29.4	99.0	0.522
30	93.9	55.2	28.7	97.9	0.491
31	93.9	56.4	29.2	98.0	0.503
32	90.9	60.5	30.6	97.2	0.514
33	84.8	66.9	32.9	95.8	0.517
34	81.8	69.2	33.8	95.2	0.510
35	72.7	71.5	32.9	93.2	0.442

Gd, gadolinium; PPV, positive predicted value; NPV, negative predicted value; YI, Youden Index.

The ROC analysis revealed that also the cumulative Gd dose received by study participants lifetime recognized with high precision the presence of brain T1-WI hyperintensity (AUC of 0.82 [95% CI: 0.75-0.88] as shown in Figure 15.

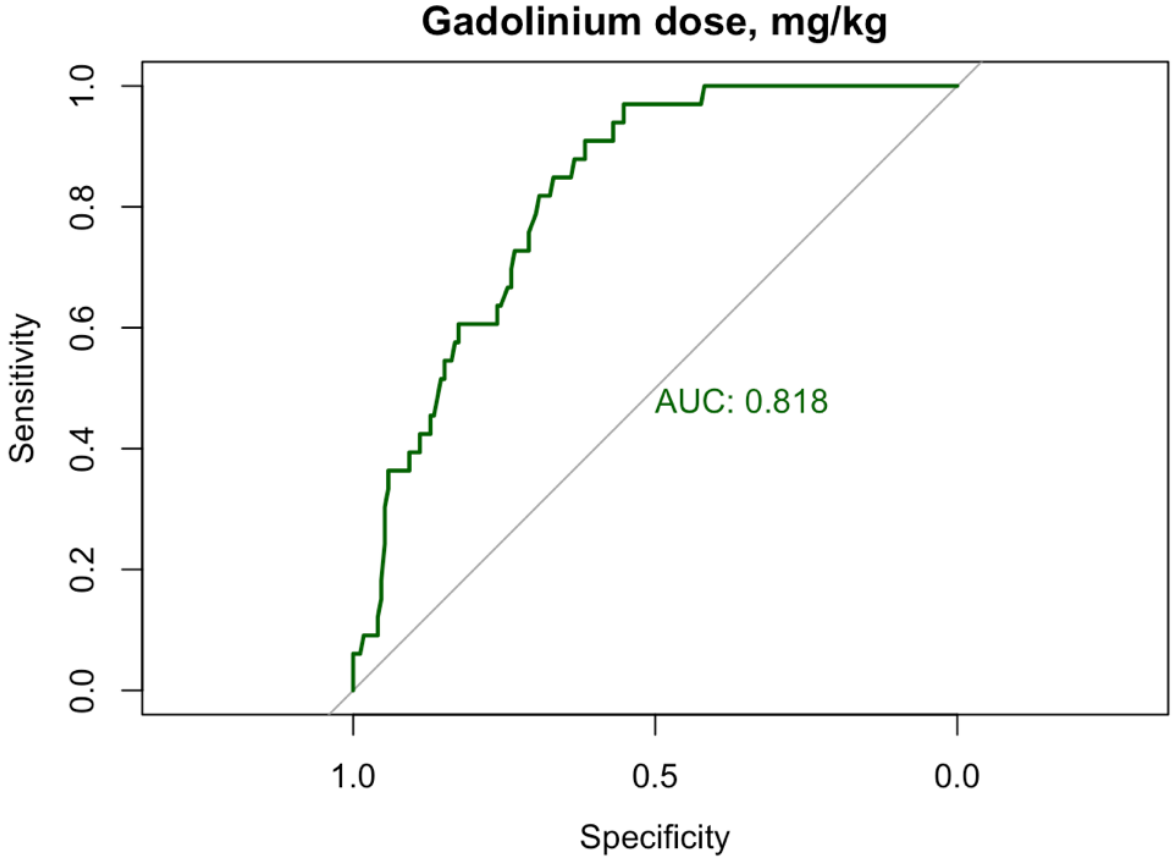

Figure 15 ROC curve showing the capability of increasing dosage of gadolinium to recognize brain deposits with specificity on the x axis and sensitivity on y axis. AUC, area under the curve.

The threshold dose of 501 mg/kg achieved the higher YI (0.525) with a sensitivity of 90.9% and a specificity of 61.6% with a NPV of 97.2% (Table 10)

Table 10 Cut-off values of gadolinium dose received lifetime and their sensitivity, specificity, positive and negative predictive values and Youden Index for the recognition of brain Gd deposits

Cut-off (mg/kg)	Sensitivity	Specificity	PPV	NPV	YI
377	100	41.9	24.8	100	0.419
392	97.0	42.4	24.4	98.6	0.394
393	97.0	43.0	24.6	98.7	0.399
403	97.0	45.9	25.6	98.8	0.429
408	97.0	46.5	25.8	98.8	0.435

409	97.0	47.1	26.0	98.8	0.441
415	97.0	47.7	26.2	98.8	0.446
419	97.0	48.3	26.4	98.8	0.452
421	97.0	48.8	26.7	98.8	0.458
424	97.0	49.4	26.9	98.8	0.464
426	97.0	52.3	28.1	98.9	0.493
439	97.0	52.9	28.3	98.9	0.499
440	97.0	53.5	28.6	98.9	0.505
447	97.0	54.1	28.8	98.9	0.510
455	97.0	54.7	29.1	98.9	0.516
463	93.9	55.2	28.7	97.9	0.492
471	93.9	55.8	29.0	98.0	0.498
485	93.9	56.4	29.2	98.0	0.503
486	93.9	57.0	29.5	98.0	0.509
487	90.9	57.0	28.8	97.0	0.479
489	90.9	59.3	30.0	97.1	0.502
491	90.9	59.9	30.3	97.2	0.508
492	90.9	60.5	30.6	97.2	0.514
494	90.9	61.0	30.9	97.2	0.519
501	90.9	61.6	31.2	97.2	0.525
503	87.9	61.6	30.5	96.4	0.495
512	84.8	64.5	31.5	95.7	0.494
513	84.8	65.1	31.8	95.7	0.499
518	84.8	65.7	32.2	95.8	0.506
519	84.8	66.9	32.9	95.8	0.517
520	81.8	67.0	32.5	95.1	0.493
522	81.8	68.0	32.9	95.1	0.498
531	81.8	68.6	33.3	95.2	0.504
534	81.8	69.2	33.8	95.2	0.510
540	72.7	70.9	32.4	93.1	0.437
550	72.7	71.5	32.9	93.2	0.442

Gd, gadolinium; PPV, positive predicted value; NPV, negative predicted value; YI, Youden Index.

Fifty-five patients started their MRI follow-up between 1991 and 2006 with a frequency of brain T1-WI hyperintensity of 32.7%; one-hundred and twenty-four underwent the first MRI between 2007 and 2016 with a frequency of brain T1-WI hyperintensity of 12.1%. No T1-WI hyperintensity was found in pwMS who started the brain MRI monitoring protocol after 2017 ($p<0.0001$; Figure 16).

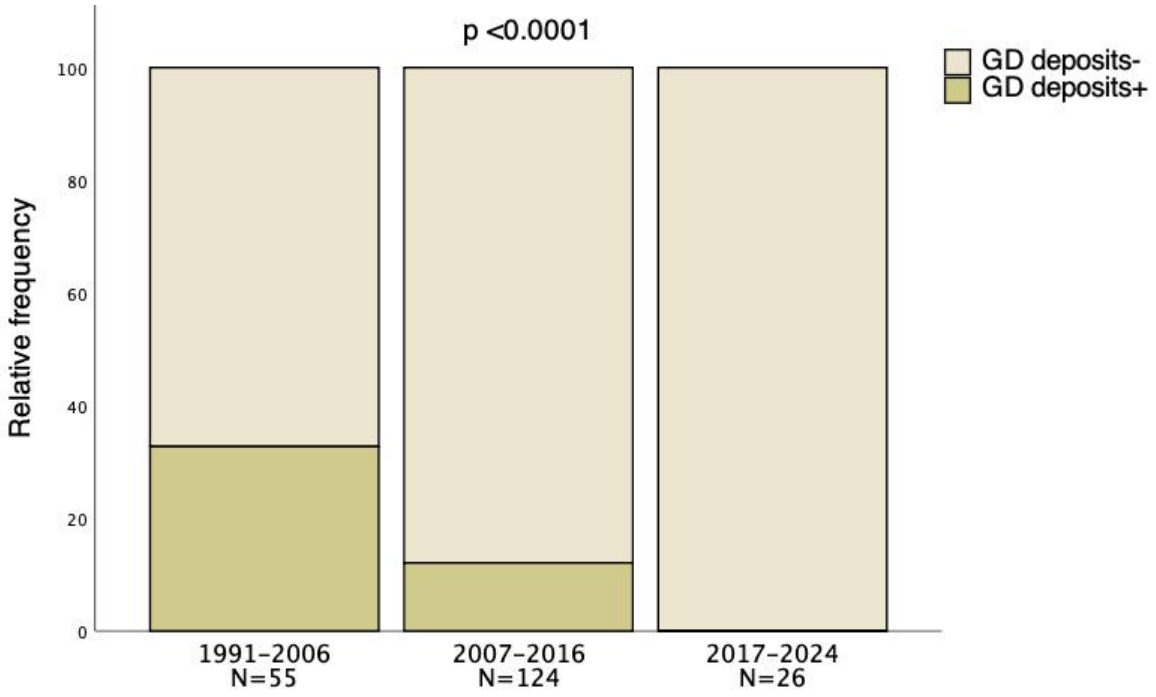

Figure 16 Bar-charts showing the relative frequency of brain Gd deposits according to the initiation era of the MRI monitoring. Gd, gadolinium.

5.3 UPDRS analyses

A total of n=124 patients consecutively underwent UPDRS evaluation. N=66 of them were included for the analyses according the inclusion criteria (Figure 10). The mean UPDRS score was 2.9 ± 4.7 and was higher in patients with T1-WI hyperintensity (6.3 ± 7.7) compared to those without (1.7 ± 2.1) and this was statistically significant (p=0.015) as depicted in Figure 17.

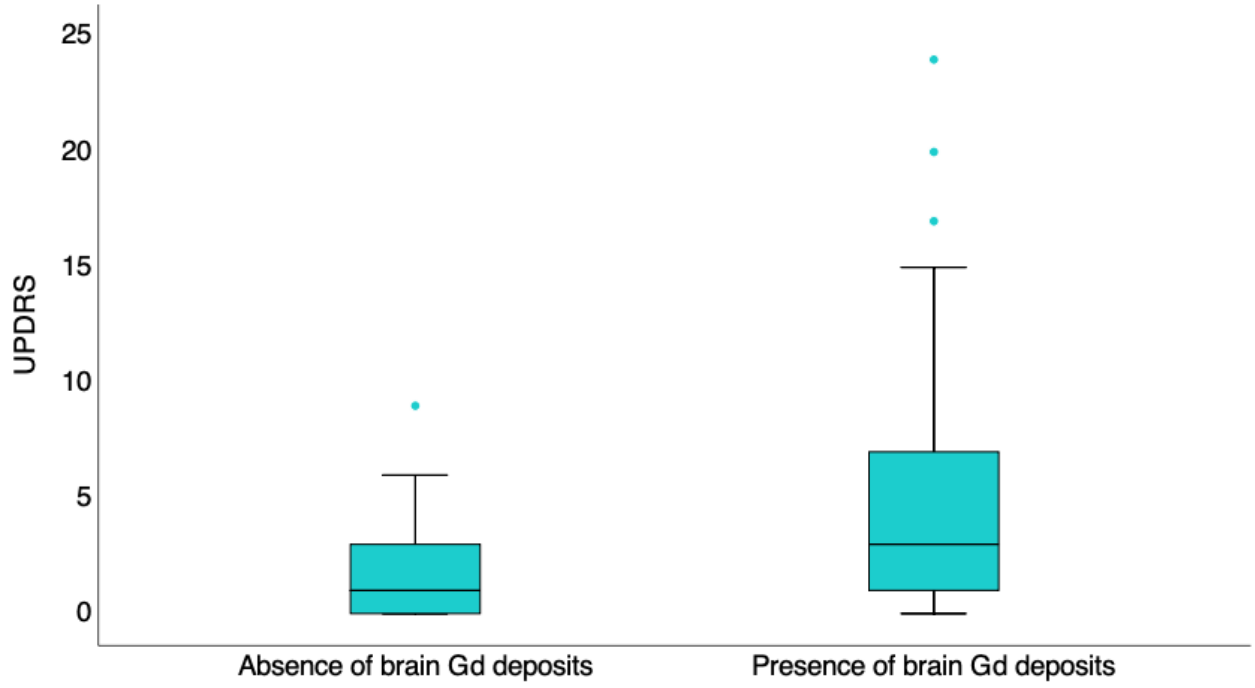

Figure 17 Box-plot showing the comparison of UPDRS scores between patients without and with globi pallidi and dentati nuclei T1-WI hyperintensity. UPDRS, Unified Parkinson Disease Rating Scale, Gd, gadolinium.

The multivariate linear regression analysis showed that age (B=0.22, p=0.049), EDSS (B=0.45, p<0.0001) and the presence of brain T1-WI hyperintensity (B=0.25, p=0.012) were associated with higher UPDRS scores while sex was inversely associated with UPDRS and no association emerged with Gd dose (mg/MRI) as shown in Table 11.

Table 6 Multivariate linear regression analysis exploring the association between demographic features, EDSS, presence of brain T1-WI hyperintensity, Gd dose and UPDRS score

	Standard error	Standardized Beta	*p*
Women	1.07	-0.21	0.035
Age	0.042	0.22	0.049
EDSS	0.28	0.45	<0.0001
T1-WI hyperintensity	1.01	0.25	0.012
*Gd dose (mg/MRI)	0.002	0.12	0.23

EDSS, Expanded Disability Status Scale, Gd, gadolinium, MRI, magnetic resonance imaging. *Gd dose expressed as mg/MRI did not correlate with brain T1-WI hyperintensity and the assumption of collinearity was not violated.

UPDRS score was higher as higher was the cumulative Gd dose (p=0.037). After the post-hoc analyses, statistically significant difference was found between Q1 and Q4 (p=0.01) as well as Q2 and Q4 (p=0.02) as depicted in Figure 18.

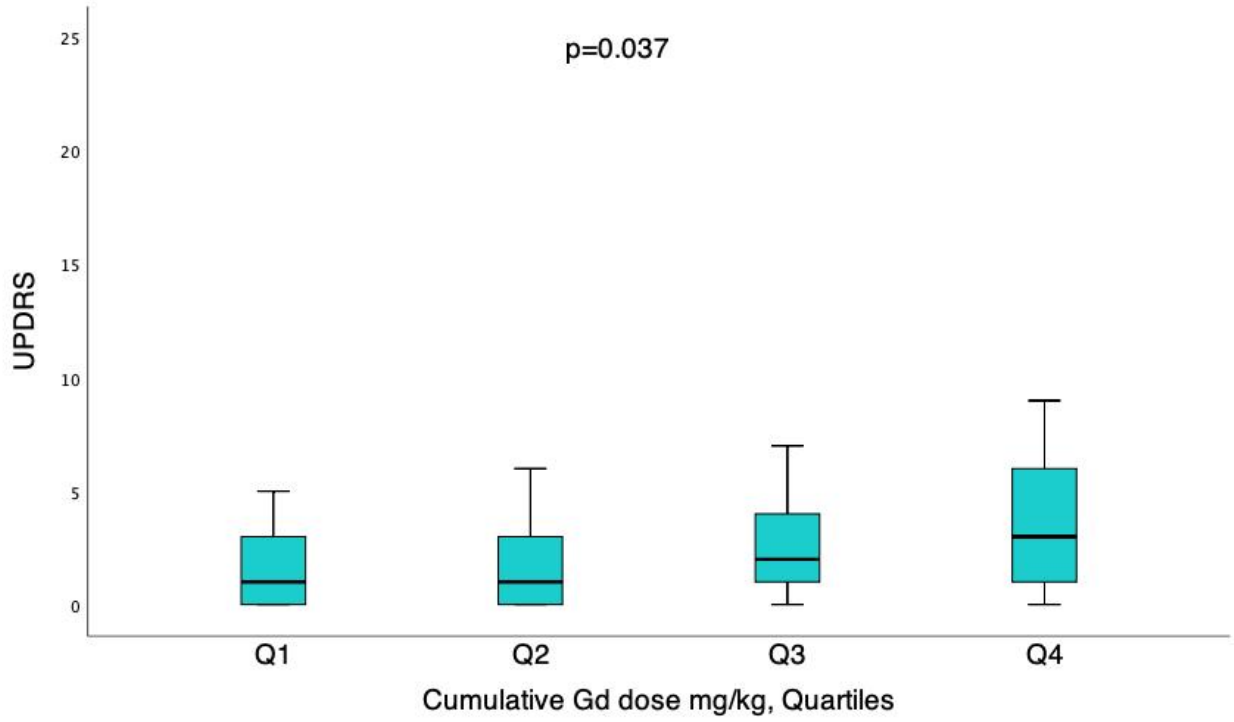

Figure 18 UPDRS comparison between the quartiles of the cumulative dose of Gd received by participants. UPDRS, Unified Parkinson Disease Rating Scale, Gd, gadolinium; Q, quartile.

5.4 SDMT analyses

A total of 148 patients of the study cohort underwent at least one SDMT assessment. Of them, thirty-six patients were eligible for analyses (Figure 10). The median score was 44.5 (37-52) and 7 patients out of 36 (19.7%) achieved a pathologic score. SDMT score was lower in patients with brain T1-WI hyperintensity (42 [33-45]) compared to those without it (48 [44-53]) and this was statistically significant (p=0.049) as shown in Figure 20.

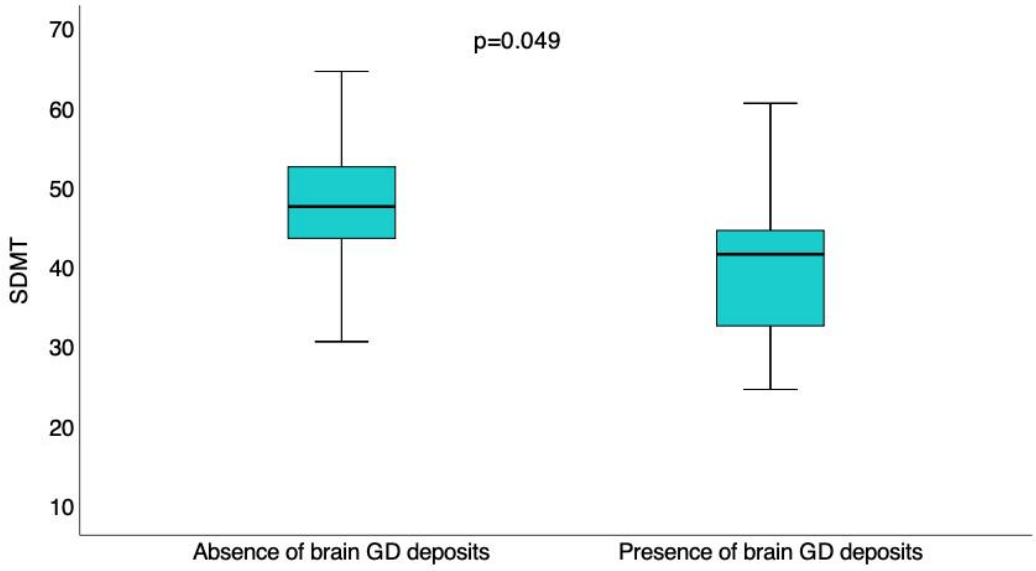

Figure 19 Box-plot showing the comparison of SDMT scoring in patients with and without brain T1-WI hyperintensity. GD, gadolinium; SDMT, symbol digit modalities test.

However, neither brain T1-WI hyperintensity (B= -0.13, p=0.40) nor Gd dose (mg/MRI) were statistically associated with SDMT scores and only age (B= -0.49, p=0.003) was related to (Table 12).

Table 7 Multivariate linear regression analysis exploring the association between age, presence of brain T1-WI hyperintensity, Gd dose and SDMT score

	Standard error	**Standardized Beta**	***p***
Age	0.15	-0.49	0.003
Brain T1-WI hyperintensity	3.5	-0.14	0.38
*Gd dose (mg/MRI)	0.008	-0.13	0.40

EDSS, Expanded Disability Status Scale, Gd, gadolinium, MRI, magnetic resonance imaging. *Gd dose expressed as mg/MRI did not correlate with T1-WI hyperintensity and the assumption of collinearity was not violated.

In addition, SDMT scores did not differ according to quartile of cumulative Gd dose exposition (p=0.42); data not shown.

5.5 Renal function analyses

A total of one-hundred and forty-three patients had a serum creatinine testing and were included in the analysis. The median creatinine level was 0.76 mg/dL (0.65-0.87) while the median GFR was 102.4 ml/min (89-113). According to 2021 CKD-EPI classification, n=105 (72.4%) and n=37 (25.9%) patients were G1 and G2, respectively, while only one patient (0.7%) was G3. Although GFR was slightly lower in patients with brain T1-WI hyperintensity (95 ml/min [89-105]) compared to those without it (103 [89-114]; p=0.089), no statistically significant association was found between renal disease and presence brain T1-WI hyperintensity (p>0.05). It is worth noting that patients exposed to higher cumulative dose of Gd showed a reduction of GFR compared other (Figure 22).

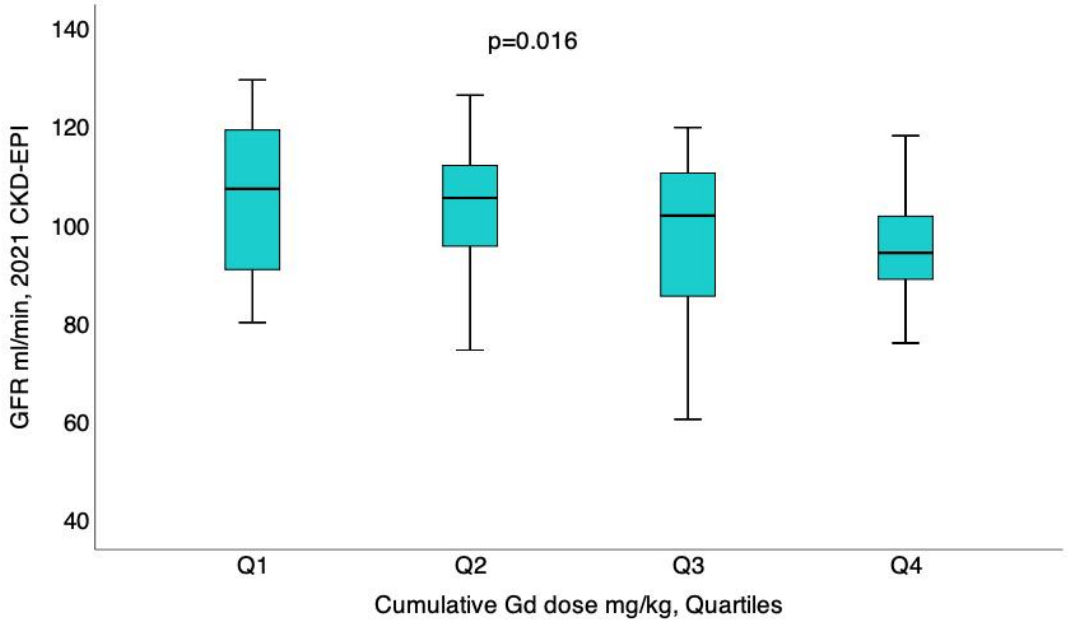

Figure 20 Box-plot showing the comparison between GFR and cumulative Gd dose received. GFR, glomerular filtration rate; CKD-EPI, chronic kidney disease epidemiological collaboration.

However, age appeared the most important contributor to the decline of renal function (Table 13).

Table 8 Multivariate linear regression analysis exploring the association between sex, age, EDSS, cumulative GD dose and 2021 CKD-EPI

	Standard error	**Standardized Beta**	***p***
Women	5.02	-0.08	0.28
Age	0.55	-6.78	<0.0001
EDSS	0.61	0.18	0.02
Cumulative Gd dose (mg/kg)	0.007	-0.10	0.20

Gd, gadolinium; EDSS, Expanded Disability Status Scale; CKD-EPI, Chronic Kidney Disease Epidemiology Collaboration.

6. DISCUSSION

The aims of this study are to 1)estimate frequency and anatomical pattern of brain T1-WI hyperintensity in a cohort of 205 pwMS; 2)identify the number of MRI scan with GBCAs administration as well as the cumulative Gd dose that predict the presence of brain T1-WI hyperintensity; 3)explore the clinical consequence of brain T1-WI hyperintensity on motor and cognitive functions by evaluating UPDRS and SDMT, respectively; 4) explore the relationship between the cumulative Gd dose and renal function. In this study, a total of 205 pwMS who had undergone routine brain MRI monitoring with GBCAs administration were enrolled. Patients underwent a median of 31 MRI with GBACs administration with a rate of 2.2 MRI/patient/year. This number was higher during NTZ treatment (Figure 11) as well as in in JCV positive patients (Figure 12). These findings were expected since patients at higher risk of PML usually undergo a peculiar MRI monitoring strategy (e.g., every 3 months). By the visual assessment of the T1-WI signal increase in DN and GP, the overall frequency of T1-WI hyperintensity was 16.1% in study participants. Interestingly, while most patients had both DN and GP involvement, the selective hyperintensity of GP was more common than DN alone (Figure 13). Whether some case report and not more than fifteen small observational studies in humans have been published, this study represents the largest cross-sectional study worldwide exploring the frequency of deep nuclei hyperintensity as a possible consequence of prolonged Gd exposition. Roccatagliata et a. found that 19.3% of a cohort of 123 pwMS had the T1-WI hyperintensity of DN but this finding was associated to MS progression rather than prolonged Gd exposition (114). Since Kanda et al. in 2014 reported the deposition of Gd into cerebral deep nuclei, most of published studies included patients undergoing MRI after brain tumours surgery with few studies on pwMS. In the present study, patients exposed to a higher cumulative Gd dose had a higher probability to have a visible T1-WI hyperintensity in GP and DN (Model 1, Table 7). Thus, there are no doubts that the T1-WI signal intensity changes in GP and DN of pwMS are related to prolonged exposition to Gd rather than natural history of MS. Moreover, the increase of BMI was even associated with brain T1-WI hyperintensity and this may be explained by the fact that obese patients receive a higher dose of GBCAs (Model 2, Table 8). Although this was not statistically significant, the clinical value of that OR should not be neglected since these results may be underestimated due to the limited number of participants in this sub-analysis (Table 8). Furthermore, the threshold of enhanced-MRI number predicting the finding of T1-WI hyperintensity in GP and DN was calculated. The ROC curves and YI showed that 29 MRI scans with GBCAs administration is the critic threshold for the finding of eye-detectable T1-WI hyperintensity of DN and GP with a sensitivity of 97%, specificity of 55.2% and a NPV of 99% (Table 9). A Gd dose of 501mg/kg achieved a 90.9% sensitivity, 61.6% specificity and 97.2% NPV to recognize T1-WI

hyperintensity of GP and DN (Table 10). Although the specificity values were lower, the higher sensitivity and NPV values acquire notable relevance in this case leading to correctly prediction of the dangerous number of MRI with GBCAs administration and critical cumulative Gd dose. These results may help neurologists and radiologists to individualize the monitoring MRI strategy avoiding to expose pwMS to an unnecessary number of enhanced-MRI. Furthermore, the trend of T1-WI hyperintensity in GP and DN frequency decreased according to the date of first MRI (Figure 16). This would lead to several interpretations. Firstly, this is may be due to the huge use of linear GBCAs before 2006 and their predominant role as causal factors of brain T1-WI hyperintensity. Since the description of NSF in 2006, the use of linear GBCAs was progressively avoided and this may explain the decreasing frequency trend across MRI era in the present study. Studies exploring the effect of prolonged exposition to macrocyclic GBCAs are conflicting. While lower brain Gd concentration were found in several in animal treated with macrocyclic GBCAs compared to linear ones, Stojanov et al. reported a significant increase of the GP-to-thalamus and DN-to-pons signal intensity ratios in pwMS who received multiple doses of gadobutrol. This signal increase correlated to the duration of the exposition since its highest values were found in patients receiving gadobutrol over a shorter period of time compared to those who received the same dose over a longer time period (169). Thus, whether linear GBCAs induce a stronger brain Gd deposition, it could be hypothesized that the brain deposition of Gd from macrocyclic GBCAs occurs under specific conditions such as a frequent administration. This hypothesis may explain the presence of patients with T1-WI changes in the 2007-2017 era when the use of macrocyclic GBCAs for CNS investigation was almost exclusive. On the other hand, since the probability to find a visible T1-WI hyperintensity of GP and DN increases with the increase of the MRI number and cumulative Gd dose, it is also possible that patients who started the MRI monitoring follow-up in the 2017-2024 era might not have reached the critical Gd dose (i.e., 501 mg/kg) or MRI number (i.e., 29). Interestingly, Bjørnerud et al. reported two patients with hyperintensity of DN on T1-WI following more than 35 doses of gadobutrol without previous exposition to linear GBCAs (182). Most observational studies employed the GP-to-thalamus and DN-to-pons signal intensity ratios as biomarker of Gd deposition while in the present study the finding of eye-detectable T1-WI hyperintensity in GP and/or DN was used to assess the presence or not of Gd deposits. (96,183)(147,184)The GP and DN belong to extrapyramidal pathways which are involved mainly in motor control and executive functions (e.g., optimization of movement in relation to motor task, motor learning, control of voluntary movement, verbal fluency, etc). Damage to the DN and GP may result in resting tremor, rigidity, bradykinesia, and gait abnormalities, as well as cognitive impairment, depression, and neurobehavioral deficits (185,186). Interestingly, the UPDRS score was significantly higher in patients who had GP and DN T1-WI hyperintensity ($p=0.015$; Figure 17). Sex

was inversely associated with UPDRS score while higher age and EDSS were associated with higher UPDRS scores. Whilst the presence of GP and DN T1-WI hyperintensity was associated to higher UPDRS score, the Gd dose (mg/MRI) was not associated to (Table 11). However, UPDRS score was higher in pwMS exposed to the fourth quartile of the cumulative Gd dose (mg/kg) while no other differences were found among other quartiles in post-hoc analysis (Figure 18). Taken together the finding may suggest that only patients with eye-detectable T1-WI hyperintensity on non-enhanced T1 sequences of GP and/or DN have clinical signs of parkinsonism and, at the same time, that the Gd deposition in GP and DN occurs when a critical threshold of cumulative Gd dose is reached that, in turn, depends from patient's weight and number of enhanced-MRI scan. It is worth noting that patients with and without DN and GP hyperintensity had a similar EDSS (Table 6) while higher EDSS was associated with higher UPDRS score indicating a possible effect of EDSS on UPDRS calculation. Notably, one population study ten years ago did not find any association to the exposition with Gd exposition and the risk of parkinsonism (187). In that case, authors estimated the risk of parkinsonism in patients exposed to ≥1 MRI with GBCAs administration compared to never exposed population. However, participants had a lower exposition to Gd since the 81.5% of them underwent a single MRI scan. Furthermore, they did not account for the presence or not of T1-WI hyperintensity in deep nuclei, thus it is not surprising that they did not find an association between Gd exposition and parkinsonism. More recently, Vymazal et al. did not find signs of parkinsonism or behavioral changes in four patients with brain Gd deposits after both linear and macrocyclic GBCAs exposure (188); in this case, the impact of Gd-deposits on motor function was evaluated through the Natural History and Neuroprotection in Parkinson Plus Syndromes—Parkinson Plus Scale. This scale was developed originally for parkinson plus syndromes and it would be less appropriate than UPDRS to estimate the clinical consequences of the GP involvement. Moreover, Scaravilli et al. and Cocozza et al. did not find any association between the T1-WI hyperintensity and R1 relaxation changes of DN with motor performance evaluated by EDSS or EDSS worsening (189,190). Accordingly, as the finding of the presented study, EDSS did not differ between patients with and without brain T1-WI hyperintensity, probably because EDSS would not the appropriate clinical tool to assess the consequence of a Gd-related disease. The extrapyramidal functioning through the evaluation of UPDRS in a large cohort of pwMS with GP and DN T1-WI hyperintensity due to prolonged exposition to Gd has been never investigated to date. The results from the present study may support a development of a Gd-related parkinsonism only in pwMS with eye-detectable T1-WI hyperintensity of GP and DN who underwent a critical number of enhanced-MRI exams and who received the critical cumulative dose of Gd. Despite patients with GP and DN T1-WI hyperintensity had lower SDMT scores compared to those without (Figure 20, p=0.049), the multivariable regression analysis showed no association between

deep nuclei T1-WI hyperintensity and SDMT score (Table 12). In addition, the SDMT scores were not different across the quartiles of cumulative Gd dose ($p>0.05$). Forslin et al. investigated the association between GP and DN signal intensity, verbal memory and SDMT. They found an inverse association between GP-to-thalamus and DN-to-cerebellum signal intensity ratio and SDMT but this was lost after correcting for MS severity (e.g., lesion volume) even if the association between signal changes and reduction of verbal fluency remained significant (191). The same author, by using relaxometry-MRI, found that the higher relaxation of DN and GP were associated with lower SDMT and verbal fluency, respectively, although they concluded that the contribution of underlying MS severity was the relevant factor influencing the cognitive functioning (192). Other authors failed to find an association between the T1-WI hyperintensity of DN and cognitive function in pwMS (137). More recently, other authors did not find any association between the presence of DN hyperintensity or changes in R1 relaxation maps with SDMT, California Verbal Learning Test and Brief Visuospatial Memory test (189). In conclusion, the results of the presented study are in line with those reported previously. The finding of new determinants of cognitive dysfunction in pwMS could be somewhat complex due to massive brain damage masking the effect of other causal factors. Finally, the association between renal function, brain Gd deposits and cumulative Gd dose was explored. Whether patients exposed to highest quartile of cumulative Gd dose showed a significant reduction of GFR compared to other, by adjusting for other clinical and demographic factors no association emerged between cumulative Gd dose and renal function (Table 13). Accordingly, the frequency of brain T1-WI hyperintensity did not differ according CKD-EPI quartiles. These finding may indicate a lack of relationship between prolonged exposition to Gd and renal dysfunction as well as that mild or moderate renal dysfunction are not predisposing factor to brain Gd deposition. Accordingly, several studies shown that the tissue deposition of Gd is independent from renal function and that NSF occurs only in cases of dramatic renal disease (GFR <30ml/min) (96,97,193). Thus, renal disease may affect tissue deposition of Gd only in special conditions but the prolonged Gd administration would have not toxic effect on renal functioning.

7. LIMITATIONS AND STRENGHT

This is a retrospective and cross-sectional study and the first limitation would be the selection bias because the enrollment of a special cohort (i.e., MRI monitoring for PML-risk surveillance) which may be not representative of the general MS population. However, given the peculiarity of these patients, the presented cohort represents a unique population for the study of toxic consequence of prolonged exposition to Gd. Furthermore, both linear and macrocyclic GBCAs were grouped together since the identical Gd dose (0.1 mmol/kg) provided per each MRI scan regardless their chemical

composition. This lack of stratification between linear and macrocyclic GBCAs may represents other limitation. Moreover, whether more than one-hundred study participants underwent UPDRS and SDMT testing, many of them were excluded from the analysis and this would lead to attrition bias. Finally, both signal intensity ratios and the absolute signal intensity increase on T1-WI may be affected by several confounding factors such as MRI parameters acquisition, type of ROI, sequence type and strength of magnetic field (96,183). Some MRI techniques such as R1 relaxometry and QSM are more sensitive tools for biometal imaging allowing a more accurate quantitative evaluation of transchelation of Gd from GBCA to competing macromolecules (147,184). Thus, it is also possible that the frequency of brain Gd deposits has been underestimated in the present study. However, as a strength, this was the biggest study worldwide investigating the frequency of Gd-related T1-WI hyperintensity of DN and GP in pwMS. Moreover, the sample size and the long history of Gd exposition allowed to estimate the threshold of the dangerous cumulative Gd dose and the critical number of enhanced-MRI subsequently. It is worth noting that, UPDRS here for first time was employed to explore the clinical consequence of Gd deposition in GP and DN.

8. CONCLUSION

The use of GBCAs in pwMS is usually recommended at diagnosis and should be limited as much as possible during the routine MRI monitoring (83). Historically, pwMS underwent several enhanced-MRI scans to monitor disease activity, particularly those in special conditions such as for the PML-risk surveillance purpose. Thus, it is not surprising that many MS patients have undergone more than 30 MRI scan with GBCAs administration lifetime. Since the identification of NSF, several strategies have been developed to minimize the consequence of Gd exposition such as screening practices and development of more stable GBCAs. According to the chemical properties of GBCAs, the American College of Radiology provided a classification of GBCAs into three groups based on NSF risk: 1) Group 1 (highest risk) includes gadopentetate dimeglumine, gadodiamide; 2)Group 2 (intermediate risk) includes gadobenate dimeglumine; 3) Group 3 (lowest risk), includes all macrocyclic agents. This turned out in a switch to macrocyclic GBCAs from 2007 in most European hospitals. Furthermore, after the publication of articles showing the increased T1-WI signal intensity in GP and DN, starting from February 2017, high risk GBCAs were withdrawn from European market while gadobenate was limited to liver MRI resulting in an exclusive use of macrocyclic GBCAs (194). The present study expands the knowledge about the effect of prolonged exposition to Gd and cerebral toxicity suggesting that the involvement of GP and DN could be not clinically irrelevant. Commonly, the management of pwMS is complex due to several reasons (e.g., chronic comorbidities, disability, DMT adverse events, etc). In this perspective, Gd toxicity may have a negative impact both at

individual (e.g., worsen patient's disability) and at healthcare level since it imposes the implementation of monitoring strategy to minimize its risk. Despite the prolonged Gd administration was not associated to the decline of renal function, the management of Gd exposure appears even more relevant in pwMS who are often elderly, undergoing concomitant DMT and burdened by chronic comorbidities that may collectively contribute to Gd toxicity. Thus, regardless the type of GBCAs, the presented results in this study supports their use only in specific conditions in pwMS limiting the exposition to a critical number of enhanced-MRI scans and cumulative Gd dose.

9. REFERENCES

1. Multiple Sclerosis International Federation (MSIF). Number of people with MS | Atlas of MS. (2020) https://www.atlasofms.org/map/united-kingdom/epidemiology/number-of-people-with-ms [Accessed October 14, 2023]
2. Kurtzke JF. Epidemiology of multiple sclerosis. Does this really point toward an etiology? Lectio Doctoralis. *Neurol Sci* (2000) 21:383–403. doi: 10.1007/S100720070055
3. Koch-Henriksen N, Sorensen PS. Why does the north-south gradient of incidence of multiple sclerosis seem to have disappeared on the northern hemisphere? *J Neurol Sci* (2011) 311:58–63. doi: 10.1016/J.JNS.2011.09.003
4. Zivadinov R, Iona L, Monti-Bragadin L, Bosco A, Jurjevic A, Taus C, Cazzato G, Zorzon M. The use of standardized incidence and prevalence rates in epidemiological studies on multiple sclerosis. A meta-analysis study. *Neuroepidemiology* (2003) 22:65–74. doi: 10.1159/000067107
5. Puthenparampil M, Perini P, Bergamaschi R, Capobianco M, Filippi M, Gallo P. Multiple sclerosis epidemiological trends in Italy highlight the environmental risk factors. *J Neurol* (2022) 269:1817–1824. doi: 10.1007/S00415-021-10782-5
6. Melcon MO, Correale J, Melcon CM. Is it time for a new global classification of multiple sclerosis? *J Neurol Sci* (2014) 344:171–181. doi: 10.1016/J.JNS.2014.06.051
7. Naseri A, Nasiri E, Sahraian MA, Daneshvar S, Talebi M. Clinical Features of Late-Onset Multiple Sclerosis: a Systematic Review and Meta-analysis. *Mult Scler Relat Disord* (2021) 50:102816. doi: 10.1016/J.MSARD.2021.102816
8. Ristori G, Cannoni S, Stazi MA, Vanacore N, Cotichini R, Alfò M, Pugliatti M, Sotgiu S, Solaro C, Bomprezzi R, et al. Multiple sclerosis in twins from continental Italy and Sardinia: a nationwide study. *Ann Neurol* (2006) 59:27–34. doi: 10.1002/ANA.20683
9. Harirchian MH, Fatehi F, Sarraf P, Honarvar NM, Bitarafan S. Worldwide prevalence of familial multiple sclerosis: A systematic review and meta-analysis. *Mult Scler Relat Disord* (2018) 20:43–47. doi: 10.1016/J.MSARD.2017.12.015
10. Moutsianas L, Jostins L, Beecham AH, Dilthey AT, Xifara DK, Ban M, Shah TS, Patsopoulos NA, Alfredsson L, Anderson CA, et al. Class II HLA interactions modulate genetic risk for multiple sclerosis. *Nat Genet* (2015) 47:1107–1113. doi: 10.1038/NG.3395
11. Manousaki D, Dudding T, Haworth S, Hsu YH, Liu CT, Medina-Gómez C, Voortman T, van der Velde N, Melhus H, Robinson-Cohen C, et al. Low-Frequency Synonymous Coding Variation in CYP2R1 Has Large Effects on Vitamin D Levels and Risk of Multiple Sclerosis. *Am J Hum Genet* (2017) 101:227–238. doi: 10.1016/J.AJHG.2017.06.014
12. Steri M, Orrù V, Idda ML, Pitzalis M, Pala M, Zara I, Sidore C, Faà V, Floris M, Deiana M, et al. Overexpression of the Cytokine BAFF and Autoimmunity Risk. *N Engl J Med* (2017) 376:1615–1626. doi: 10.1056/NEJMOA1610528
13. Gregory AP, Dendrou CA, Attfield KE, Haghikia A, Xifara DK, Butter F, Poschmann G, Kaur G, Lambert L, Leach OA, et al. TNF receptor 1 genetic risk mirrors outcome of anti-TNF therapy in multiple sclerosis. *Nature* (2012) 488:508–511. doi: 10.1038/NATURE11307
14. Maier LM, Lowe CE, Cooper J, Downes K, Anderson DE, Severson C, Clark PM, Healy B, Walker N, Aubin C, et al. IL2RA genetic heterogeneity in multiple sclerosis and type 1 diabetes susceptibility and soluble interleukin-2 receptor production. *PLoS Genet* (2009) 5: doi: 10.1371/JOURNAL.PGEN.1000322
15. Lundmark F, Duvefelt K, Iacobaeus E, Kockum I, Wallström E, Khademi M, Oturai A, Ryder LP, Saarela J, Harbo HF, et al. Variation in interleukin 7 receptor alpha chain (IL7R) influences risk of multiple sclerosis. *Nat Genet* (2007) 39:1108–1113. doi: 10.1038/NG2106
16. Beecham AH, Patsopoulos NA, Xifara DK, Davis MF, Kemppinen A, Cotsapas C, Shah TS, Spencer C, Booth D, Goris A, et al. Analysis of immune-related loci identifies 48 new

susceptibility variants for multiple sclerosis. *Nat Genet* (2013) 45:1353–1362. doi: 10.1038/NG.2770
17. Palacios N, Alonso A, BrØnnum-Hansen H, Ascherio A. Smoking and increased risk of multiple sclerosis: parallel trends in the sex ratio reinforce the evidence. *Ann Epidemiol* (2011) 21:536–542. doi: 10.1016/J.ANNEPIDEM.2011.03.001
18. Mokry LE, Ross S, Timpson NJ, Sawcer S, Davey Smith G, Richards JB. Obesity and Multiple Sclerosis: A Mendelian Randomization Study. *PLoS Med* (2016) 13: doi: 10.1371/JOURNAL.PMED.1002053
19. Hassani A, Corboy JR, Al-Salam S, Khan G. Epstein-Barr virus is present in the brain of most cases of multiple sclerosis and may engage more than just B cells. *PLoS One* (2018) 13: doi: 10.1371/JOURNAL.PONE.0192109
20. Bjornevik K, Cortese M, Healy BC, Kuhle J, Mina MJ, Leng Y, Elledge SJ, Niebuhr DW, Scher AI, Munger KL, et al. Longitudinal analysis reveals high prevalence of Epstein-Barr virus associated with multiple sclerosis. *Science* (2022) 375:296–301. doi: 10.1126/SCIENCE.ABJ8222
21. Fanara S, Aprile M, Iacono S, Schirò G, Bianchi A, Brighina F, Dominguez LJ, Ragonese P, Salemi G. The Role of Nutritional Lifestyle and Physical Activity in Multiple Sclerosis Pathogenesis and Management: A Narrative Review. *Nutrients* (2021) 13: doi: 10.3390/NU13113774
22. Greenfield AL, Hauser SL. B-cell Therapy for Multiple Sclerosis: Entering an era. *Ann Neurol* (2018) 83:13–26. doi: 10.1002/ANA.25119
23. Filippi M, Bar-Or A, Piehl F, Preziosa P, Solari A, Vukusic S, Rocca MA. Multiple sclerosis. *Nat Rev Dis Primers* (2018) 4: doi: 10.1038/S41572-018-0041-4
24. Kunkl M, Frascolla S, Amormino C, Volpe E, Tuosto L. T Helper Cells: The Modulators of Inflammation in Multiple Sclerosis. *Cells* (2020) 9: doi: 10.3390/CELLS9020482
25. Murúa SR, Farez MF, Quintana FJ. The Immune Response in Multiple Sclerosis. *Annu Rev Pathol* (2022) 17:121–139. doi: 10.1146/ANNUREV-PATHOL-052920-040318
26. Comi G, Bar-Or A, Lassmann H, Uccelli A, Hartung HP, Montalban X, Sørensen PS, Hohlfeld R, Hauser SL. Role of B Cells in Multiple Sclerosis and Related Disorders. *Ann Neurol* (2021) 89:13–23. doi: 10.1002/ANA.25927
27. Liu R, Du S, Zhao L, Jain S, Sahay K, Rizvanov A, Lezhnyova V, Khaibullin T, Martynova E, Khaiboullina S, et al. Autoreactive lymphocytes in multiple sclerosis: Pathogenesis and treatment target. *Front Immunol* (2022) 13: doi: 10.3389/FIMMU.2022.996469
28. Lassmann H. Pathology and disease mechanisms in different stages of multiple sclerosis. *J Neurol Sci* (2013) 333:1–4. doi: 10.1016/J.JNS.2013.05.010
29. Prineas JW, Kwon EE, Cho ES, Sharer LR, Barnett MH, Oleszak EL, Hoffman B, Morgan BP. Immunopathology of secondary-progressive multiple sclerosis. *Ann Neurol* (2001) 50:646–657. doi: 10.1002/ANA.1255
30. Lassmann H. Multiple Sclerosis Pathology. *Cold Spring Harb Perspect Med* (2018) 8: doi: 10.1101/CSHPERSPECT.A028936
31. Absinta M, Sati P, Masuzzo F, Nair G, Sethi V, Kolb H, Ohayon J, Wu T, Cortese ICM, Reich DS. Association of Chronic Active Multiple Sclerosis Lesions with Disability in Vivo. *JAMA Neurol* (2019) 76:1474–1483. doi: 10.1001/JAMANEUROL.2019.2399,
32. Cunniffe N, Coles A. Promoting remyelination in multiple sclerosis. *J Neurol* (2021) 268:30–44. doi: 10.1007/S00415-019-09421-X
33. Lemus HN, Warrington AE, Rodriguez M. Multiple Sclerosis: Mechanisms of Disease and Strategies for Myelin and Axonal Repair. *Neurol Clin* (2018) 36:1–11. doi: 10.1016/J.NCL.2017.08.002
34. Mahad DH, Trapp BD, Lassmann H. Pathological mechanisms in progressive multiple sclerosis. *Lancet Neurol* (2015) 14:183–193. doi: 10.1016/S1474-4422(14)70256-X

35. Dendrou CA, Fugger L, Friese MA. Immunopathology of multiple sclerosis. *Nat Rev Immunol* (2015) 15:545–558. doi: 10.1038/NRI3871
36. Lassmann H. Multiple Sclerosis Pathology. *Cold Spring Harb Perspect Med* (2018) 8: doi: 10.1101/CSHPERSPECT.A028936
37. Machado-Santos J, Saji E, Tröscher AR, Paunovic M, Liblau R, Gabriely G, Bien CG, Bauer J, Lassmann H. The compartmentalized inflammatory response in the multiple sclerosis brain is composed of tissue-resident CD8+ T lymphocytes and B cells. *Brain* (2018) 141:2066–2082. doi: 10.1093/BRAIN/AWY151
38. Magliozzi R, Howell OW, Nicholas R, Cruciani C, Castellaro M, Romualdi C, Rossi S, Pitteri M, Benedetti MD, Gajofatto A, et al. Inflammatory intrathecal profiles and cortical damage in multiple sclerosis. *Ann Neurol* (2018) 83:739–755. doi: 10.1002/ANA.25197
39. Magliozzi R, Howell OW, Reeves C, Roncaroli F, Nicholas R, Serafini B, Aloisi F, Reynolds R. A Gradient of neuronal loss and meningeal inflammation in multiple sclerosis. *Ann Neurol* (2010) 68:477–493. doi: 10.1002/ANA.22230
40. Zrzavy T, Hametner S, Wimmer I, Butovsky O, Weiner HL, Lassmann H. Loss of "homeostatic" microglia and patterns of their activation in active multiple sclerosis. *Brain* (2017) 140:1900–1913. doi: 10.1093/BRAIN/AWX113
41. Magliozzi R, Serafini B, Rosicarelli B, Chiappetta G, Veroni C, Reynolds R, Aloisi F. B-cell enrichment and Epstein-Barr virus infection in inflammatory cortical lesions in secondary progressive multiple sclerosis. *J Neuropathol Exp Neurol* (2013) 72:29–41. doi: 10.1097/NEN.0B013E31827BFC62
42. Lisak RP, Nedelkoska L, Benjamins JA, Schalk D, Bealmear B, Touil H, Li R, Muirhead G, Bar-Or A. B cells from patients with multiple sclerosis induce cell death via apoptosis in neurons in vitro. *J Neuroimmunol* (2017) 309:88–99. doi: 10.1016/J.JNEUROIM.2017.05.004
43. Lisak RP, Benjamins JA, Nedelkoska L, Barger JL, Ragheb S, Fan B, Ouamara N, Johnson TA, Rajasekharan S, Bar-Or A. Secretory products of multiple sclerosis B cells are cytotoxic to oligodendroglia in vitro. *J Neuroimmunol* (2012) 246:85–95. doi: 10.1016/J.JNEUROIM.2012.02.015
44. Mey GM, Mahajan KR, DeSilva TM. Neurodegeneration in multiple sclerosis. *WIREs mechanisms of disease* (2023) 15: doi: 10.1002/WSBM.1583
45. Dobson R, Giovannoni G. Multiple sclerosis - a review. *Eur J Neurol* (2019) 26:27–40. doi: 10.1111/ENE.13819
46. Lublin FD, Reingold SC, Cohen JA, Cutter GR, Sørensen PS, Thompson AJ, Wolinsky JS, Balcer LJ, Banwell B, Barkhof F, et al. Defining the clinical course of multiple sclerosis: the 2013 revisions. *Neurology* (2014) 83:278–286. doi: 10.1212/WNL.0000000000000560
47. Klineova S, Lublin FD. Clinical Course of Multiple Sclerosis. *Cold Spring Harb Perspect Med* (2018) 8: doi: 10.1101/CSHPERSPECT.A028928
48. Cree BAC, Arnold DL, Chataway J, Chitnis T, Fox RJ, Pozo Ramajo A, Murphy N, Lassmann H. Secondary Progressive Multiple Sclerosis: New Insights. *Neurology* (2021) 97:378–388. doi: 10.1212/WNL.0000000000012323
49. Lublin FD, Häring DA, Ganjgahi H, Ocampo A, Hatami F, Čuklina J, Aarden P, Dahlke F, Arnold DL, Wiendl H, et al. How patients with multiple sclerosis acquire disability. *Brain* (2022) 145:3147–3161. doi: 10.1093/BRAIN/AWAC016
50. Ontaneda D. Progressive Multiple Sclerosis. *Continuum (Minneap Minn)* (2019) 25:736–752. doi: 10.1212/CON.0000000000000727
51. SCHUMACHER GA. MULTIPLE SCLEROSIS. *Med Clin North Am* (1963) 47:1603–1617. doi: 10.1016/S0025-7125(16)33512-X
52. Poser CM, Paty DW, Scheinberg L, McDonald WI, Davis FA, Ebers GC, Johnson KP, Sibley WA, Silberberg DH, Tourtellotte WW. New diagnostic criteria for multiple sclerosis:

Guidelines for research protocols. *Ann Neurol* (1983) 13:227–231. doi: 10.1002/ANA.410130302,
53. Thompson AJ, Banwell BL, Barkhof F, Carroll WM, Coetzee T, Comi G, Correale J, Fazekas F, Filippi M, Freedman MS, et al. Diagnosis of multiple sclerosis: 2017 revisions of the McDonald criteria. *Lancet Neurol* (2018) 17:162–173. doi: 10.1016/S1474-4422(17)30470-2
54. Schwenkenbecher P, Wurster U, Konen FF, Gingele S, Sühs KW, Wattjes MP, Stangel M, Skripuletz T. Impact of the McDonald Criteria 2017 on Early Diagnosis of Relapsing-Remitting Multiple Sclerosis. *Front Neurol* (2019) 10: doi: 10.3389/FNEUR.2019.00188
55. Solomon AJ, Naismith RT, Cross AH. Misdiagnosis of multiple sclerosis: Impact of the 2017 McDonald criteria on clinical practice. *Neurology* (2019) 92:26–33. doi: 10.1212/WNL.0000000000006583
56. Kurtzke JF. Rating neurologic impairment in multiple sclerosis: an expanded disability status scale (EDSS). *Neurology* (1983) 33:1444–1452. doi: 10.1212/WNL.33.11.1444
57. Degenhardt A, Ramagopalan S V., Scalfari A, Ebers GC. Clinical prognostic factors in multiple sclerosis: a natural history review. *Nat Rev Neurol* (2009) 5:672–682. doi: 10.1038/NRNEUROL.2009.178
58. Magyari M, Sorensen PS. Comorbidity in Multiple Sclerosis. *Front Neurol* (2020) 11: doi: 10.3389/FNEUR.2020.00851
59. Cortese R, Giorgio A, Severa G, De Stefano N. MRI Prognostic Factors in Multiple Sclerosis, Neuromyelitis Optica Spectrum Disorder, and Myelin Oligodendrocyte Antibody Disease. *Front Neurol* (2021) 12: doi: 10.3389/FNEUR.2021.679881
60. Hauser SL, Cree BAC. Treatment of Multiple Sclerosis: A Review. *Am J Med* (2020) 133:1380-1390.e2. doi: 10.1016/J.AMJMED.2020.05.049
61. Barnes MP, Bateman DE, Cleland PG, Dick DJ, Walls TJ, Newman PK, Saunders M, Tilley PJ. Intravenous methylprednisolone for multiple sclerosis in relapse. *J Neurol Neurosurg Psychiatry* (1985) 48:157–159. doi: 10.1136/JNNP.48.2.157,
62. Fierro B, Salemi G, Brighina F, Buffa D, Conte S, La Bua V, Piazza A, Savettieri G. A transcranial magnetic stimulation study evaluating methylprednisolone treatment in multiple sclerosis. *Acta Neurol Scand* (2002) 105:152–157. doi: 10.1034/J.1600-0404.2002.1O369.X,
63. Iacono S, Schirò G, Salemi G, Scirè E, Aridon P, Melfa M, Andolina M, Sorbello G, Calì A, Brighina F, et al. Efficacy and Safety of Rescue Treatment with Plasma Exchange in Patients with Acute Inflammatory Neurological Disorders: A Single Center Experience. *Neurol Int* (2024) 16:761–775. doi: 10.3390/NEUROLINT16040056,
64. Rae-Grant A, Day GS, Marrie RA, Rabinstein A, Cree BAC, Gronseth GS, Haboubi M, Halper J, Hosey JP, Jones DE, et al. Practice guideline recommendations summary: Disease-modifying therapies for adults with multiple sclerosis: Report of the Guideline Development, Dissemination, and Implementation Subcommittee of the American Academy of Neurology. *Neurology* (2018) 90:777–788. doi: 10.1212/WNL.0000000000005347
65. Filippi M, Amato MP, Centonze D, Gallo P, Gasperini C, Inglese M, Patti F, Pozzilli C, Preziosa P, Trojano M. Early use of high-efficacy disease-modifying therapies makes the difference in people with multiple sclerosis: an expert opinion. *J Neurol* (2022) 269:5382–5394. doi: 10.1007/S00415-022-11193-W,
66. Jakimovski D, Kolb C, Ramanathan M, Zivadinov R, Weinstock-Guttman B. Interferon β for Multiple Sclerosis. *Cold Spring Harb Perspect Med* (2018) 8: doi: 10.1101/CSHPERSPECT.A032003
67. Axisa PP, Hafler DA. Multiple sclerosis: genetics, biomarkers, treatments. *Curr Opin Neurol* (2016) 29:345–353. doi: 10.1097/WCO.0000000000000319
68. Polman CH, O'Connor PW, Havrdova E, Hutchinson M, Kappos L, Miller DH, Phillips JT, Lublin FD, Giovannoni G, Wajgt A, et al. A Randomized, Placebo-Controlled Trial of

Natalizumab for Relapsing Multiple Sclerosis. *New England Journal of Medicine* (2006) 354:899–910. doi: 10.1056/NEJMOA044397,
69. McGinley MP, Cohen JA. Sphingosine 1-phosphate receptor modulators in multiple sclerosis and other conditions. *The Lancet* (2021) 398:1184–1194. doi: 10.1016/S0140-6736(21)00244-0
70. Kappos L, Radue E-W, O'Connor P, Polman C, Hohlfeld R, Calabresi P, Selmaj K, Agoropoulou C, Leyk M, Zhang-Auberson L, et al. A placebo-controlled trial of oral fingolimod in relapsing multiple sclerosis. *N Engl J Med* (2010) 362:387–401. doi: 10.1056/NEJMOA0909494
71. Carotenuto A, Di Monaco C, Papetti L, Borriello G, Signoriello E, Masciulli C, Tomassini V, De Luca G, Ianniello A, Lus G, et al. Pediatric-onset Multiple Sclerosis treatment: a multicentre observational study comparing natalizumab with fingolimod. *J Neurol* (2024) 271:6773–6781. doi: 10.1007/S00415-024-12610-Y,
72. Cree BAC, Arnold DL, Fox RJ, Gold R, Vermersch P, Benedict RHB, Bar-Or A, Piani-Meier D, Rouyrre N, Ritter S, et al. Long-term efficacy and safety of siponimod in patients with secondary progressive multiple sclerosis: Analysis of EXPAND core and extension data up to >5 years. *Mult Scler* (2022) 28:1591–1605. doi: 10.1177/13524585221083194
73. Kappos L, Fox RJ, Burcklen M, Freedman MS, Havrdová EK, Hennessy B, Hohlfeld R, Lublin F, Montalban X, Pozzilli C, et al. Ponesimod Compared with Teriflunomide in Patients with Relapsing Multiple Sclerosis in the Active-Comparator Phase 3 OPTIMUM Study: A Randomized Clinical Trial. *JAMA Neurol* (2021) 78:558–567. doi: 10.1001/JAMANEUROL.2021.0405,
74. Gärtner J, Hauser SL, Bar-Or A, Montalban X, Cohen JA, Cross AH, Deiva K, Ganjgahi H, Häring DA, Li B, et al. Efficacy and safety of ofatumumab in recently diagnosed, treatment-naive patients with multiple sclerosis: Results from ASCLEPIOS I and II. *Multiple Sclerosis Journal* (2022) 28:1562–1575. doi: 10.1177/13524585221078825,
75. Rizzo MA, Hadjimichael OC, Preiningerova J, Vollmer TL. Prevalence and treatment of spasticity reported by multiple sclerosis patients. *Mult Scler* (2004) 10:589–595. doi: 10.1191/1352458504MS1085OA
76. Young IR, Hall AS, Pallis CA, Bydder GM, Legg NJ, Steiner RE. NUCLEAR MAGNETIC RESONANCE IMAGING OF THE BRAIN IN MULTIPLE SCLEROSIS. *The Lancet* (1981) 318:1063–1066. doi: 10.1016/S0140-6736(81)91273-3,
77. McDonald WI, Compston A, Edan G, Goodkin D, Hartung HP, Lublin FD, McFarland HF, Paty DW, Polman CH, Reingold SC, et al. Recommended diagnostic criteria for multiple sclerosis: guidelines from the International Panel on the diagnosis of multiple sclerosis. *Ann Neurol* (2001) 50:121–127. doi: 10.1002/ANA.1032
78. Sati P, Oh J, Todd Constable R, Evangelou N, Guttmann CRG, Henry RG, Klawiter EC, Mainero C, Massacesi L, McFarland H, et al. The central vein sign and its clinical evaluation for the diagnosis of multiple sclerosis: A consensus statement from the North American Imaging in Multiple Sclerosis Cooperative. *Nat Rev Neurol* (2016) 12:714–722. doi: 10.1038/NRNEUROL.2016.166,
79. Filippi M, Rocca MA, Ciccarelli O, De Stefano N, Evangelou N, Kappos L, Rovira A, Sastre-Garriga J, Tintorè M, Frederiksen JL, et al. MRI criteria for the diagnosis of multiple sclerosis: MAGNIMS consensus guidelines. *Lancet Neurol* (2016) 15:292–303. doi: 10.1016/S1474-4422(15)00393-2
80. Rovira Á, Wattjes MP, Tintoré M, Tur C, Yousry TA, Sormani MP, De Stefano N, Filippi M, Auger C, Rocca MA, et al. Evidence-based guidelines: MAGNIMS consensus guidelines on the use of MRI in multiple sclerosis - Clinical implementation in the diagnostic process. *Nat Rev Neurol* (2015) 11:471–482. doi: 10.1038/NRNEUROL.2015.106,
81. Bakshi R, Minagar A, Jaisani Z, Wolinsky JS. Imaging of multiple sclerosis: Role in neurotherapeutics. *NeuroRx* (2005) 2:277–303. doi: 10.1602/NEURORX.2.2.277,

82. Bagnato F, Sati P, Hemond CC, Elliott C, Gauthier SA, Harrison DM, Mainero C, Oh J, Pitt D, Shinohara RT, et al. Imaging chronic active lesions in multiple sclerosis: a consensus statement. *Brain* (2024) 147:2913–2933. doi: 10.1093/BRAIN/AWAE013,
83. Wattjes MP, Ciccarelli O, Reich DS, Banwell B, de Stefano N, Enzinger C, Fazekas F, Filippi M, Frederiksen J, Gasperini C, et al. 2021 MAGNIMS–CMSC–NAIMS consensus recommendations on the use of MRI in patients with multiple sclerosis. *Lancet Neurol* (2021) 20:653–670. doi: 10.1016/S1474-4422(21)00095-8,
84. Gasperini C, Prosperini L, Tintoré M, Sormani MP, Filippi M, Rio J, Palace J, Rocca MA, Ciccarelli O, Barkhof F, et al. Unraveling treatment response in multiple sclerosis: A clinical and MRI challenge. *Neurology* (2019) 92:180–192. doi: 10.1212/WNL.0000000000006810,
85. Thormann A, Magyari M, Koch-Henriksen N, Laursen B, Sørensen PS. Vascular comorbidities in multiple sclerosis: a nationwide study from Denmark. *J Neurol* (2016) 263:2484–2493. doi: 10.1007/S00415-016-8295-9,
86. Grebenciucova E, Pruitt A. Infections in Patients Receiving Multiple Sclerosis Disease-Modifying Therapies. *Curr Neurol Neurosci Rep* (2017) 17: doi: 10.1007/S11910-017-0800-8,
87. Jordan ALM, Yang J, Fisher CJ, Racke MK, Mao-Draayer Y. Progressive multifocal leukoencephalopathy in dimethyl fumarate-treated multiple sclerosis patients. *Multiple Sclerosis Journal* (2022) 28:7–15. doi: 10.1177/1352458520949158,
88. Gerevini S, Capra R, Bertoli D, Sottini A, Imberti L. Immune profiling of a patient with alemtuzumab-associated progressive multifocal leukoencephalopathy. *Multiple Sclerosis Journal* (2019) 25:1196–1201. doi: 10.1177/1352458519832259,
89. Nakahara J, Tomaske L, Kume K, Takata T, Kamada M, Deguchi K, Kufukihara K, Schneider R, Gold R, Ayzenberg I. Three cases of non-carryover fingolimod-PML: Is the risk in Japan increased? *Neurol Neuroimmunol Neuroinflamm* (2019) 6: doi: 10.1212/NXI.0000000000000559,
90. Sørensen PS, Bertolotto A, Edan G, Giovannoni G, Gold R, Havrdova E, Kappos L, Kieseier BC, Montalban X, Olsson T. Risk stratification for progressive multifocal leukoencephalopathy in patients treated with natalizumab. *Multiple Sclerosis Journal* (2012) 18:143–152. doi: 10.1177/1352458511435105,
91. Yousry TA, Pelletier D, Cadavid D, Gass A, Richert ND, Radue EW, Filippi M. Magnetic resonance imaging pattern in natalizumab-associated progressive multifocal leukoencephalopathy. *Ann Neurol* (2012) 72:779–787. doi: 10.1002/ANA.23676,
92. Wattjes MP, Richert ND, Killestein J, De Vos M, Sanchez E, Snaebjornsson P, Cadavid D, Barkhof F. The chameleon of neuroinflammation: Magnetic resonance imaging characteristics of natalizumab-associated progressive multifocal leukoencephalopathy. *Multiple Sclerosis Journal* (2013) 19:1826–1840. doi: 10.1177/1352458513510224/ASSET/8447A5F7-EC7E-43E9-8D8C-68F9F05399B3/ASSETS/IMAGES/LARGE/10.1177_1352458513510224-FIG11.JPG
93. Ryerson LZ, Foley J, Chang I, Kister I, Cutter G, Metzger RR, Goldberg JD, Li X, Riddle E, Smirnakis K, et al. Risk of natalizumab-associated PML in patients with MS is reduced with extended interval dosing. *Neurology* (2019) 93:e1452–e1462. doi: 10.1212/WNL.0000000000008243,
94. Dong-Si T, Richman S, Wattjes MP, Wenten M, Gheuens S, Philip J, Datta S, McIninch J, Bozic C, Bloomgren G, et al. Outcome and survival of asymptomatic PML in natalizumab-treated MS patients. *Ann Clin Transl Neurol* (2014) 1:755–764. doi: 10.1002/ACN3.114,
95. Scarpazza C, Signori A, Cosottini M, Sormani MP, Gerevini S, Capra R. Should frequent MRI monitoring be performed in natalizumab-treated MS patients? A contribution to a recent debate. *Multiple Sclerosis Journal* (2020) 26:1227–1236. doi: 10.1177/1352458519854162,

96. van der Molen AJ, Quattrocchi CC, Mallio CA, Dekkers IA. Ten years of gadolinium retention and deposition: ESMRMB-GREC looks backward and forward. *Eur Radiol* (2024) 34:600–611. doi: 10.1007/S00330-023-10281-3,
97. Domingo JL, Semelka RC. Gadolinium toxicity: mechanisms, clinical manifestations, and nanoparticle role. *Arch Toxicol* (2025) doi: 10.1007/S00204-025-04124-X,
98. Frenzel T, Lengsfeld P, Schirmer H, Hütter J, Weinmann HJ. Stability of gadolinium-based magnetic resonance imaging contrast agents in human serum at 37°C. *Invest Radiol* (2008) 43:817–828. doi: 10.1097/RLI.0B013E3181852171,
99. Sørensen TJ, Faulkner S. Multimetallic Lanthanide Complexes: Using Kinetic Control to Define Complex Multimetallic Arrays. *Acc Chem Res* (2018) 51:2493–2501. doi: 10.1021/ACS.ACCOUNTS.8B00205,
100. Marckmann P, Skov L, Rossen K, Dupont A, Damholt MB, Heaf JG, Thomsen HS. Nephrogenic systemic fibrosis: Suspected causative role of gadodiamide used for contrast-enhanced magnetic resonance imaging. *Journal of the American Society of Nephrology* (2006) 17:2359–2362. doi: 10.1681/ASN.2006060601,
101. Lancelot E. Revisiting the Pharmacokinetic Profiles of Gadolinium-Based Contrast Agents. *Invest Radiol* (2016) 51:691–700. doi: 10.1097/RLI.0000000000000280,
102. Fur M Le, Moon BF, Zhou IY, Zygmont S, Boice A, Rotile NJ, Ay I, Pantazopoulos P, Feldman AS, Rosales IA, et al. Gadolinium-based Contrast Agent Biodistribution and Speciation in Rats. *Radiology* (2023) 309: doi: 10.1148/RADIOL.230984/ASSET/IMAGES/LARGE/RADIOL.230984.TBL2.JPEG
103. Idée JM, Port M, Raynal I, Schaefer M, Le Greneur S, Corot C. Clinical and biological consequences of transmetallation induced by contrast agents for magnetic resonance imaging: A review. *Fundam Clin Pharmacol* (2006) 20:563–576. doi: 10.1111/J.1472-8206.2006.00447.X,
104. Rasschaert M, Weller RO, Schroeder JA, Brochhausen C, Idée JM. Retention of Gadolinium in Brain Parenchyma: Pathways for Speciation, Access, and Distribution. A Critical Review. *Journal of Magnetic Resonance Imaging* (2020) 52:1293–1305. doi: 10.1002/JMRI.27124,
105. Taoka T, Naganawa S. Gadolinium-based contrast media, cerebrospinal fluid and the glymphatic system: Possible mechanisms for the deposition of gadolinium in the brain. *Magnetic Resonance in Medical Sciences* (2018) 17:111–119. doi: 10.2463/MRMS.REV.2017-0116,
106. Deike-Hofmann K, Reuter J, Haase R, Paech D, Gnirs R, Bickelhaupt S, Forsting M, Heußel CP, Schlemmer HP, Radbruch A. Glymphatic Pathway of Gadolinium-Based Contrast Agents Through the Brain: Overlooked and Misinterpreted. *Invest Radiol* (2019) 54:229–237. doi: 10.1097/RLI.0000000000000533,
107. Kanda T, Matsuda M, Oba H, Toyoda K, Furui S. Gadolinium deposition after contrastenhanced MR imaging. *Radiology* (2015) 277:924–925. doi: 10.1148/RADIOL.2015150697;WEBSITE:WEBSITE:RSNA-SITE;REQUESTEDJOURNAL:JOURNAL:RADIOLOGY;WGROUP:STRING:RSNA
108. Laurent S, Vander Elst L, Copoix F, Muller RN. Stability of MRI paramagnetic contrast media: A proton relaxometric protocol for transmetallation assessment. *Invest Radiol* (2001) 36:115–122. doi: 10.1097/00004424-200102000-00008,
109. Uzal-Varela R, Rodríguez-Rodríguez A, Wang H, Esteban-Gómez D, Brandariz I, Gale EM, Caravan P, Platas-Iglesias C. Prediction of Gd(III) complex thermodynamic stability. *Coord Chem Rev* (2022) 467:214606. doi: 10.1016/J.CCR.2022.214606
110. Gianolio E, Bardini P, Arena F, Stefania R, Gregorio E DI, Iani R, Aime S. Gadolinium retention in the rat brain: Assessment of the amounts of insoluble gadolinium-containing species and intact gadolinium complexes after repeated administration of gadolinium-based contrast agents. *Radiology* (2017) 285:839–849. doi: 10.1148/RADIOL.2017162857;PAGEGROUP:STRING:PUBLICATION

111. Henderson IM, Benevidez AD, Mowry CD, Watt J, Bachand GD, Kirk ML, Dokładny K, DeAguero J, Escobar GP, Wagner B. Precipitation of gadolinium from magnetic resonance imaging contrast agents may be the Brass tacks of toxicity. *Magn Reson Imaging* (2025) 119:110383. doi: 10.1016/J.MRI.2025.110383
112. Lansman JB. Blockade of current through single calcium channels by trivalent lanthanide cations: Effect of ionic radius on the rates of ion entry and exit. *Journal of General Physiology* (1990) 95:679–696. doi: 10.1085/JGP.95.4.679,
113. Kanda T, Ishii K, Kawaguchi H, Kitajima K, Takenaka D. High signal intensity in the dentate nucleus and globus pallidus on unenhanced T1-weighted MR images: Relationship with increasing cumulative dose of a gadoliniumbased contrast material. *Radiology* (2014) 270:834–841. doi: 10.1148/RADIOL.13131669,
114. Roccatagliata L, Vuolo L, Bonzano L, Pichiecchio A, Mancardi GL. Multiple sclerosis: Hyperintense dentate nucleus on unenhanced T1-weighted MR images is associated with the secondary progressive subtype. *Radiology* (2009) 251:503–510. doi: 10.1148/RADIOL.2511081269,
115. Errante Y, Cirimele V, Mallio CA, Di Lazzaro V, Zobel BB, Quattrocchi CC. Progressive increase of T1 signal intensity of the dentate nucleus on unenhanced magnetic resonance images is associated with cumulative doses of intravenously administered gadodiamide in patients with normal renal function, suggesting dechelation. *Invest Radiol* (2014) 49:685–690. doi: 10.1097/RLI.0000000000000072,
116. Minaeva O, Hua N, Franz ES, Lupoli N, Mian AZ, Farris CW, Hildebrandt AM, Kiernan PT, Evers LE, Griffin AD, et al. Nonhomogeneous gadolinium retention in the cerebral cortex after intravenous administration of gadolinium-based contrast agent in rats and humans. *Radiology* (2020) 294:377–385. doi: 10.1148/RADIOL.2019190461,
117. El Hamrani D, Vives V, Buchholz R, Même W, Factor C, Fingerhut S, Sperling M, Karst U, Robert P, Même S. Effect of Long-Term Retention of Gadolinium on Metabolism of Deep Cerebellar Nuclei after Repeated Injections of Gadodiamide in Rats. *Invest Radiol* (2020) 55:120–128. doi: 10.1097/RLI.0000000000000621,
118. Davies J, Marino M, Smith APL, Crowder JM, Larsen M, Lowery L, Castle J, Hibberd MG, Evans PM. Repeat and single dose administration of gadodiamide to rats to investigate concentration and location of gadolinium and the cell ultrastructure. *Sci Rep* (2021) 11:13950. doi: 10.1038/S41598-021-93147-2,
119. Robert P, Lehericy S, Grand S, Violas X, Fretellier N, Ideé JM, Ballet S, Corot C. T1-Weighted Hypersignal in the Deep Cerebellar Nuclei after Repeated Administrations of Gadolinium-Based Contrast Agents in Healthy Rats: Difference between Linear and Macrocyclic Agents. *Invest Radiol* (2015) 50:473–480. doi: 10.1097/RLI.0000000000000181,
120. Jost G, Lenhard DC, Sieber MA, Lohrke J, Frenzel T, Pietsch H. Signal increase on unenhanced T1-weighted images in the rat brain after repeated, extended doses of gadolinium-based contrast agents comparison of linear and macrocyclic agents. *Invest Radiol* (2016) 51:83–89. doi: 10.1097/RLI.0000000000000242,
121. Guo BJ, Yang ZL, Zhang LJ. Gadolinium Deposition in Brain: Current Scientific Evidence and Future Perspectives. *Front Mol Neurosci* (2018) 11: doi: 10.3389/FNMOL.2018.00335,
122. Mallio CA, Lo Vullo G, Messina L, Beomonte Zobel B, Parizel PM, Quattrocchi CC. Increased T1 signal intensity of the anterior pituitary gland on unenhanced magnetic resonance images after chronic exposure to gadodiamide. *Invest Radiol* (2020) 55:25–29. doi: 10.1097/RLI.0000000000000604,
123. Wang S, Hesse B, Roman M, Stier D, Castillo-Michel H, Cotte M, Suuronen JP, Lagrange A, Radbruch H, Paul F, et al. Increased Retention of Gadolinium in the Inflamed Brain after Repeated Administration of Gadopentetate Dimeglumine: A Proof-of-Concept Study in Mice

Combining ICP-MS and Micro- A nd Nano-SR-XRF. *Invest Radiol* (2019) 54:617–626. doi: 10.1097/RLI.0000000000000571,
124. Robert P, Fingerhut S, Factor C, Vives V, Letien J, Sperling M, Rasschaert M, Santus R, Ballet S, Idée JM, et al. One-year retention of gadolinium in the brain: Comparison of gadodiamide and gadoterate meglumine in a rodent model. *Radiology* (2018) 288:424–433. doi: 10.1148/RADIOL.2018172746,
125. Jost G, Frenzel T, Boyken J, Lohrke J, Nischwitz V, Pietsch H. Long-term Excretion of Gadolinium-based Contrast Agents: Linear versus Macrocyclic Agents in an Experimental Rat Model. *Radiology* (2019) 290:340–348. doi: 10.1148/RADIOL.2018180135,
126. Frenzel T, Apte C, Jost G, Schöckel L, Lohrke J, Pietsch H. Quantification and assessment of the chemical form of residual gadolinium in the brain after repeated administration of gadolinium-based contrast agents comparative study in rats. *Invest Radiol* (2017) 52:396–404. doi: 10.1097/RLI.0000000000000352,
127. Strzeminska I, Factor C, Jimenez-Lamana J, Lacomme S, Subirana MA, Le Coustumer P, Schaumlöffel D, Robert P, Szpunar J, Corot C, et al. Comprehensive Speciation Analysis of Residual Gadolinium in Deep Cerebellar Nuclei in Rats Repeatedly Administered With Gadoterate Meglumine or Gadodiamide. *Invest Radiol* (2022) 57:283–292. doi: 10.1097/RLI.0000000000000846,
128. Strzeminska I, Factor C, Robert P, Szpunar J, Corot C, Lobinski R. Speciation Analysis of Gadolinium in the Water-Insoluble Rat Brain Fraction after Administration of Gadolinium-Based Contrast Agents. *Invest Radiol* (2021) 56:535–544. doi: 10.1097/RLI.0000000000000774,
129. Gianolio E, Bardini P, Arena F, Stefania R, Gregorio E DI, Iani R, Aime S. Gadolinium retention in the rat brain: Assessment of the amounts of insoluble gadolinium-containing species and intact gadolinium complexes after repeated administration of gadolinium-based contrast agents. *Radiology* (2017) 285:839–849. doi: 10.1148/RADIOL.2017162857,
130. Fretellier N, Granottier A, Rasschaert M, Grindel AL, Baudimont F, Robert P, Idée JM, Corot C. Does age interfere with gadolinium toxicity and presence in brain and bone tissues?: A comparative gadoterate versus gadodiamide study in juvenile and adult rats. *Invest Radiol* (2019) 54:61–71. doi: 10.1097/RLI.0000000000000517,
131. Smith APL, Marino M, Roberts J, Crowder JM, Castle J, Lowery L, Morton C, Hibberd MG, Evans PM. Clearance of gadolinium from the brain with no pathologic effect after repeated administration of gadodiamide in healthy rats: An analytical and histologic study. *Radiology* (2017) 282:743–751. doi: 10.1148/RADIOL.2016160905,
132. Davies J, Marino M, Smith APL, Crowder JM, Larsen M, Lowery L, Castle J, Hibberd MG, Evans PM. Repeat and single dose administration of gadodiamide to rats to investigate concentration and location of gadolinium and the cell ultrastructure. *Sci Rep* (2021) 11:13950. doi: 10.1038/S41598-021-93147-2,
133. El Hamrani D, Vives V, Buchholz R, Même W, Factor C, Fingerhut S, Sperling M, Karst U, Robert P, Même S. Effect of Long-Term Retention of Gadolinium on Metabolism of Deep Cerebellar Nuclei after Repeated Injections of Gadodiamide in Rats. *Invest Radiol* (2020) 55:120–128. doi: 10.1097/RLI.0000000000000621,
134. Robert P, Violas X, Grand S, Lehericy S, Idée JM, Ballet S, Corot C. Linear gadolinium-based contrast agents are associated with brain gadolinium retention in healthy rats. *Invest Radiol* (2016) 51:73–82. doi: 10.1097/RLI.0000000000000241,
135. Jost G, Lenhard DC, Sieber MA, Lohrke J, Frenzel T, Pietsch H. Signal increase on unenhanced T1-weighted images in the rat brain after repeated, extended doses of gadolinium-based contrast agents comparison of linear and macrocyclic agents. *Invest Radiol* (2016) 51:83–89. doi: 10.1097/RLI.0000000000000242,

136. Oh H, Chung YE, You JS, Joo CG, Kim PK, Lim JS, Kim MJ. Gadolinium retention in rat abdominal organs after administration of gadoxetic acid disodium compared to gadodiamide and gadobutrol. *Magn Reson Med* (2020) 84:2124–2132. doi: 10.1002/MRM.28249,
137. Kühn I, Maschke H, Großmann A, Hauenstein K, Weber MA, Zettl UK, Storch A, Walter U. Dentate-nucleus gadolinium deposition on magnetic resonance imaging: ultrasonographic and clinical correlates in multiple sclerosis patients. *Neurol Sci* (2022) 43:2631–2639. doi: 10.1007/S10072-021-05702-4
138. Robert P, Fingerhut S, Factor C, Vives V, Letien J, Sperling M, Rasschaert M, Santus R, Ballet S, Idée JM, et al. One-year retention of gadolinium in the brain: Comparison of gadodiamide and gadoterate meglumine in a rodent model. *Radiology* (2018) 288:424–433. doi: 10.1148/RADIOL.2018172746,
139. Nakamura R, Takanezawa Y, Ohshiro Y, Uraguchi S, Kiyono M. Effects of chemical forms of gadolinium on the spleen in mice after single intravenous administration. *Biochem Biophys Rep* (2022) 29: doi: 10.1016/j.bbrep.2022.101217
140. Jost G, Frenzel T, Boyken J, Pietsch H. Impact of brain tumors and radiotherapy on the presence of gadolinium in the brain after repeated administration of gadolinium-based contrast agents: an experimental study in rats. *Neuroradiology* (2019) 61:1273–1280. doi: 10.1007/S00234-019-02256-3,
141. Smith APL, Marino M, Roberts J, Crowder JM, Castle J, Lowery L, Morton C, Hibberd MG, Evans PM. Clearance of gadolinium from the brain with no pathologic effect after repeated administration of gadodiamide in healthy rats: An analytical and histologic study. *Radiology* (2017) 282:743–751. doi: 10.1148/RADIOL.2016160905,
142. Jost G, Frenzel T, Boyken J, Lohrke J, Nischwitz V, Pietsch H. Long-term Excretion of Gadolinium-based Contrast Agents: Linear versus Macrocyclic Agents in an Experimental Rat Model. *Radiology* (2019) 290:340–348. doi: 10.1148/RADIOL.2018180135,
143. Wang S, Hesse B, Roman M, Stier D, Castillo-Michel H, Cotte M, Suuronen JP, Lagrange A, Radbruch H, Paul F, et al. Increased Retention of Gadolinium in the Inflamed Brain after Repeated Administration of Gadopentetate Dimeglumine: A Proof-of-Concept Study in Mice Combining ICP-MS and Micro- A nd Nano-SR-XRF. *Invest Radiol* (2019) 54:617–626. doi: 10.1097/RLI.0000000000000571,
144. Barisano G, Bigjahan B, Metting S, Cen S, Amezcua L, Lerner A, Toga AW, Law M. Signal hyperintensity on unenhanced T1-weighted brain and cervical spinal cord MR images after multiple doses of linear gadolinium-based contrast agent. *American Journal of Neuroradiology* (2019) 40:1274–1281. doi: 10.3174/AJNR.A6148,
145. Conte G, Preda L, Cocorocchio E, Raimondi S, Giannitto C, Minotti M, De Piano F, Petralia G, Ferrucci PF, Bellomi M. Signal intensity change on unenhanced T1-weighted images in dentate nucleus and globus pallidus after multiple administrations of gadoxetate disodium: an intraindividual comparative study. *Eur Radiol* (2017) 27:4372–4378. doi: 10.1007/S00330-017-4810-3,
146. Young JR, Qiao J, Orosz I, Salamon N, Franke MA, Kim HJ, Pope WB. Gadolinium deposition within the paediatric brain: no increased intrinsic T1-weighted signal intensity within the dentate nucleus following the administration of a minimum of four doses of the macrocyclic agent gadobutrol. *Eur Radiol* (2018) 28:4882–4889. doi: 10.1007/S00330-018-5464-5,
147. Werner P, Taupitz M, Schröder L, Schuenke P. An NMR relaxometry approach for quantitative investigation of the transchelation of gadolinium ions from GBCAs to a competing macromolecular chelator. *Sci Rep* (2021) 11: doi: 10.1038/S41598-021-00974-4,
148. Bussi S, Coppo A, Bonafè R, Rossi S, Colombo Serra S, Penard L, Kirchin MA, Maisano F, Tedoldi F. Gadolinium Clearance in the First 5 Weeks After Repeated Intravenous Administration of Gadoteridol, Gadoterate Meglumine, and Gadobutrol to rats. *Journal of Magnetic Resonance Imaging* (2021) 54:1636–1644. doi: 10.1002/JMRI.27693,

149. Bussi S, Coppo A, Celeste R, Fanizzi A, Fringuello Mingo A, Ferraris A, Botteron C, Kirchin MA, Tedoldi F, Maisano F. Macrocyclic MR contrast agents: evaluation of multiple-organ gadolinium retention in healthy rats. *Insights Imaging* (2020) 11: doi: 10.1186/S13244-019-0824-5,
150. Fretellier N, Granottier A, Rasschaert M, Grindel AL, Baudimont F, Robert P, Idée JM, Corot C. Does age interfere with gadolinium toxicity and presence in brain and bone tissues?: A comparative gadoterate versus gadodiamide study in juvenile and adult rats. *Invest Radiol* (2019) 54:61–71. doi: 10.1097/RLI.0000000000000517,
151. Robert P, Lehericy S, Grand S, Violas X, Fretellier N, Ideé JM, Ballet S, Corot C. T1-Weighted Hypersignal in the Deep Cerebellar Nuclei after Repeated Administrations of Gadolinium-Based Contrast Agents in Healthy Rats: Difference between Linear and Macrocyclic Agents. *Invest Radiol* (2015) 50:473–480. doi: 10.1097/RLI.0000000000000181,
152. Errante Y, Cirimele V, Mallio CA, Di Lazzaro V, Zobel BB, Quattrocchi CC. Progressive increase of T1 signal intensity of the dentate nucleus on unenhanced magnetic resonance images is associated with cumulative doses of intravenously administered gadodiamide in patients with normal renal function, suggesting dechelation. *Invest Radiol* (2014) 49:685–690. doi: 10.1097/RLI.0000000000000072,
153. Ramalho J, Semelka RC, AlObaidy M, Ramalho M, Nunes RH, Castillo M. Signal intensity change on unenhanced T1-weighted images in dentate nucleus following gadobenate dimeglumine in patients with and without previous multiple administrations of gadodiamide. *Eur Radiol* (2016) 26:4080–4088. doi: 10.1007/S00330-016-4269-7,
154. Quattrocchi CC, Mallio CA, Errante Y, Cirimele V, Carideo L, Ax A, Zobel BB. Gadodiamide and dentate nucleus T1 hyperintensity in patients with meningioma evaluated by multiple follow-up contrast-enhanced magnetic resonance examinations with no systemic interval therapy. *Invest Radiol* (2015) 50:470–472. doi: 10.1097/RLI.0000000000000154
155. Mallio CA, Lo Vullo G, Messina L, Beomonte Zobel B, Parizel PM, Quattrocchi CC. Increased T1 signal intensity of the anterior pituitary gland on unenhanced magnetic resonance images after chronic exposure to gadodiamide. *Invest Radiol* (2020) 55:25–29. doi: 10.1097/RLI.0000000000000604,
156. Mallio CA, Messina L, Parillo M, Lo Vullo G, Beomonte Zobel B, Parizel PM, Quattrocchi CC. Anterior pituitary gland T1 signal intensity is influenced by time delay after injection of gadodiamide. *Sci Rep* (2020) 10: doi: 10.1038/S41598-020-71981-0,
157. Mallio CA, Parillo M, Zobel BB, Parizel PM, Quattrocchi CC. Effect of Exposure to Gadodiamide and Brain Irradiation on T1-Weighted Images and ADC Maps of the Dentate Nucleus. *Journal of Magnetic Resonance Imaging* (2020) 52:1525–1530. doi: 10.1002/JMRI.27198,
158. Zhang Y, Cao Y, Shih GL, Hecht EM, Prince MR. Extent of signal hyperintensity on unenhanced T1-weighted brain MR images after more than 35 administrations of linear gadolinium-based contrast agents. *Radiology* (2017) 282:516–525. doi: 10.1148/RADIOL.2016152864,
159. Nguyen NC, Molnar TT, Cummin LG, Kanal E. Dentate nucleus signal intensity increases following repeated gadobenate dimeglumine administrations: A retrospective analysis. *Radiology* (2020) 296:122–130. doi: 10.1148/RADIOL.2020190246,
160. Adin ME, Kleinberg L, Vaidya D, Zan E, Mirbagheri XS, Yousem XDM. Hyperintense dentate nuclei on t1-weighted mri: Relation to repeat gadolinium administration. *American Journal of Neuroradiology* (2015) 36:1859–1865. doi: 10.3174/AJNR.A4378,
161. Radbruch A, Weberling LD, Kieslich PJ, Eidel O, Burth S, Kickingereder P, Heiland S, Wick W, Schlemmer HP, Bendszus M. Gadolinium retention in the dentate nucleus and globus pallidus is dependent on the class of contrast agent. *Radiology* (2015) 275:783–791. doi: 10.1148/RADIOL.2015150337,

162. Bi Q, Li H, Du J, Li Q, Wang J, Huang Y, Gong X. Gadolinium deposition in the brain is related to various contrast agents: a matched case–control study. *Clin Radiol* (2022) 77:299–306. doi: 10.1016/J.CRAD.2021.12.020,
163. Schlemm L, Chien C, Bellmann-Strobl J, Dörr J, Wuerfel J, Brandt AU, Paul F, Scheel M. Gadopentetate but not gadobutrol accumulates in the dentate nucleus of multiple sclerosis patients. *Mult Scler* (2017) 23:963–972. doi: 10.1177/1352458516670738,
164. Kuno H, Jara H, Buch K, Qureshi MM, Chapman MN, Sakai O. Global and regional brain assessment with quantitative MR imaging in patients with prior exposure to linear gadolinium-based contrast agents. *Radiology* (2017) 283:195–204. doi: 10.1148/RADIOL.2016160674,
165. Weberling LD, Kieslich PJ, Kickingereder P, Wick W, Bendszus M, Schlemmer HP, Radbruch A. Increased signal intensity in the dentate nucleus on unenhanced t1-weighted images after gadobenate dimeglumine administration. *Invest Radiol* (2015) 50:743–748. doi: 10.1097/RLI.0000000000000206,
166. Kinner S, Schubert TB, Bruce RJ, Rebsamen SL, Diamond CA, Reeder SB, Rowley HA. Deep brain nuclei t1 shortening after gadobenate dimeglumine in children: Influence of radiation and chemotherapy. *American Journal of Neuroradiology* (2018) 39:24–30. doi: 10.3174/AJNR.A5453,
167. Kahn J, Posch H, Steffen IG, Geisel D, Bauknecht C, Liebig T, Denecke T. Is there long-Term signal intensity increase in the central nervous system on t1-weighted images after MR imaging with the hepatospecific contrast agent gadoxetic acid? A crosssectional study in 91 patients. *Radiology* (2017) 282:708–716. doi: 10.1148/RADIOL.2016162535,
168. Tedeschi E, Cocozza S, Borrelli P, Ugga L, Morra VB, Palma G. Longitudinal assessment of dentate nuclei relaxometry during massive gadobutrol exposure. *Magnetic Resonance in Medical Sciences* (2018) 17:100–104. doi: 10.2463/MRMS.CR.2016-0137,
169. Stojanov DA, Aracki-Trenkic A, Vojinovic S, Benedeto-Stojanov D, Ljubisavljevic S. Increasing signal intensity within the dentate nucleus and globus pallidus on unenhanced T1W magnetic resonance images in patients with relapsing-remitting multiple sclerosis: correlation with cumulative dose of a macrocyclic gadolinium-based contrast agent, gadobutrol. *Eur Radiol* (2016) 26:807–815. doi: 10.1007/S00330-015-3879-9,
170. Splendiani A, Perri M, Marsecano C, Vellucci V, Michelini G, Barile A, Di Cesare E. Effects of serial macrocyclic-based contrast materials gadoterate meglumine and gadobutrol administrations on gadolinium-related dentate nuclei signal increases in unenhanced T1-weighted brain: a retrospective study in 158 multiple sclerosis (MS) patients. *Radiologia Medica* (2018) 123:125–134. doi: 10.1007/S11547-017-0816-9,
171. Deike-Hofmann K, Reuter J, Haase R, Kuder T, Paech D, Bickelhaupt S, Forsting M, Schlemmer HP, Heußel CP, Radbruch A. No Changes in T1 Relaxometry after a Mean of 11 Administrations of Gadobutrol. *Invest Radiol* (2020) 55:381–386. doi: 10.1097/RLI.0000000000000650,
172. Lim WH, Choi SH, Yoo RE, Kang KM, Yun TJ, Kim JH, Sohn CH. Does radiation therapy increase gadolinium accumulation in the brain?: Quantitative analysis of T1 shortening using R1 relaxometry in glioblastoma multiforme patients. *PLoS One* (2018) 13: doi: 10.1371/JOURNAL.PONE.0192838,
173. Hinoda T, Fushimi Y, Okada T, Arakawa Y, Liu C, Yamamoto A, Okada T, Yoshida K, Miyamoto S, Togashi K. Quantitative assessment of gadolinium deposition in dentate nucleus using quantitative susceptibility mapping. *Journal of Magnetic Resonance Imaging* (2017) 45:1352–1358. doi: 10.1002/JMRI.25490,
174. Choi Y, Jang J, Kim J, Nam Y, Shin NY, Ahn KJ, Jeon SS, Kim BS. MRI and quantitative magnetic susceptibility maps of the brain after serial administration of gadobutrol: A longitudinal follow-up study. *Radiology* (2020) 297:143–150. doi: 10.1148/RADIOL.2020192579,

175. Neal CH, Pujara AC, Srinivasan A, Chenevert TL, Malyarenko D, Khalatbari S, Helvie MA, Noroozian M, Jeruss JS, Pearlman MD, et al. Prospective Imaging Trial Assessing Gadoteridol Retention in the Deep Brain Nuclei of Women Undergoing Breast MRI. *Acad Radiol* (2020) 27:1734–1741. doi: 10.1016/j.acra.2020.01.007
176. Kurtzke JF. Rating neurologic impairment in multiple sclerosis: an expanded disability status scale (EDSS). *Neurology* (1983) 33:1444–1452. doi: 10.1212/WNL.33.11.1444
177. Goetz CG, Tilley BC, Shaftman SR, Stebbins GT, Fahn S, Martinez-Martin P, Poewe W, Sampaio C, Stern MB, Dodel R, et al. Movement Disorder Society-Sponsored Revision of the Unified Parkinson's Disease Rating Scale (MDS-UPDRS): Scale presentation and clinimetric testing results. *Movement Disorders* (2008) 23:2129–2170. doi: 10.1002/MDS.22340,
178. Benedict RHB, Deluca J, Phillips G, LaRocca N, Hudson LD, Rudick R. Validity of the Symbol Digit Modalities Test as a cognition performance outcome measure for multiple sclerosis. *Multiple Sclerosis* (2017) 23:721–733. doi: 10.1177/1352458517690821/ASSET/57A1452F-8280-432D-AE7D-CA6ADACA6E15/ASSETS/IMAGES/LARGE/10.1177_1352458517690821-FIG2.JPG
179. Smith, A. (1982). Symbol Digit Modalities Test (SDMT). Manual (Revised). Los Angeles Western Psychological Services. https://www.scirp.org/reference/referencespapers?referenceid=975903 [Accessed September 7, 2025]
180. Nocentini U, Giordano A, Di Vincenzo S, Panella M, Pasqualetti P. The Symbol Digit Modalities Test - Oral version: Italian normative data. *Funct Neurol* (2006) 21:93–96. https://pubmed.ncbi.nlm.nih.gov/16796824/ [Accessed September 7, 2025]
181. Delgado C, Baweja M, Crews DC, Eneanya ND, Gadegbeku CA, Inker LA, Mendu ML, Miller WG, Moxey-Mims MM, Roberts G V., et al. A Unifying Approach for GFR Estimation: Recommendations of the NKF-ASN Task Force on Reassessing the Inclusion of Race in Diagnosing Kidney Disease. *American Journal of Kidney Diseases* (2022) 79:268-288.e1. doi: 10.1053/j.ajkd.2021.08.003
182. Bjørnerud A, Vatnehol SAS, Larsson C, Due-Tønnessen P, Hol PK, Groote IR. Signal Enhancement of the Dentate Nucleus at Unenhanced MR Imaging after Very High Cumulative Doses of the Macrocyclic Gadolinium-based Contrast Agent Gadobutrol: An Observational Study. *Radiology* (2017) 285:434–444. doi: 10.1148/RADIOL.2017170391
183. McDonald RJ, Levine D, Weinreb J, Kanal E, Davenport MS, Ellis JH, Jacobs PM, Lenkinski RE, Maravilla KR, Prince MR, et al. Gadolinium retention: A research roadmap from the 2018 NIH/ACR/RSNA workshop on gadolinium chelates. *Radiology* (2018) 289:517–534. doi: 10.1148/RADIOL.2018181151,
184. Harada T, Kudo K, Fujima N, Yoshikawa M, Ikebe Y, Sato R, Shirai T, Bito Y, Uwano I, Miyata M. Quantitative Susceptibility Mapping: Basic Methods and Clinical Applications. *Radiographics* (2022) 42:1161–1176. doi: 10.1148/RG.210054
185. Gillies MJ, Hyam JA, Weiss AR, Antoniades CA, Bogacz R, Fitzgerald JJ, Aziz TZ, Whittington MA, Green AL. The Cognitive Role of the Globus Pallidus interna; Insights from Disease States. *Exp Brain Res* (2017) 235:1455–1465. doi: 10.1007/S00221-017-4905-8
186. Münchau A, Mathen D, Cox T, Quinn NP, Marsden CD, Bhatia KP. Unilateral lesions of the globus pallidus: report of four patients presenting with focal or segmental dystonia. *J Neurol Neurosurg Psychiatry* (2000) 69:494–498. doi: 10.1136/JNNP.69.4.494
187. Welk B, McArthur E, Morrow SA, MacDonald P, Hayward J, Leung A, Lum A. Association Between Gadolinium Contrast Exposure and the Risk of Parkinsonism. *JAMA* (2016) 316:96–98. doi: 10.1001/JAMA.2016.8096
188. Vymazal J, Krámská L, Brožová H, Růžička E, Rulseh AM. Does serial administration of gadolinium-based contrast agents affect patient neurological and neuropsychological status?

Fourteen-year follow-up of patients receiving more than fifty contrast administrations. *J Magn Reson Imaging* (2020) 51:1912–1913. doi: 10.1002/JMRI.26948
189. Scaravilli A, Tranfa M, Pontillo G, Falco F, Criscuolo C, Moccia M, Monti S, Lanzillo R, Morra VB, Palma G, et al. MR Imaging Signs of Gadolinium Retention Are Not Associated with Long-Term Motor and Cognitive Outcomes in Multiple Sclerosis. *AJNR Am J Neuroradiol* (2023) 44:396. doi: 10.3174/AJNR.A7807
190. Cocozza S, Pontillo G, Lanzillo R, Russo C, Petracca M, Di Stasi M, Paolella C, Vola EA, Criscuolo C, Moccia M, et al. MRI features suggestive of gadolinium retention do not correlate with Expanded Disability Status Scale worsening in Multiple Sclerosis. *Neuroradiology* (2019) 61:155–162. doi: 10.1007/S00234-018-02150-4
191. Forslin Y, Shams S, Hashim F, Aspelin P, Bergendal G, Martola J, Fredrikson S, Kristoffersen-Wiberg M, Granberg T. Retention of Gadolinium-Based Contrast Agents in Multiple Sclerosis: Retrospective Analysis of an 18-Year Longitudinal Study. *AJNR Am J Neuroradiol* (2017) 38:1311–1316. doi: 10.3174/AJNR.A5211
192. Forslin Y, Martola J, Bergendal, Fredrikson S, Wiberg MK, Granberg T. Gadolinium Retention in the Brain: An MRI Relaxometry Study of Linear and Macrocyclic Gadolinium-Based Contrast Agents in Multiple Sclerosis. *AJNR Am J Neuroradiol* (2019) 40:1265–1273. doi: 10.3174/AJNR.A6112
193. Guo BJ, Yang ZL, Zhang LJ. Gadolinium Deposition in Brain: Current Scientific Evidence and Future Perspectives. *Front Mol Neurosci* (2018) 11: doi: 10.3389/FNMOL.2018.00335
194. Gadolinium-containing contrast agents - referral | European Medicines Agency (EMA). https://www.ema.europa.eu/en/medicines/human/referrals/gadolinium-containing-contrast-agents [Accessed September 6, 2025]